Towards seamless value-oriented forecasting and data-driven market valorisation of photovoltaic production

Thomas Carriere

PSL
UNIVERSITÉ PARIS

THÈSE DE DOCTORAT
DE L'UNIVERSITÉ PSL

Préparée à MINES ParisTech

Prévision et valorisation de la production photovoltaïques par méthodes orientées données

Towards seamless value-oriented forecasting and data-driven market valorization of photovoltaic production

Soutenue par

Thomas Carriere

Le 27 Février 2020

École doctorale n°621

Ingénierie des Systèmes, Matériaux, Mécanique, Energétique

Spécialité

Energétique et procédés

Composition du jury :

Julio Usaola	Professor, University Carlos III de Madrid	*Président, Rapporteur*
Pierre Pinson	Professor, Technical University of Denmark DTU	*Rapporteur*
Anastasios Bakirtzis	Professor, Aristotle University of Thessaloniki	*Rapporteur*
Lars Landberg	Doctor, DNV GL	*Examinateur*
Elke Lorenz	Doctor, Fraunhofer ISE	*Examinatrice*
Stefano Alessandrini	Doctor, National Center for Atmospheric Research NCAR	*Examinateur*
François-Pascal Neirac	Professor, MINES ParisTech	*Examinateur*
Georges Kariniotakis	Directeur de Recherche, MINES ParisTech	*Directeur de thèse*

MINES ParisTech | PSL

Acknowledgements

I would like to thank my supervisors Georges Kariniotakis and François-Pascal Neirac for their care and support during the realization of the thesis, on both a scientific and personal level. This work could not have been done without their precious advice.

I also want to thank Christophe Vernay, Sebastien Pitaval and Philippe Blanc who accompanied me during these three years, for their insights and more importantly their friendship. And also the numerous proofreadings that I inflicted to them !

The realization of this thesis was possible thanks to numerous companies. First, I want to thank MINES Paristech for the organization of the PhD. I would like to thank the company Solaïs and Third Step Energy for providing funds, data and guidance on the research. I also want to thank the Association Nationale Recherche Technologie for providing funds through a CIFRE agreement. I would also like to thank the European Centre for Medium Range Weather Forecasts that provided weather data and forecasts used throughout the thesis. Finally, I would like to thank the company EPEX SPOT for providing electricity prices data that was used in the thesis.

On a more personal level, I want to thank all the staff of MINES Paristech that helped me in various ways for the technical realization of the thesis. It goes without saying that these thanks are also addressed to my colleagues and fellow PhD candidates for all the laughs we had together. Their friendship made these three years a very pleasant and happy journey.

Finally, I want to thank my family for their love and support, and especially my parents and brothers who helped me get to this point in many ways, way before the beginning of this PhD. Claire, thank you for sharing your time with me and for always giving me a sympathetic ear and a shoulder to lean on.

Contents

List of Figures

List of Tables

Chapter 1

Introduction

Contents

1.1 The role of photovoltaic (PV) power in the energy transition

1.1.1 Current environmental issues

One of the major challenges of the coming years is to define a society model that can address the many environmental problems that have emerged in recent decades. These problems are all somehow related to the overexploitation of the Earth's natural resources. Although they have been identified since more than a century ago (see [1] or [2]), it is only in the recent decades that their effects have become noticeable.

However, these problems are interrelated and it seems difficult to solve one without affecting the others. The main major environmental problems are briefly presented in the next parts.

1.1.1.1 Global warming

Global warming is one of the main consequences of the large-scale combustion of fossil fuels. This combustion releases large amount of greenhouse gases (GHGs), and in particular carbon dioxide, CO_2. The increased proportion of CO_2 in the atmosphere contributes significantly to its warming.

This warming has been measured for several decades. Figure 1.1 represents the evolution of temperature anomalies, defined as the difference between the average temperature of the current year and the "smoothed" average temperature over several years. It is clear that there has been a significant increase in temperature since around the 1960s.

The consequences of global warming are numerous. They include rising ocean water levels, increased frequency of extreme weather events, and biodiversity loss. According to a 2007 report from the United Nations Environment Programme (UNEP), many geopolitical consequences should be expected [3], partly caused by increased pressure on resources, and the risk of civil migration associated with environmental change.

While the human contribution to global warming was discussed for a long time, it is now proved that the observed temperature variations are directly caused by human activities and the scientific consensus is unequivocal, as summarized in the latest report from the Intergovernmental Panel on Climate Change (IPCC) [4]. It seems therefore necessary to drastically reduce greenhouse gas emissions in all areas of human activity.

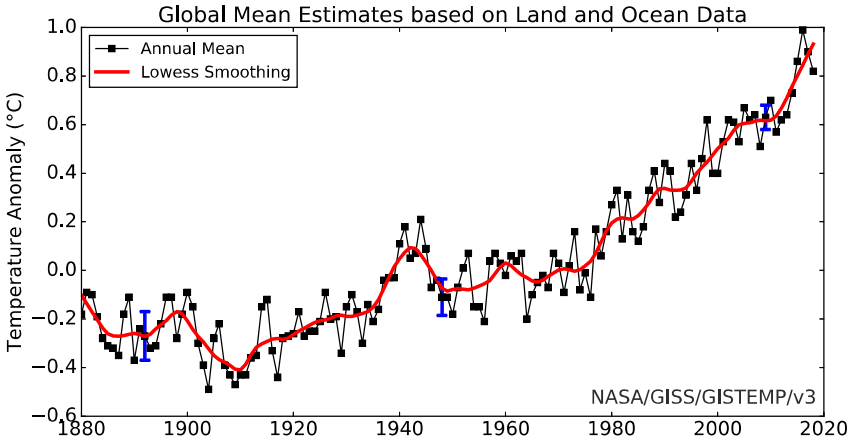

Figure 1.1: Temperature anomalies. Source: Hansen et al., 2010 [5]

1.1.1.2 Biodiversity loss

Biodiversity loss is the increased rate of disappearing of living species, both in term of population and number of species. According to a 2018 report from the World Wide Fund for Nature (WWF), vertebrate population sizes have seen a decline of 60% in the last 50 years [6]. Figure 1.2 compares the number of animal species extinction during different eras.

Biodiversity loss is also linked to human activity. It is partly caused by global warming, but also by the loss of natural habitats due to the transformation of natural environments into agricultural land, by pollution of the existing natural habitats and finally by the appearance of invasive species with the development of trade and travel. These different causes were identified in a report commissioned by the United Nations (UN) [7].

Apart from the natural heritage or moral value that can be attributed to biodiversity, it is also undeniable that biodiversity provides many services to human society. These are referred to as ecosystem services. Ecosystem services provide material resources: food, raw materials, water or medical resources. They also include regulation services that contribute to maintaining conditions favorable to life on Earth: oxygen production, soil fertility maintenance, pollination or CO_2 trapping. The value of these services was estimated in 2014 in reference [8] between \$125 and \$145 trillion/yr.

As a consequence, feedback loops are emerging. Increasing global warming reduces biodiversity and therefore the capture cycle of CO_2, which further increases global warming, and so on. This shows that it is impossible to deal with these subjects separately.

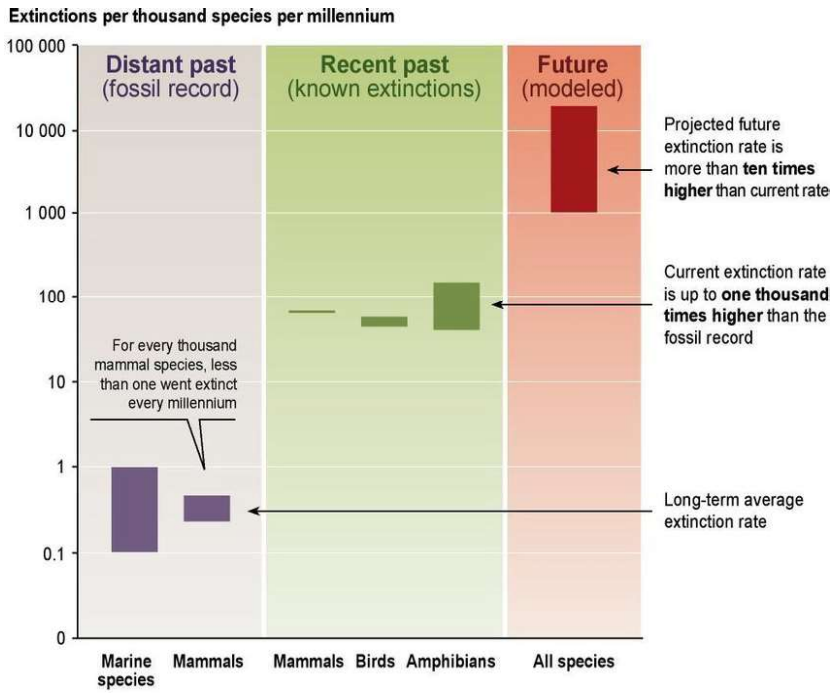

Figure 1.2: Animal species extinctions. Source: Hassan et al., 2005 [7]

1.1.1.3 Air, soil and water pollution

Various types of pollution are also caused by human activities and interrelated with the above-mentioned problems. Among the most problematic, we can cite:

- Air pollution, which is mainly caused by the excessive emission of toxic gases, particles and biological molecules in the atmosphere. Air pollution is a major health issue. A 2015 paper published in Nature estimated that air pollution causes 3.3 billion premature deaths per year, predominantly in Asia [9].

- Soil pollution, mainly caused by contamination of the soils with chemicals from industrial activity or intensive agriculture. This type of pollution is detrimental to human health through direct contact or consumption of groundwater contaminated from soils, and to ecosystems by modifying the chemical composition of the ground, thus perturbing the local food chain.

- Water pollution. This pollution has several causes, including industrial and agricultural waste, oil combustion wastes, untreated used waters or plastic waste. This type of pollution affects greatly the biodiversity loss for marine life, and causes significant

human health issues, especially in developing countries.

1.1.2 The energy transition

The growing pressure caused by all the issues described in section 1.1.1 pushes numerous governments to develop more sustainable policies. Many of these issues are somehow related to the increases in energy production and consumption. For example, global warming and air pollution are accelerated by the combustion of hydrocarbons for electricity production and transport. Biodiversity is under pressure from oil-intensive agricultural techniques, which also cause soil pollution. The same applies to plastic production, which has historically been linked to the development of the oil sector and is one of the main contributors to water pollution.

Therefore, many countries set up policies to limit the impact of our energy consumption on the ecosystem. These policies are commonly referred to as energy transition policies. They include many components, both on the energy production and consumption sides. The main objectives of such policies are to slow the depletion of Earth's natural resources and to lower the CO_2 emissions by moving to a system where energy production is based on renewable resources. They also push to lower the overall consumption by having more energy-efficient technologies and be globally more sober in terms of energy consumption.

Among all sources of energy, the electricity production sector plays a significant role in these environmental issues and should be performed in the most environmentally friendly possible manner. Conventional electricity production methods based on coal, oil or natural gas are a major source of CO_2 emissions. However, they developed strongly throughout the 20^{th} century thanks to the abundance of hydrocarbon reserves. They still provide the majority of the world's electricity today, as represented in Fig. 1.3.

However, the increasing awareness of environmental problems and the gradual depletion of deposits contribute to disadvantage these production methods. Low-carbon alternatives to these means of production exist, each with their advantages and disadvantages. They are different levers of the energy transition for the electricity production sector.

1.1.3 Low-carbon electricity production: the role of PV power

1.1.3.1 Low-carbon electricity production

One objective of the energy transition is to produce low-carbon electricity to avoid CO_2, while minimizing the production's impact on the environment. It is also necessary to take into account the cost of electricity production and the easy access to resources in order to achieve the production from an economic point of view. Figures 1.4a and 1.4b represent

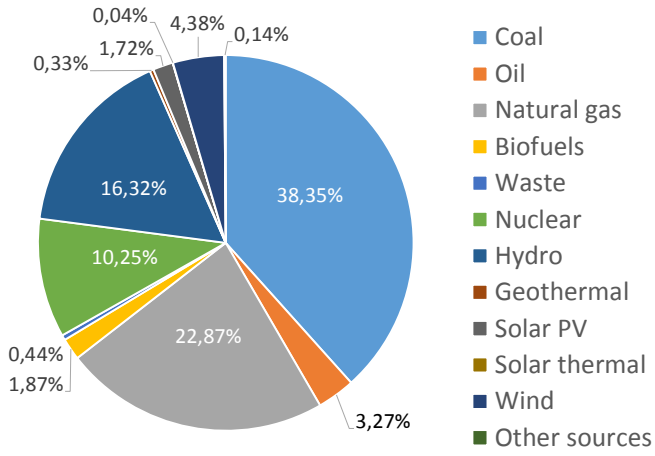

Figure 1.3: Proportion of different energy sources in the world electricity production.
Total: 25,720 TWh.
Source: International Energy Agency [10]

some of these characteristics. On Figure 1.4a, CO_2 emissions from different production sources are compared. On Figure 1.4b, the Levelised Cost of Electricity (LCOE) is shown. It is a calculation of the total cost of production of an energy unit, taking into account investment costs (CAPEX), maintenance costs (OPEX), as well as fuel costs if necessary, and the discount rate over the lifetime of the generation. Nuclear power is included in the category "fossil-fueled" in Fig. 1.4b. Low-carbon electricity production sources are briefly presented in the following parts.

1.1.3.2 Nuclear power

Nuclear power generation based on fission is a mature technology for producing electricity with very low CO_2 emissions. The main advantages of this sector are the very low CO_2 emissions and its low production cost, although there is some controversy over the cost of decommissioning old nuclear power plants.

However, nuclear power has several disadvantages. Producing electricity by nuclear fission generates pollution with radioactive wastes, for which there are no known treatments. For the time being, radioactive waste is buried or stored. Another problem is the risk of accidents. While accidents are in fact very rare, their consequences are dramatic. For example, the nuclear incident at the Fukushima Daiichi power plant caused the evacuation of more than a hundred thousand people and a large radioactive pollution of sea water [13] and had lasting effects on the local wildlife [14], [15]. Besides, the impacts on ecosystems

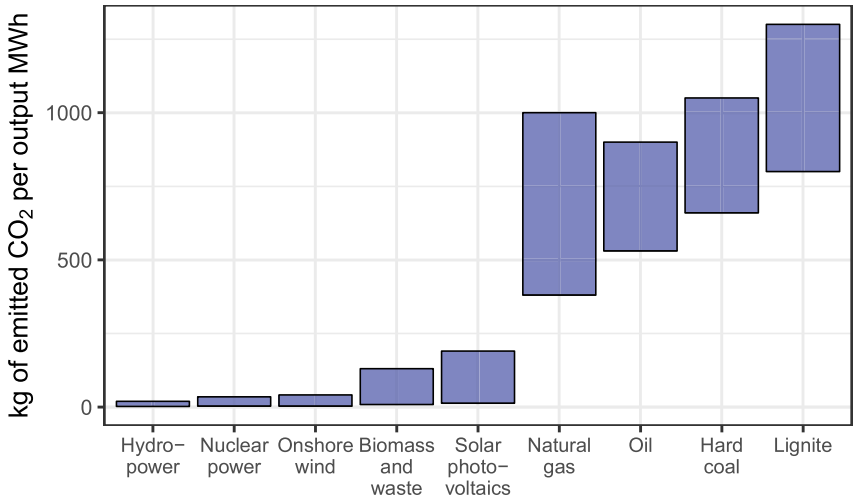

(a) Range of CO_2 emissions for different electricity production sources.
Source: Adapted from Turconi et al., 2013 [11]

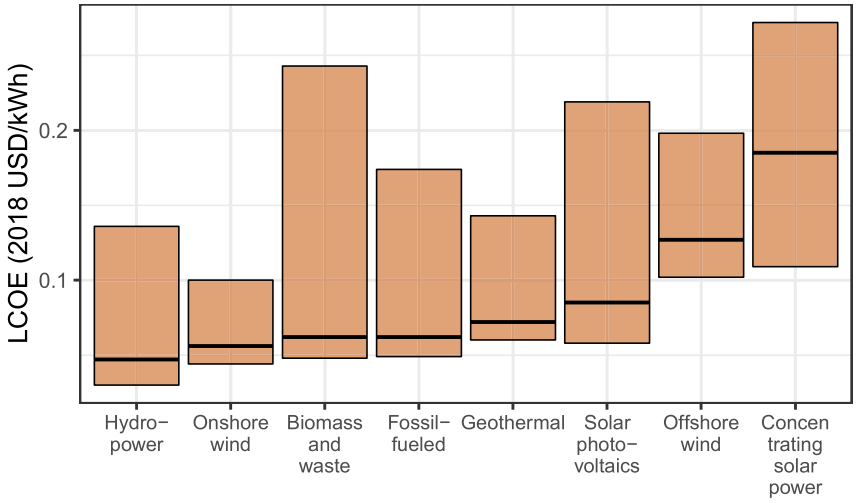

(b) LCOE for different electricity production sources. Horizontal lines indicate the mean LCOE, lower and upper values show the 5-th and 95-th percentile.
Source: Adapted from report *Renewable Power Generation Costs in 2018* [12]

Figure 1.4: LCOE and CO_2 emissions for different sources of electricity production

and the radioactive pollution generated from nuclear power plants are undeniable, making some areas affected for decades.

There are also many geopolitical risks surrounding nuclear power generation, as it requires a resource, that is uranium. Access to this resource could become a problem if the proportion of nuclear energy in the global energy mix increases. In addition, uranium is not widely distributed throughout the world, with some countries providing most of the production. This can contribute to geopolitical instability, especially if there is a lot of pressure on the access to the resource, as was the case for oil in the oil crisis in 1973, 1979 or the oil price shock of 1990 [16]. Finally, there is also the risk of nuclear proliferation. Indeed, nuclear energy can also be used for weapon production, and there is concern that the growth of nuclear energy could globally increase the presence of extremely destructive nuclear weapons in the world.

1.1.3.3 Renewable energy sources

Renewable Energy Sources (RES) are another option for producing low-carbon electricity. They are electricity production methods where the initial source of energy that is converted into electricity is not a fossil source such as coal, oil derivatives or uranium (to be more precise, these resources are also renewable in the sense that they are naturally produced, but on extremely long time scales compared to those of renewable resources). RES refers to a large number of electricity production techniques. Among the most developed are:

- Hydroelectricity relying on the water cycle to produce electricity using the flow of rivers.
- Wind energy that converts the wind's kinetic energy into electricity.
- Photovoltaic energy, that converts solar irradiance into electricity.
- Concentrated Solar Power CSP that powers a heat engine using heat from the Sun concentrated through lenses or mirrors.
- Cogeneration using biomass that produces both heat and electricity.
- Geothermal energy, that converts heat from the inner parts of the Earth into electricity.
- Tidal energy that converts cinetic energy from the tide into electricity.

These energies have different levels of maturity. Hydroelectricity is one of the oldest sources of electricity production and is well controlled. Wind and solar energies have an

advanced technological and commercial maturity, and these two sources of energy have experienced particularly high growth rates since the last decade (see section 1.4). Biomass usage has developed in the recent years, although there is a risk of overexploitation of the natural resource. Tidal and geothermal power, although mature technologies, can generally only be developed in specific parts of the world where the resource is significant. Other RES are also only at the demonstration scale of their development.

Wind energy allows electricity production with very low CO_2 emissions. In addition, the resources specific to the manufacture of wind turbines are not sparse, except for direct-drive systems that use rare-earth components [17]. However, direct-drive systems represent only 2% of the wind turbines in the US [18]. The main disadvantages of wind power are the variability of the production and the visual pollution. Wind power production is not or only partially controllable, since it is driven by wind speed. To ensure the stability of the power grid, it is thus necessary to ensure in real time the balance between supply and demand, which is usually made by activating controllable means of production that can be started up quickly (typically gas turbines) to compensate for the variations in the production. This represents a cost that is difficult to estimate since it depends on the variability of production, the available backup production means, as well as the way the electricity grid manages the supply/demand balance in real time. Due to the complexity of these costs, they are rarely included in LCOE calculations. The spatial smoothing effect refers to the fact that a collection of spatially distributed wind turbines have an overall smaller variability than a single turbine, and can mitigate the variability's cost. Offshore wind power can also mitigate the variability, but it still suffers from relatively high production costs.

Photovoltaic energy has also low CO_2 emissions, although they are higher than wind and nuclear power. This is mainly due to the manufacturing process of solar panels, which includes the extraction of silica, which is polluting, and an energy-intensive step of purifying silica, to the point that solar panels can take a few years to "refund" their initial energy cost, which is the Energy Payback Time (EPBT). In southern Europe, recent studies estimate the EPBT to roughly 1.5 years [19]. However, if the panels are manufactured using a low-carbon energy mix, the CO_2 emissions of the photovoltaic sector greatly reduce. One of the major advantages is that the initial energy source (solar radiation), as well as the resources needed to manufacture the panels (mainly silica) are present in most regions of the world. Besides, in areas with high solar irradiation, the LCOE of PV power is very competitive. The disadvantages of this sector are its high CO_2 emissions compared to other RES and nuclear energy, but also the large area required to capture solar radiation (around 1ha per MWp in 2019 for ground-mounted PV), the unavailability of the resource during

night hours, and the variability of production. CSP shows less variability since it primarily produces heat, which can easily be stored. However, it also suffers from higher costs than PV as shown in Fig. 1.4b.

In the end, wind and solar energy are expected to develop at an increased rate, as they have low impacts in terms of CO_2 emissions and pollution and their costs steadily decrease. One of the biggest challenge for their integration remains the management of the variability of their production. In this thesis, we focus on the photovoltaic sector, and particularly on large (> 10 MW) ground-mounted PV plants. Such plants have the lowest LCOE in the photovoltaic sector, and thus are expected to grow significantly in the coming years.

1.2 Characteristics of PV power production

1.2.1 Photovoltaic effect

The production of electricity by photovoltaic panels is based on the photoelectric effect that occurs in each of the photovoltaic cells that compose in the panel. Simply put, an incident photon with sufficient energy can separate an electron within the material, creating an electron/hole pair. By an assembly of so-called "doped" layers, the electron and the hole separate, each moving towards one end of the material, thus creating a potential difference. Finally, by inserting conductive metal contacts at both ends, a direct electrical current can flow.

The physical phenomenon that generates the current is the number of incident photons, and therefore production is primarily dependent on solar irradiance, defined as the power per unit area received from the Sun, in W/m^2. However, the components of photovoltaic cells are also affected by temperature: the lower the temperature, the more efficient the panels. In addition, photovoltaic cells have a spectral sensitivity, that is, their efficiency is different according to the wavelength of the incident photons, which itself depends mainly on the radiative transfer in the atmoshpere.

More precisely, the basic quantity that is frequently used to explain and characterize photovoltaic production is the Global Horizontal Irradiance (GHI). This quantity represents the power received from the Sun per unit of horizontal surface area. It is composed of the direct solar radiation BHI (Beam Horizontal Irradiance) and the diffuse radiation resulting from the multiple reflections taking place in the atmosphere, the DHI (Diffuse Horizonal Irradiance), as shown in Fig. 1.5.

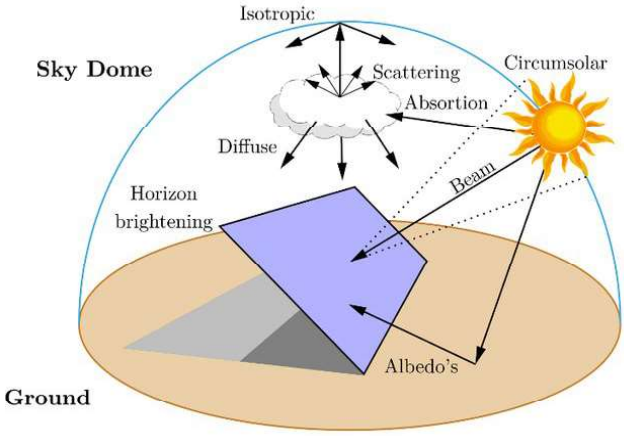

Figure 1.5: Illustration of the different components of solar irradiance
Source: De Simòn-Martìn et al., 2016 [20]

1.2.2 Predictability of photovoltaic power

The variability of photovoltaic production is strongly related to that of solar irradiance. This variability is present at different time scales and is caused by different physical phenomena. These variabilities generate uncertainty on the upcoming PV power generation and thus limit its predictability. Variability on long-time scale i.e. daily or seasonal is important for maintenance planning of the plants or prospective generation assessment for new projects. Variability on short-time scale i.e. a few minutes to a few hours is important for grid operation or market participation. There are different causes for the variability depending on the time scale.

There are two causes of variability for long time scales: the day/night alternation related to the Earth's rotation on a daily scale, and the seasonal cycle related to the Earth's revolution around the Sun on an annual scale. However, the equations describing the motion of the Sun are very precise, and thus this variability does not limit much the predictability of PV power [21]. Irradiance in clear sky conditions ("Clear-Sky") is a useful quantity to characterize this variability. It refers to the irradiance that would be received at Earth's surface if there were no clouds. Many models exist to calculate it, and although it depends mainly on the position of the Sun, models are often enhanced to take into account the composition of the atmosphere or other relevant quantities. In the rest of the manuscript, we will always use the McClear model [22].

Variability on short time scales is mainly caused by the movement of clouds. These movements can be very quick and consequently, because PV production has no inertia, it

can exhibit strong ramps, i.e. very rapid power variations, when a cloud passes over the plant. On an intra-day scale, the proportion of water vapour, the composition of aerosols i.e. fine particles suspended in the atmosphere, or temperature variations can also cause power variations, although in a much less significant manner than cloud movements. The variability caused by clouds is the one that generates the most uncertainty about PV production, as it is difficult to accurately predict the formation and movement of clouds over a long forecast horizon.

Therefore, cloud movements and formations strongly limit the predictability of PV power. As for wind power, the variability of PV power can be mitigated by the spatial smoothing effect: cloud movements are a very local phenomenon. Thus, when the output of several power plants is summed, the overall uncertainty is reduced since an unexpected event only affects one power plant at a time, and therefore only a part of the output.

Another important characteristic of the PV power predictability is the autocorrelation of forecast errors. This refers to the fact that PV power forecast error is highly correlated with itself, shifted over time. This is caused by the persistence of climatic conditions, which is the tendency that the weather has to remain the same over consecutive time steps. Simply put, it reflects the fact that if the PV production is lower than expected at a time t, it is more likely that the production at the time $t + 1$ is also lower than expected. This effect can be problematic if we try to reduce the variability of production using a storage system with limited capacity, as we will see in the next chapters.

Finally, the movement of the clouds from one plant to another creates a correlation between the production from a specific plant and a distant one shifted in time. The further away these plants are from each other, the lower the correlation. This effect can be used to generate production forecasts from the production observed in other plants. However, it is not exploited in this thesis, where we consider only individual power plants.

1.3 Regulated context, electricity market

1.3.1 Support mechanisms for PV power

There are numerous ways of valorizing the energy produced by PV sources. Historically, PV power was largely subsidized as for most of renewable energies, to help its development. However, the costs for installing PV power systems reduced greatly in the recent years, due to the decrease of PV modules costs which still represents roughly one third of the total installation cost [12]. Consequently, financial support from government reduced also in many countries. There are three common kind of financial incentives for PV power:

investment subsidies, feed-in tariffs and Solar Renewable Energy Credits (SRECs).

The earliest form of financial incentive for solar power was in the form of investment subsidies. That is, PV power plants developers used to recover a part of the capital they invested from their government. This mechanism proved an efficient way of increasing the share of PV power, but it was criticized for not providing to the PV plant developers an incentive to build efficient plants since the remuneration was only based on the investment and not on the actual energy output of the plant.

To solve this problem, another form of financial incentive was introduced with feed-in tariffs. With this system, national entities have to buy the output of PV power producers at a fixed price that is either set by the authorities, or negotiated between the PV producer and the entity. Since the PV producer is paid proportionally to the energy output of their plant, they are encouraged to build and operate efficient plants. However, a problem arised from this mechanism. The buying price is usually set at a price higher than the grid electricity price, which results in the overpayment of the PV plant owner. Thus, it is a very strong incentive to develop new PV plants. These buying prices reduced to follow the reduction of PV modules costs. However, the LCOE of PV power plants has reduced in the recent years, and in many countries it is now approaching the real market electricity prices. As a result, there is no point in having dedicated feed-in tariffs systems.

A more subtle mechanism was introduced, mostly in the United States [23] with the development of SREC. This was introduced to imitate an electricity market, so that the actual price for PV power energy was based on a market mechanism that pushes PV power producers to be cost-effective. The principle is that each PV power producer is awarded a SREC for every MWh of electricity they produce, and each electricity utility has to buy a fixed amount of SREC, set by the authorities. Then, the SRECs are negotiated through a market system, with the price depending on the actual demand and offer for PV power.

There is still a problem caused by these mechanisms, which is that the financial costs caused by the variability of the PV power generation are entirely left to the Transmission System Operator (TSO). Since the PV producers are either remunerated at a fixed price with feed-in tariffs, or with SRECs generated for each MWh, they do not have any incentive to mitigate the variability of the PV generation, and thus they are not financially responsible for the cost it entails for TSOs.

Recent support mechanisms tend to make the PV plant owners responsible for the variability of their production. For example, with the last tender in France [24], PV plant owners have to sell their energy in the French electricity market, where they are financially responsible for any difference between the amount of energy they sold the day before and

their actual energy output. Afterwards, they get from the authorities a payment to compensate the difference between the mean electricity price on the electricity market and a fixed tariff negociated through the tender. In that way, PV plant owners must tackle the issue of the variability of PV power generation.

1.3.2 Electricity production valorization

Usually, there are three options to valorize the electricity produced by a power plant.

The first option is to distribute directly the electricity to the consumers. This is frequently the case for large electricity utilities that are both producers and distributors of electricity (e.g. EDF, E.ON or British Gas). The selling price is determined by a contract between the consumer and the utility. This option is not relevant for a PV plant operator that has no intention to become an electricity distributor.

The second option is to sell the electricity directly to a specific consumer through so-called OTC (Over The Counter) contracts, or PPA (Power Purchase Agreements). These contracts are negotiated in agreement between the parties (buyer and seller of electricity), as opposed to the standard contracts with mandatory clauses that are signed between the parties in an organized market. Usually, these contracts are negotiated between an electricity producer and a large consumer such as a factory or an electricity distributor without production resources. It is a possible option for selling PV power, however both parties have to consider the fact that the PV plant will not produce during night hours, and have a variable production on daylight hours. For the moment, such contracts are rare in Europe. For example, in France, the first PPA was signed between the companies Voltalia and SNCF Energies, which is the main French railway company, in May 2019.

Finally, the last option is to sell the electricity in an organized market. This is the default option, since the other options require either to have consumer clients, or to find a party that is interested in signing a PPA. In this thesis, we assume that these specific conditions are not fulfilled and we focus on the most general case of market participation as the only mean of PV production valorization. A first introduction to electricity markets is provided below.

1.3.3 Electricity markets

On day-ahead electricity markets, energy producers and consumers submit their selling or buying bids to the market operator. A bid is constituted of an energy volume, a Market Time Unit (MTU) and a price in €/MWh. A positive (resp. negative) energy volume means that the bidder is willing to sell (resp. buy) the specified volume at the time indicated by

the MTU for a price higher (resp. lower) or equal than the specified price.

All the actors can submit bids until a specified time called the GCT (Gate Closure Time). After this time, all the selling and buying bids are aggregated to build the offer and demand curves, and their intersection defines the market price. The selling (resp. buying) bids that have a price lower (resp. higher) than the market price are accepted. The entity that calculated the market prices organizes the financial flows and usually retrieves a fee for that.

Based on these general principles, several variations of these markets exist. The way the prices are calculated, the time resolution of the MTUs (hourly, half-hourly or less), the GCT can vary a lot. Furthermore, on electricity markets, actors are usually responsible for matching the electricity production and consumption over a given perimeter that includes their production and consumption resources. Therefore, if they are not able to actually produce (resp. consume) the volume they sold (resp. bought) on the market, they must pay a compensation to the TSO that manages their perimeter. Thus, the limited predictability of PV power generation can incur significant losses for PV power producers participating in electricity markets. These costs are called the balancing costs, and the way they are calculated also depends on the TSOs. In the end, the valorization of the PV power production depends on both the electricity market and the TSO.

1.4 Motivation and objective of the thesis

1.4.1 Motivation

From the industry perspective, several governments voted laws promoting the energy transition to renewable sources, while PV installation costs are decreasing steadily. This creates very favorable conditions for development of new PV plants projects. For example, in France, the "Programmation Pluriannuelle de l'Energie" (PPE) was published in 2018 according to the 2014 law "Loi relative à la Transition Energétique pour la Croissance Verte" (LTECV). This document specifies the French strategy regarding the energy transition. Regarding PV power, the objectives are to install 20.6 GW of PV power by 2023 and between 35.6 and 44.5 GW by 2028 [25]. These objectives set a sharp trajectory for the development of PV power plants since there was only 8.5 GW of PV power installed in 2018 in France. This is, however, a worldwide tendency. Figure 1.6 shows the growth in the installation of solar power in the world.

However, PV plants are now expected to bear the costs caused by the balancing of their production, since it is variable and has a limited predictability. New support mechanisms

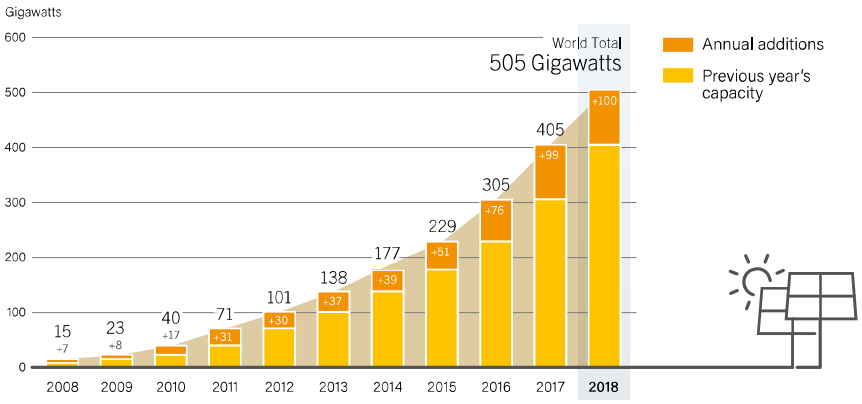

Figure 1.6: PV power growth in the world. Source : Murdock et al., 2019 [26]

force PV plant operators to participate in electricity markets instead of benefiting from feed-in tariffs or similar support schemes. Thus, the return on investment of PV plants becomes variable, as it depends from market prices. Besides, the penalties mentioned above depend on forecast errors, which makes the revenue also dependent on PV power variability.

1.4.2 Objectives

Considering these elements, the overarching goal of this thesis is to maximize the revenue obtained from the production of PV power with regard to electricity market prices and PV generation variability. To do so, we will study the value chain of PV generation, that is the chain of data streams, models and decision-making tools that a PV power producer has to consider to generate revenue from its production.

This chain is summarized on figure Fig. 1.7. In the literature, most attempts to increase the PV power value do so by incrementally improving parts of the chain. For example, there is a significant research activity in improving Numerical Weather Prediction (NWP) forecasts quality, PV power forecasting models or trading strategies in electricity markets. Although such attempts certainly increase the value of PV power, we propose a different approach by directly addressing systematical issues in the chain itself. These issues are represented on Fig. 1.7.

We identified four main systematical issues in the value chain, that each constitute a scientific objective to overcome in the thesis. The solutions we propose to address these issues are presented in the next section.

1. The first issue is a lack of adequacy between the PV power forecasting models used in the scientific literature and the forecasting products required in electricity markets.

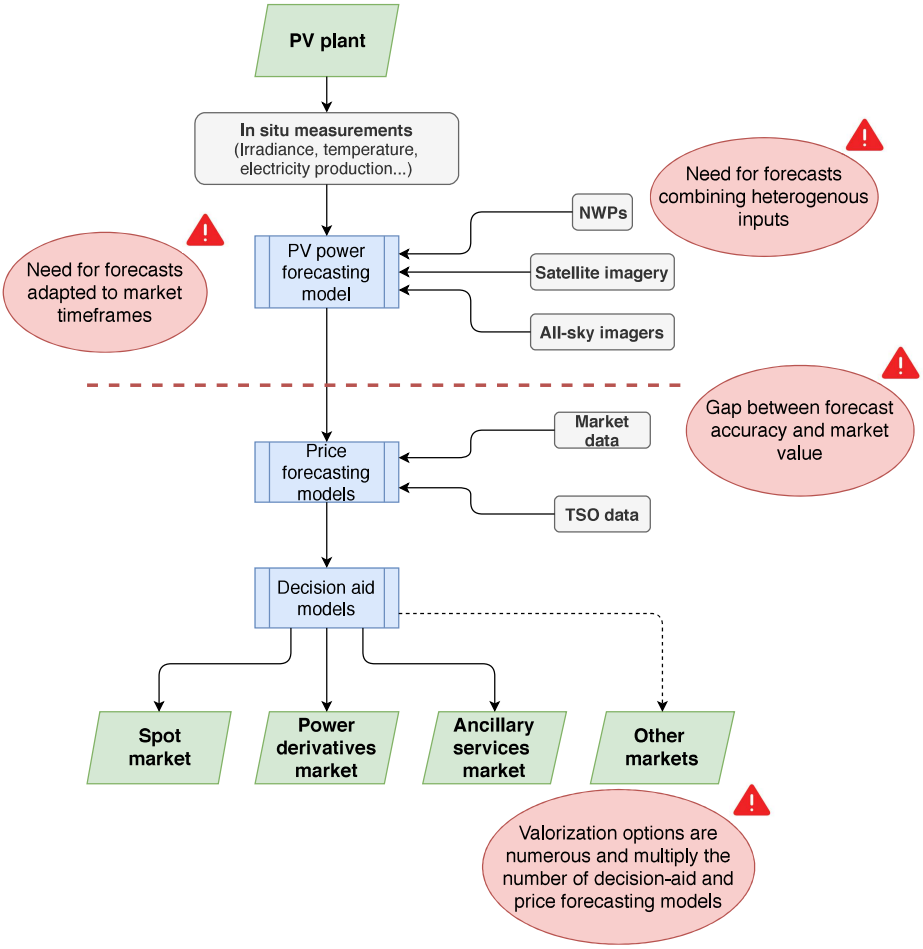

Figure 1.7: General valorization process of PV power and technological gaps

The main problem is that generally, different models are used depending on the forecast horizon in the literature. At the same time, electricity markets require forecasts with heterogeneous time frames. For example, spot electricity markets usually require day-ahead forecasts, while intra-day continuous markets can require forecasts from a few minutes up to a few hours ahead. Thus, participating in all these markets requires developing and maintaining different models, and thus causes continuity issues in the forecasts, with discrepancies at the horizon threshold between models.

2. The second issue is linked to the first one, in the sense that models in the scientific literature use different sources of data as input depending on their forecast horizon. Thus, the models are not only dependent on the horizon but also on the source of data, and they lack the ability to combine information from all available data. Since more

and more data sets and resources can be found online, we think that is important that PV power forecasting models can deal with large amounts of data and combine them to provide forecasts for all horizons without continuity issues.

3. The third issue is the gap between the PV power forecasting part of the value chain and the market trading part. In the literature, these two parts are usually developed and trained separately, and it is thus not clear how an improvement in the PV power forecast quality can improve the revenue generated from the PV power production. However, we expect that taking into account the market mechanisms and the value of the forecasts from the beginning of the value chain, that is, when developing and training the PV power forecasting models would naturally lead to an increase in the value of the forecasts.

4. Finally, the last issue is that there is a large number of ways to valorize the PV power, which makes the value chain more complex as it multiplies the number of price forecasting and decision-aid models, which in turn increases the variability of the revenue. In Fig. 1.7, we reported three major markets types, that are the spot market, the power derivatives market and the ancillary services market. However, there are many variations of these markets depending on the country or the TSO in charge of the grid where the plant is connected. It is not unusual for a power plant to be able to participate in several instances of the same kind of market. Besides, local markets operated by the TSO to help him ensure the supply/demand balance exist in many countries. Finally, some countries can offer tenders for developing PV power, which have specific remunerations conditions. Since the revenue is also dependent on the PV power variability, we can also consider decisions that hedge this variability such as the operation of a storage system as another trading option.

1.5 Methodology and contributions

We aim to improve the value of the PV power, but the term ”value” can have different meanings depending on the valorization options that the PV plant operator uses to sell its production. Thus, the first step of the methodology of this thesis is to define a formalism that allows modeling the participation of a PV plant operator in any series of valorization options in a generalized manner, so that any ”value function” can be used to estimate the revenue generated by the PV plant operator, and so the participation of the PV plant operator on any subset of the existing valorization options can be evaluated. Using this formalism, we explore different approaches for generating revenue with contributions that

address the scientific objectives of the thesis. These contributions are the following:

- We propose a seamless PV power forecasting model, that is, a model that provides forecasts that are consistent across time scales, with the same modelling for all forecast horizons. To do so, an automatic weighting of the input features of the model is performed for each forecast. The weighting process takes into account both the start time of the forecast and the forecast horizon, so that the model provides consistent results across all start times and forecast horizons. Finally, the model can use multiple data sources as input e.g. measurements, NWP, or satellite data. This seamless model addresses the objectives 1. and 2. of the thesis. This work was published in a journal article [27].

- We combine this PV power forecasting model with appropriate price forecasting models and decision-aid models to have a first approach for generating revenue on the market. However, to address objective 3. of the thesis, we propose a different paradigm to train the model. Instead of training each model to maximize its own performance, we train all the models involved at once to maximize the revenue. This effectively creates a link between the forecasting model and the trading models, ultimately increasing the revenue. This work was published in a journal article [28].

- We propose an alternative approach where we generate the revenue in a systematic manner by using appropriate Artificial Neural Networks (ANN). For each of the decision required in the value chain, an ANN performs a Policy Function Approximation in order to directly learn an efficient policy from the data, effectively using the computing power and generalization abilites of ANNs. This drastically reduces the number of models involved in the value chain and bypasses the need for intermediate forecasting models. Besides, the ANNs can be trained directly to maximize the value associated with their decision. Thus, this contribution addresses the objectives 3. and 4. of the thesis. This work was also published in the same article as the above contribution [28].

1.6 Outline of the thesis

This thesis is divided in five chapters, considering this introduction as the first chapter.

The second chapter details the operation of the different ways of valorizing PV power. Then, we propose a generic notation of the value chain for PV power as a series of decision-making processes, which allows for defining the different solutions that we propose to address

the third and fourth objectives of the thesis. These solutions include two different approaches for trading PV power, using either dedicated forecasting models (approach 1) or a single ANN model learning to trade PV power from historical data (approach 2).

In the third chapter, we present the seamless forecasting model that we developed to address the first and second objective of the thesis. This model is required to perform approach 1. This model combines in situ measurements, satellite data and weather forecasts, and can be used at any time of the day for any forecast horizon ranging from 5 minutes to 36 hours.

In the fifth chapter, we apply the different solutions presented in the previous chapters for selling the PV production on a day-ahead electricity market and a balancing market where the PV plant operator must financially compensate the balancing costs caused by its variable production. This first test case requires no additional investment, since the access to all the options considered in the value chain is free.

In the fourth chapter, we add a storage system to the PV plant and the possibility to participate in an intra-day market, which adds two decision-making processes to the value chain. However, since there are a lot of constraints associated with the usage of a storage system with limited capacity, the implementations of the different solutions for providing the decision are more complex. For the specific models approach, we have to develop a controller for operating the storage system based on the updates of PV power forecasts and the state-of-charge of the storage system. Since these constraints involve temporal interdependencies, we reflect them in the second approach by using a Recurrent Neural Network (RNN) instead of a simple ANN. The added value of storage systems is studied and compared to their investment costs, and a sensitivity analysis on the storage system sizing and market prices is proposed.

Finally, the last chapter summarizes the content of the thesis and draws the conclusion of the studies.

1.7 Publications of the thesis

Parts of this thesis have been published in the following journal articles:

[A] T. Carriere and G. Kariniotakis, 'An Integrated Approach for Value-Oriented Energy Forecasting and Data-Driven Decision-Making Application to Renewable Energy Trading', in **IEEE Transactions on Smart Grid**, vol. 10, no. 6, pp. 6933-6944, Nov. 2019. doi: 10.1109/TSG.2019.2914379, https://ieeexplore.ieee.org/document/8706264. Post-print available at https://hal.archives-ouvertes.fr/hal-02124851.

[B] T. Carriere, C. Vernay, S. Pitaval, F.P. Neirac and G. Kariniotakis, 'Strategies for combined operation of PV/storage systems integrated into electricity markets', in **IET Renewable Power Generation**, vol. 14, iss. 1, pp. 71-79, May 2019. doi: 10.1049/iet-rpg.2019.0375, https://ieeexplore.ieee.org/document/8957899. Post-print available at https://hal.archives-ouvertes.fr/hal-02124855/.

[C] T. Carriere, C. Vernay, S. Pitaval and G. Kariniotakis, 'A Novel Approach for Seamless Probabilistic Photovoltaic Power Forecasting Covering Multiple Time Frames', in **IEEE Transactions on Smart Grid**, vol. 11, no. 3, pp. 2281-2292, May 2020. doi: 10.1109/TSG.2019.2951288, https://ieeexplore.ieee.org/document/8890659. Post-print available at https://hal.archives-ouvertes.fr/hal-02369413/.

Parts were also communicated in conferences:

[D] T. Carriere, C. Vernay, S. Pitaval and G. Kariniotakis, 'Strategies for Combined Operation of PV/Storage Systems Integrated to Electricity Markets', in **11th Mediterranean Conference on Power Generation, Transmission, Distribution and Energy Conversion (MEDPOWER)**, Dubrovnik, November 2018.

[E] T. Carriere, C. Vernay, S. Pitaval and G. Kariniotakis, 'Probabilistic photovoltaic forecasting combining heterogenous sources of input data for multiple time-frames', in **6th Internation Conference on Energy and Meteorology (ICEM)**, Copenhagen, June 2019.

[F] T. Carriere, C. Vernay, S. Pitaval and G. Kariniotakis, 'Sizing of a PV/Battery System through Stochastic Control and Plant Aggregation', in **36th European PV Solar Energy Conference and Exhibition (EU PVSEC)**, Marseille, September 2019.

[G] T. Carriere, and G. Kariniotakis, 'Towards a seamless approach for photovoltaic forecasting', in **EGU General Assembly 2020**, Online, 4–8 May 2020, EGU2020-21753, https://doi.org/10.5194/egusphere-egu2020-21753,2020

Chapter summary in French

Contexte

L'activité humaine crée de nombreux problèmes environnementaux qui ont des impacts négatifs à la fois sur les écosystèmes locaux mais aussi sur la société dans son ensemble. Parmi eux, on trouve :

- Le réchauffement climatique;
- La disparition de la biodiversité;
- La pollution de l'air, de l'eau et des sols.

Ces différents problèmes sont tous liés d'une certaine façon à l'activité humaine, et plus précisément à l'augmentation de la production et de la consommation d'énergie à échelle mondiale. Dans ce contexte, la transition énergétique cherche à développer des alternatives durables et à faible impact sur l'environnement au model actuel de production et de consommation d'énergie. Cette transition se caractérise par des changements profonds d'un point de vue social et comportemental, mais aussi des solutions techniques pour réduire l'empreinte énergétique des différentes activités humaines.

Parmi elles, la production d'électricité est une activité qui participe à de nombreux problèmes environnementaux, et en particulier au réchauffement climatique. En effet, la plupart de l'électricité produite dans le monde est produite par combustion de combustibles fossiles, ce qui émet d'importantes quantités de gaz à effet de serre.

De nombreux moyens de production d'électricité ayant un plus faible impact environnemental que les moyens traditionnels existent. Parmi eux, les moyens de production d'énergie renouvelable, c'est-à-dire qui utilisent une source d'énergie dont le renouvellement naturel est rapide, connaissent un développement rapide depuis les années 2000. Dans cette thèse, nous nous intéresserons particulièrement à la filière photovoltaïque, qui convertit l'irradiation solaire en électricité par le moyen de l'effet photoélectrique.

L'un des défauts de la filière photovoltaïque est que la production est dépendante de l'ensoleillement, et donc présente une importante variabilité. Cette variabilité est présente à plusieurs échelles de temps. La mouvement périodique de la Terre sur son orbite génère une variabilité saisonnière et sa rotation sur elle-même une variabilité journalière avec l'alternance jour/nuit. Finalement, la formation et le passage de nuages au-dessus des centrales photovoltaïques créent une variabilité intra-journalière. Le mouvement de la Terre est bien connu et génère peu d'incertitudes sur la production, mais la formation et le mouvement

des nuages est un phénomène complexe et local qu'il est difficile de prévoir. Ceci génère une importante incertitude sur la variabilité intra-journalière de la production photovoltaïque, et limite finalement la prévisibilité de la production.

En parallèle, les subventions accordées à la production photovoltaïque diminuent graduellement pour accompagner la baisse des coûts de cette filière. Les tarifs d'achat ont maintenant disparu dans de nombreux pays et les producteurs d'énergie photovoltaïque doivent maintenant vendre leur production sur les marchés de l'électricité comme pour toute autre filière. Cependant, les participants au marché de l'électricité doivent payer des pénalités financières pour tout écart entre leur production et la quantité vendue sur le marché, ce qui est problématique pour l'énergie photovoltaïque puique sa prévisibilité est limitée.

Motivation

Du point de vue industriel, la filière photovoltaïque a bénéficié de fortes réduction des coûts dans les dernières années, acompagnée par une forte volonté politique de développement de cette filière. Cependant, elle doit maintenant assumer elle-même les coûts crées par sa variabilité, ce qui génère une importante incertitude sur le revenue.

L'objectif de cette thèse est donc de maximiser le revenu géneré par une centrale photovoltaïque sur le marché de l'électricité, en tenant compte de l'incertitude de la production et celle des prix de l'électricité. La chaîne de valorisation qui conduit à la géneration de revenu sur les marchés est complexe et implique de nombreux modèles de prévisions fonctionnant à divers horizons temporels (voir figure 2.4). La plupart des approches existantes tentent d'améliorer le revenu lié à la vente de la production en améliorant incrémentalement certaines parties de la chaîne, par exemple en améliorant la performance du modèle de prévision de la production. Dans cette thèse, nous explorons d'autres perspectives d'amélioration en étudiant les problèmes structurels de la chaîne de valorisation. Nous avons identifié quatre problèmes structurels, qui constituent chacun un objectif scientifique de la thèse à surmonter :

- Le manque d'adéquation entre les modèles de prévision proposés dans la littérature scientifique qui sont géneralement différents selon l'horizon de prévision, et les besoins de la vente de la production photovoltaïque qui fonctionnent de façon continue sur une multiplicité d'horizons de prévisions.

- Le besoin de modèles de prévision de la production capables d'exploiter des sources d'information diverses, telles que les mesures, les prévisions météorologiques ou les images satellites.

- Le manque de lien entre la performance des modèles de prévisions (prix ou production) individuels et le revenu géneré. Les modèles sont géneralement entraînés pour avoir la meilleure performance de prévision, ce qui ne garantit pas qu'ils génèrent le meilleur revenu possible.

- La complexité de la chaîne de valorisation qui nécessite une grande variété de modèles et de données d'entrée, ce qui complique son utilisation de façon opérationelle.

Méthodologie

Nous proposons différentes approches pour traiter les problèmes structurels de la chaîne de valorisation de la production photovoltaïque. Le terme "valeur" peut avoir un sens différent selon les options de valorisation choisies : le calcul du revenu est différent selon que l'électricité est vendue sur un marché day-ahead uniquement ou day-ahead et intra-day, selon que la centrale PV est couplée à une batterie ou non, et ainsi de suite.

La première étape de la méthodologie de la thèse est donc de proposer une notation générique qui permet de modéliser n'importe quelle option de valorisation de la production. Cette notation permet de définir facilement les différentes solutions proposées pour traiter les objectifs scientifiques de la thèse.

Pour traiter les deux premiers objectifs, nous développons un modèle de prévision de la production photovoltaïque exploitant une procédure automatique de pondération des données d'entrées selon l'horizon, de façon à ce que le modèle puisse être utilisé facilement pour n'importe quel option de valorisation.

Pour traiter le troisième objectif, nous proposons de prendre en compte le revenu géneré par les modèles de prévision en les entraînant pour maximiser ce revenu au lieu de maximiser leur performance de prévision.

Pour traiter le quatrième objectif de la thèse, nous proposons une approche alternative à l'approche classique qui consiste à combiner des prévisions issues de nombreux modèles de prévision individuels pour obtenir la décision optimale pour chaque option de valorisation. Cette approche alternative utilise des réseaux de neurones artificiels. L'avantage de ces modèles est qu'ils sont capables d'apprendre directement à maximiser le revenu en fonction de l'historique de données et de la forme de la fonction de calcul du revenu. Ils permettent ainsi de traiter n'importe quelle option de valorisations de façon systématique, sans avoir à développer de nombreux modèles de prévisions individuels.

Plan

Le chapitre 2 présente en détail le fonctionnement des marchés de l'électricité, puis introduit les notations géneriques utilisées pour définir les différents solutions proposées. Le chapitre 3 présente en détail le modèle de prévision photovoltaïque développé dans cette thèse. Le chapitre 4 est une première application des solutions proposées pour le cas de la vente d'électricité sur le marché day-ahead seul, ce qui est une simplification de la chaîne de valorisation. Ce cas d'étude permet cependant d'identifier certaines caractéristiques des différents solutions proposées. Le chapitre 5 est une seconde application sur la chaîne de valorisation complète, incluant la possibilité de participer à un marché intra-day, et la possibilité de coupler une centrale avec un moyen de stockage. Finalement, le chapitre 6 tire les conclusions de la thèse et propose des directions de recherche.

Chapter 2

A generic formulation for PV power valorization in electricity markets

Contents

In this chapter we describe the different electricity markets, and propose generic notations to describe the participation in any market. From these notation, we state explicitly the different solutions that we propose to improve the PV power value chain. Parts of this chapter were published in the article [A] in section 1.7.

2.1 Overview of electricity market mechanisms

As explained in chapter 1, we consider PV power trading only through electricity markets, because we do not assume that the producer has consumer clients, or enough clients to cover his production with PPAs. However, electricity markets can differ by several criteria.

The purpose of electricity markets is to anonymously exchange commodities based on electricity generation or power depending on the market, through buying or selling bids. They are defined by their products, that is the definition of the exchanged commodity, but also their timings and their pricing rules. We can broadly define three types of markets for electricity generation:

- Long-term energy exchanges where electricity is sold from a few days up to a few years in the future.
- Day-ahead markets where electricity is sold for the following day.
- Intra-day markets where electricity is traded for the current day.

There are also markets for providing power instead of actual energy generation. The provisions of a given amount of available power are called "Ancillary services" and help TSOs manage the power grid. Markets for ancillary services are also differentiated depending on their timings.

In this section, we propose a detailed explanation of these markets operations.

2.1.1 Long-term energy exchanges

Long-term energy exchanges allow for the trading of electricity derivatives. Derivatives are contracts that derive their value from a given indicator called the underlying. In the case of electricity derivatives, the underlying is generally the electricity spot price. Such markets include EEX in Europe, NYMEX or NASDAQ in the USA, PXE (part of EEX group) in eastern Europe, OMIP in the Iberian Peninsula or KPX in South Korea.

There are usually two major kinds of contracts for electricity derivatives: futures and options. Some other derivatives exist, but they are less commonly traded, such as swaps, strike spread or swing options, tolling and load-serving full-requirement contracts [29].

Futures are the agreement between two parties, the buyer and the seller, to buy (resp. sell) a specific amount of a given product at a specific time in the future and for a price specified in the contract. In most cases, these contracts are cash-settled, which means that at the expiration of the contract, the buyer pays to the seller the difference between the

price specified in the contract and the underlying value. This difference can be positive in which case the seller is paid by the buyer, or negative in which case the buyer is paid. When the contracts are cash-settled, there is no real exchange of goods. As a result, these contracts are generally used as hedging options to be less vulnerable to price variations. For example, an electricity producer could be concerned by a potential decrease of energy spot price. Thus, he would sign a future contract with a buyer to the amount of its production for the minimum price that he would accept to sell its electricity, called the contract price. If the spot price falls lower that this minimum price, the buyer would pay him the difference, and so the seller is guaranteed to get at least the contract price for its electricity, no matter the spot price variations. On the contrary, if the spot price increases, the seller pays the buyer the difference between the spot price and the contract price, and thus gets a lower revenue that if he had not contracted a future. Essentially, power futures are a bet on the variation of the electricity price.

Options are similar to futures. The owner of an option pays a premium to get the right to buy (”call” option) or to sell (”put” option) a specified amount of goods at a future time. They are again hedging options. If an electricity producer suspects that the spot price will decrease, he can buy a ”put” option on its production for the minimum price he can sell its electricity, that is the contract price. Then, at the expiry of the option, if the spot price did decrease, he can use the option to sell its electricity at the contract price. Otherwise, if the spot price increased, he can abandon the option to sell the electricity at the spot price. The difference between futures and options is mainly that with an option, the owner of the option always pays a premium, but gets in return the right to choose if he sells the goods for the spot price or the contract price. As for the futures, these contracts are usually cash-settled, and so there is no actual delivery of electricity.

Futures and options are usually traded for periods ranging from one day to one year. In other words, the product that is sold with such contracts is a constant output of a given amount of power during a one-day to one-year period. This is not convenient for variable energies such as PV power since a constant output requires a storage system and an accurate PV power forecasting model.

There is a possibility to contract physically-settled futures where the fulfilment of the contract is conditioned on the actual delivery of electricity on the grid, but in such cases the future is converted to bids on the day-ahead market for each day of the delivery period. Thus, contracting either a physically-settled future or a cash-settled future then participating in the day-ahead market are equivalent options.

In any case, both futures and options do not give the right to inject the electricity into

the grid. In the end, they are not really a way to valorize the production but a way to hedge the risk for electricity price variations; the only way to get the right to inject energy in the grid is trough physical markets such as the day-ahead or intra-day markets.

2.1.2 Day-ahead markets

Day-ahead markets allow for the trading of electricity for the next day, on an hourly or sub-hourly basis depending on the market. Day-ahead markets are physical, so that any electricity sold on day-ahead market must be injected on the grid. Otherwise, the market participant must pay financial penalties (see 2.1.4). Day-ahead markets usually exist at a national level, or at least at the TSO level. In Europe, the EPEX SPOT market operates the day-ahead market in most of Western European countries. Similarly, the MIBEL market operates the day-ahead market in the Iberian Peninsula, while NORDPOOL operates it in Northern Europe. Examples of national-level day-ahead markets include APX in the UK, CROPEX in Croatia or IEX in India or JEPX in Japan. Examples of day-ahead markets at the TSO-level can be found in the USA with PJM in the East or ERCOT in Texas.

On day-ahead markets, each participant must submit buying or selling bids before the GCT. Then, all the buying and selling bids are combined to derive aggregated demand and supply curves for each MTU of the following day. The intersection of these curves defines the spot market price, which is usually the underlying for power derivatives such as futures and options (see 2.1.1). The calculation of the spot price after the GCT is called the market clearing.

After the spot prices have been calculated, the market participants are nominated for injection on the grid if their bid has been accepted. All selling bids with a price lower than the spot price are fully accepted, and all buying bids with a price higher than the spot price are fully accepted. Since we are interested in the selling of energy, we will always adopt the point of view of an energy producer in the remaining of the thesis.

In any case, all accepted transactions are settled with the spot price, independently of the initial bid. For example, if a market participant accepts to sell up to 1 MWh for 20 €/MWh and then the spot price is 40 €/MWh after clearing, the participant's bid is fully accepted and he gets
1 MWh $\times$40 €/MWh = 40 €. Thus, the revenue of a market participant that sells energy can be written:

$$R = \pi_s E_c \tag{2.1}$$

where π_s is the spot price and E_c is the amount of energy contracted on the spot market.

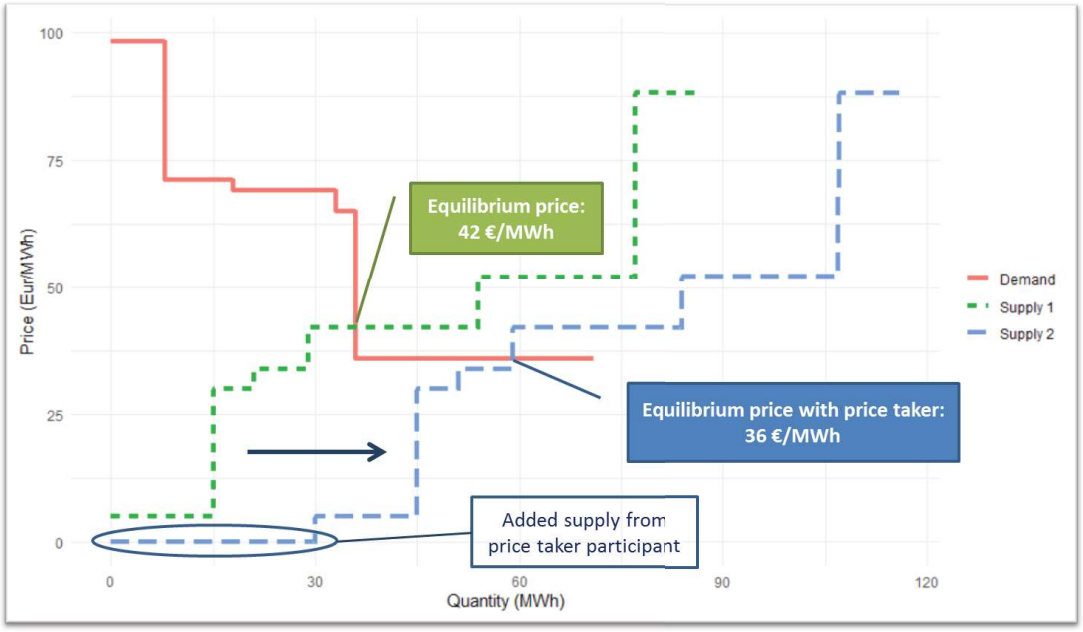

Figure 2.1: Effect of a price taker participant on the clearing price

This revenue is then subject to financial penalties if the actual energy injected is different than the amount sold (see 2.1.4).

In these kinds of markets, it is usual to sell electricity for a price higher or equal to the marginal cost i.e. the unitary cost required to increase the production. In such a case, a participant that sells electricity always generates profit from an accepted bid. However, the marginal cost has no sense for a fatal energy, since there is no cost associated with the production increase because production is completely dependent on the weather. Thus, most variable electricity producers bid following a "price-taker" strategy, that is bid at the minimum allowed price. Thus, they are sure to be accepted since they necessarily have the lower bid, and they are still paid for the spot price. However, bidding at the minimum allowed price lowers the spot price calculated at the clearing because it shifts the supply curve to the right as illustrated on Fig. 2.1. This is why prices tend to be lower when conditions are favorable to renewable energy production resources.

2.1.3 Intra-day markets

Intra-day markets are physical markets that allow trading electricity after the GCT of the day-ahead market. They are especially useful for variable energy sources that can use updated forecasts to correct the positions they took on the day-ahead market.

As for day-ahead markets, intra-day markets are characterized by a MTU, and a closure time. For example, on the EPEX SPOT intra-day market in France, the MTU is the same as the day-ahead market i.e. one hour, and the closure is five minutes before the start of the delivery period.

The pricing can be the same as for day-ahead markets, with an auction mechanism and a settlement price that applies for all participants. However, it is also very common to have continuous markets, where buying and selling bids are matched as they appear, directly using the bid price. This is for example the case on the EPEX SPOT intra-day market in France. Recent research suggested that the penetration of RES on these markets have a non-linear effect on the intra-day market price, and also tend to increase its volatility [30].

2.1.4 Balancing mechanism

At any time, electricity production must match consumption. Thus, after the intra-day market closes, the TSO takes the responsibility to ensure the supply/demand balance by activating or stopping production resources, so that any discrepancy between the consumption and the production at the TSO level is compensated. The period between the closure of the intra-day market and the delivery is called the operational window.

The term "balancing mechanism" refers to the method used by the TSO to ensure the supply/demand balance. The term "balancing market" define the different market-based tools that the TSO can use to perform the supply/demand balancing. Therefore, the balancing markets implement the balancing mechanism. The balancing markets usually include two major components:

- The imbalance settlement rules for the Balance Responsible Parties (BRPs). A BRP is an actor that has to ensure that the supply/demand balance is met on a given perimeter i.e. a set of production and consumption resources. The imbalance settlement rules define the financial penalties that the BRPs have to pay for each difference between production and consumption, called imbalance, on their perimeters. Typically, day-ahead market participants have to be BRPs and their transactions in the electricity market are accounted for in the supply/demand balance of their perimeters (buying energy is counted as an additional production, selling as an additional consumption).

- The balancing service provision, which defines the different markets in which individual actors can offer balancing capacity to the TSO. They include ancillary services, balancing energy or balancing capacity markets.

We will give a brief overview of these components in the following sections.

2.1.4.1 Imbalance settlement

Imbalance settlement rules are different for all TSOs. Still, there are two broad categories: single-pricing and dual-pricing.

In both cases, the penalties are proportional to the imbalance of the BRP, as measured by the TSO. For an electricity producer, the imbalance is the difference between the energy sold and the actual energy produced. The imbalance can be positive when the actual injection is higher than the amount sold. It can also be negative in the opposite situation, that is when the injection is lower than the amount sold. The proportionality coefficient between the imbalance and the penalty is a price derived by the TSO called the imbalance price. As a general rule, the penalties Pen can write:

$$Pen = \pi_B(E - E_c) \tag{2.2}$$

where π_B is the imbalance price, E is the actual energy injected into the grid and E_c is the energy contracted in the day-ahead and intra-day electricity markets.

With single-pricing rules, the balancing price is independent of the sign of the imbalance. On the opposite, with dual-pricing, the balancing price is different for positive and negative imbalances. This has important consequences when combining the penalty formula with the revenue generated on the electricity market from 2.1:

$$\begin{aligned} R &= \pi_s E_c + \pi_B(E - E_c) \\ R &= \pi_s E - (E - E_c)(\pi_s - \pi_B) \end{aligned} \tag{2.3}$$

We can see that penalties can be negative, which means having imbalances can increase the revenue. For example, if $\pi_s < \pi_B$, then any positive imbalance $E - E_c > 0$ would increase the revenue. So when a producer expects the balancing price to be higher than the spot price, then the most profitable bid would be the lowest possible bid allowed by the market. However, this would be very risky because if the balancing price ends up lower than the spot price, the penalties would be very important. Since the balancing prices are very uncertain, it seems difficult to have a trading strategy that relies that much on the balancing price forecast.

With dual-pricing rules, there are actually two balancing prices: one for positive imbalances and one for negative imbalances. Usually, the method used to calculate the balancing prices prevents the situation described previously when penalties are negative. To do so,

	Imbalance settlement pricing mechanism	Imbalance settlement price (imbalance pricing for imbalances that aggravates system imbalance)	Reverse imbalance settlement price (imbalance pricing for imbalances that reduce system imbalance)
Austria	Single	MAX((net cost/GRV); DAM ; IDM) + sign(NRV) * MIN(U_{max}, U_{min} + (U_{max} - U_{min}) * (NRV/V_{max})^2, if NRV > 0 MIN((net cost/GRV); DAM ; IDM) + sign(NRV) * MIN(U_{max}, U_{min} + (U_{max} - U_{min}) * (NRV/V_{max})^2, if NRV < 0 U_{min} = min surcharge, U_{max} = monthly max surcharge, V_{max} = min volume max surcharge	
Belgium	Single, if abs(SI) < 140 MW	MAX(aFRR; mFRR), if NRV > 0 MIN(aFRR; mFRR), if NRV < 0	
	Dual, if abs(SI) > 140 MW	MAX(aFRR; mFRR) + α_2, if NRV > 0 MIN(aFRR; mFRR) - α_1, if NRV < 0 α_1, α_2 = (1/8) * $\sum_{(t-7)}$(SI per ISP)^2/15,000	MAX(aFRR; mFRR) - β_1, if NRV >0 MIN(aFRR; mFRR) + β_2, if NRV <0 β_1, β_2 = 0
France[70]	Dual	MAX((net cost/GRV) * (1+k); DAM), if system is short MIN((net cost/GRV) / (1+k); DAM), if system is long k = 0.08	DAM
Germany	Single	MAX(IDM; sign(NRV) * MIN(abs(net cost/NRV); abs(MAX(FRR; RR))) + surcharge, if NRV > 0 MIN(IDM; sign(NRV) * MIN(abs(net cost/NRV); abs(MAX(FRR; RR))) + surcharge, if NRV < 0 surcharge = sign(NRV) * min(50% * balancing energy price, 100€/MWh), if SI > 80% contracted FRR	
The Netherlands	Hybrid[71]	MAX(aFRR; mFRR; ER) + incentive component, if regulation volume is positive MIN(aFRR; mFRR; ER) - incentive component, if regulation volume is negative incentive component mostly zero	MAX(aFRR; mFRR; ER) - incentive component, if regulation volume is positive MIN(aFRR; mFRR; ER) + incentive component, if regulation volume is negative incentive component mostly zero
Switzerland	Dual	(MIN(DAM; FRR; RR) - P_2) * α_2, if BRP is long & NRV > 0 (MAX(DAM; FRR; RR) + P_1) * α_1, if BRP is short & NRV < 0 P_1 = 10 €/MWh, P_2 = 5 €/MWh, α_1 = 1.1, α_2 = 0.9	(MAX(DAM; FRR; RR) + P_1) * α_1, if BRP is short & NRV > 0 (MIN(DAM; FRR; RR) - P_2) * α_2, if BRP is long & NRV < 0 P_1 = 10 €/MWh, P_2 = 5 €/MWh, α_1 = 1.1, α_2 = 0.9

CE Delft and Microeconomix based on TSO information.
Abbreviations: GRV = Gross Regulation Volume, NRV = Net Regulation Volume, SI = System Imbalance, ER Emergency Reserves.

Figure 2.2: Imbalance settlement rules in some European countries.
Source: Study from CE Delft and Microeconomix [31]

the balancing price is usually higher than the spot price for negative imbalances and lower than the spot price for positive imbalances, so that the penalty term $(E - E_c)(\pi_s - \pi_B)$ is always positive. Figure 2.2 shows the rules used by several TSOs to derive the balancing prices depending on the volumes used for regulation in the operating phase.

When making a transaction on the intra-day market, the revenue from the transaction adds to the amount initially sold, and the volume bought or sold adds to the actual production for calculating the imbalance penalty. The complete revenue of a producer that sells an energy E_c on the day-ahead market, then makes a transaction on the intra-day market of an energy volume E_{ID} (positive when energy is bought, negative when energy is sold) for a price π_{ID} is:

$$\begin{aligned} R &= \pi_s E_c - \pi_{ID} E_{ID} + (E + E_{ID} - E_c)\pi_B \\ R &= \pi_s E + (\pi_s - \pi_{ID}) E_{ID} - (E + E_{ID} - E_c)(\pi_s - \pi_B) \end{aligned} \tag{2.4}$$

2.1.4.2 Balancing service provision

Balancing service provision is organized by most TSOs with markets, where energy producers can offer available power for the TSO during the operational window for remuneration. There is a wide diversity of balancing service provision markets among the TSOs and to avoid focusing on a specific scheme, we do not consider them in this thesis.

Similarly, ancillary services markets are markets where participants can sell supporting services to the TSO called ancillary services. These services are usually categorized between frequency and voltage ancillary services. Frequency services consist in providing the TSO the opportunity to increase or decrease the injection of active power in the grid depending on the grid's frequency deviation. Voltage services consist in providing the TSO the opportunity to increase or decrease the injection of reactive power in the grid depending on the grid's voltage deviation. Voltage ancillary services are not commonly provided with markets, but are often mandatory and remunerated for a fixed price or obtained through yearly tenders.

Ancillary services "products" are defined at a TSO-level and thus are dependent on the localization of the market participants. Still, based on the existing services as defined by TSOs, we can broadly distinguish ancillary services in three categories:

- Frequency Containment Reserve (FCR). This service consists in implementing an automatic control of the active power, proportional to the grid's frequency deviation to its nominal value. The control is made in real-time.
- Automatic Frequency Restoration Reserve (aFRR). This service consists in allowing the TSO to increase or decrease the production of the power plant in a matter of minutes to restore the grid's frequency nominal value when the FCR is not enough. The nomination of the actual service providers that must increase or decrease their power plants injection is generally made by merit-order and is automatic.
- Manual Frequency Restoration Reserve (mFRR). This service is similar to the aFRR, but service providers must increase or decrease their production in a matter of a dozen of minutes. The nomination of the service providers that must modify their production is also made by merit-order and is manual.
- Replacement Reserve (RR). This service is the service that has the longest time of activation, from 15 minutes up to hours. It is intended to release the activated Frequency Restoration Reserves after an incident occurred.

The decision to use an organized market to buy the ancillary services, to buy them through a tender, or to make them mandatory for energy providers and remunerate them at

a fixed price is up to the TSO. Thus, there are no standard ancillary services market, and the procurement mechanisms are very diverse [32]. Still, there is an effort coming from the European Union to standardize ancillary services definitions to allow for implementation of international ancillary services market at the European level. One example of a successful unification of ancillary services products in an European market is the FCR reserve market operated on the platform *regelleistung.net*. On this platform, participants can participate to weekly tenders to provide a given volume of FCR at the European level. However, it is difficult to derive a value for this service for variable sources, because FCR was historically provided by spinning machines operators with a controllable production. Thus, it was very uncommon for the service providers to be unable to provide FCR at a given time. As a result, there are no clear rules on how the participants are penalized if they fail to provide FCR, which gives this system low visibility for variable electricity production resources.

The integration of variable resources in power systems increases the need for ancillary services [33]. Besides, the provision of such services from variable energy sources is difficult because of their uncertainty and their distributed nature, which makes the use of an optimal centralized controller difficult. Still, it is possible for variable energy sources to participate in electricity markets with limited periods of failure [34]. In [35], the authors studied the possibility for a wind power plant to participate in both energy and frequency reserve markets. They found that the relative profitability of energy and reserve markets is the main driver of the wind power plant strategy. Thus, under the current market framework, a profit-driven wind power plant would not always provide ancillary services even if it has the technical possibility to do so. In [36], the authors studied the participation of a Virtual Power Plant (VPP) in a similar joint market. They found that participating in both markets provides an higher revenue, but the probability of failing to provide reserve is still higher for variable energies, especially when going for more profit-driven participation strategies. In [37] and [38], the authors showed that the combination of a variable resource with a storage system can significantly improve the revenue obtained from ancillary services markets.

The penalty price for failing to provide ancillary services is generally estimated using the current penalties for providers of ancillary services that fail to comply with the TSO rules after a technical fault was observed. However, current electricity markets are not quite adapted to variable energies [39], [32]. These markets are still maturing and the future penalty prices or market designs could be different. In [40], the authors find that scheduling the reserve as close to real-time as possible would improve the capability of wind power to provide reserve. Studying the participation of resources with variable production to ancillary markets would then require a supplementary effort of prospective modeling of

the ancillary services market design. Since we want to avoid prospective studies and only consider actual existing valorization processes for PV power, we do not consider ancillary services in this thesis.

2.1.5 Scope

Figure 2.3 summarizes the different markets from long-term exchanges and reserve contractualization up to the balancing market. In this thesis, we will not consider the long-term exchange because it is used as a financial hedging tool and not as a tool to valorize the actual energy with physical injection to the grid.

Ancillary services and balancing service provision markets are also not considered in the thesis, because they lack maturity and clear rules adapted to variable electricity production sources. Thus, we will focus on the combination of day-ahead, intra-day and balancing markets to valorize the energy.

2.2 Generic formulation of the PV energy valorization process

2.2.1 Value chain for PV power trading

At this point, we identified all the market options that are in the scope of the thesis. However, we will also consider storage systems in the value chain as a mean for hedging financial risk. Although it is not a market option *per se*, it can contribute to maximizing PV power value in two ways.

On day-ahead markets, a storage system can increase the PV power value by shifting the production to times where the electricity price is higher. Typically, day-ahead prices are higher at times where the demand is high i.e. in the evening in European countries. They are also low during the day, when demand is generally lower. As a result, a benefit can be obtained by storing PV power in the storage system during the day and discharge the storage in the evening.

During imbalance settlement, the storage system can be used to compensate an imbalance, and thus reduce the penalties paid by the producer. However, this usage of the storage system is concurrent with the usage on the day-ahead market, and so the comparative benefit of these two usages has to be estimated at all times, based on the expectation of both day-ahead and imbalance electricity prices.

Considering all the options that are in the thesis, the value chain for PV production trading can be represented as in Fig. 2.4.

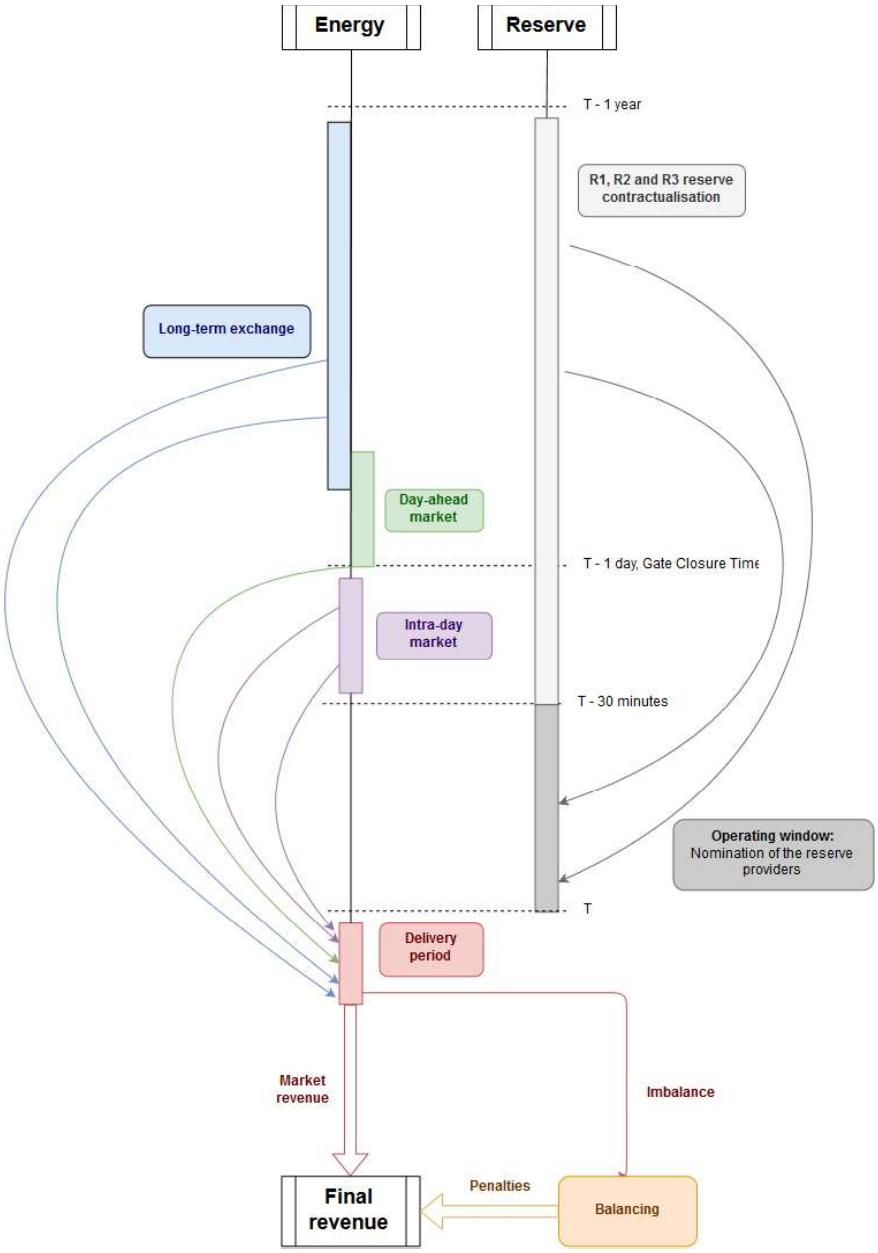

Figure 2.3: Consecutive markets leading to the supply/demand balance for electricity. Several offers can be proposed for the same MTU except on the day-ahead market.

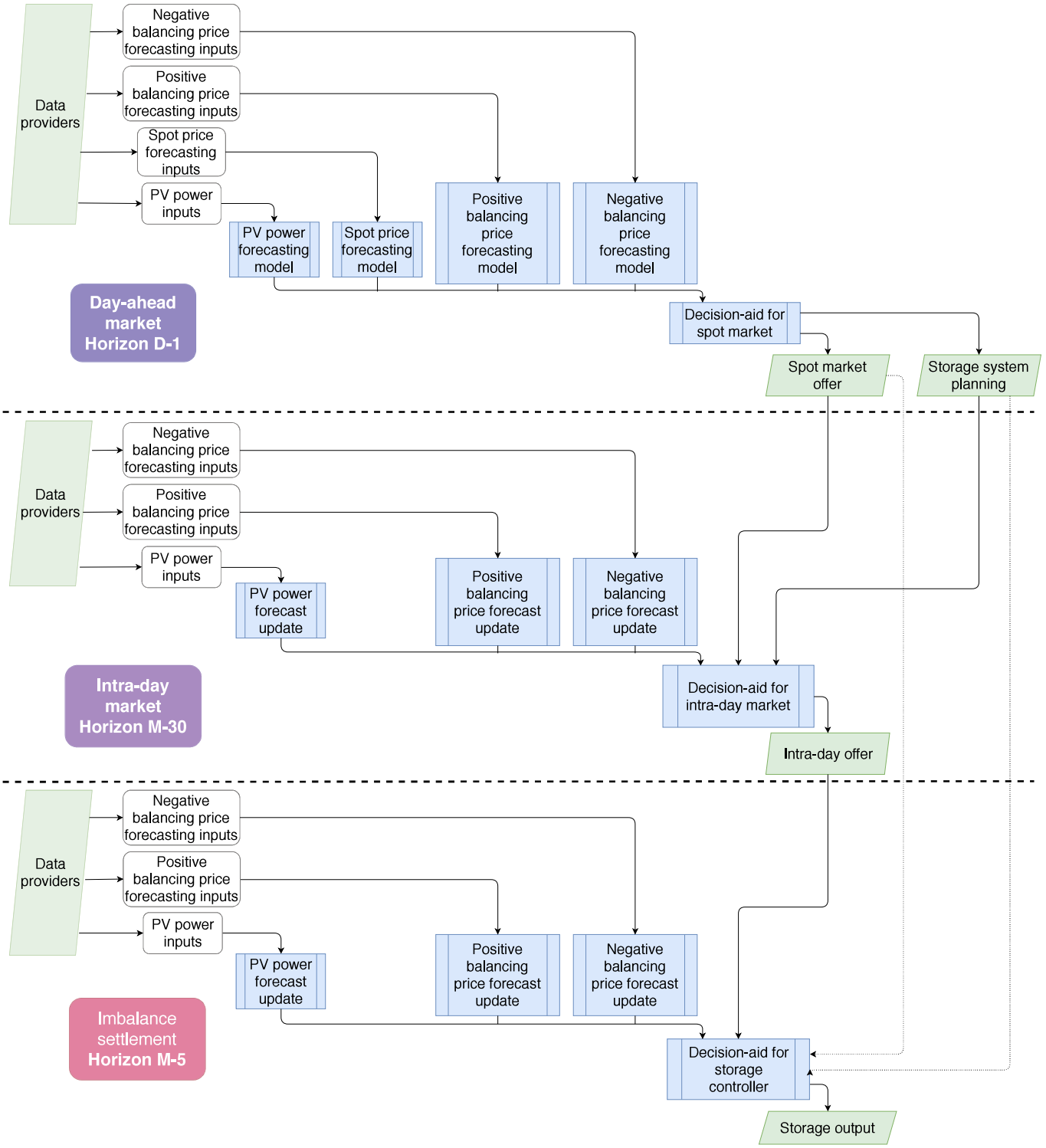

Figure 2.4: Value chain for PV production trading

On this value chain, the systematic issues identified in chapter 1 for trading PV power are clear. The first issue, which is the requirement for seamless PV power forecasting models that can provide good forecasts for any horizon independently from the start time is justified by the need for three different forecast products: one at D-1 for the day-ahead market, one at M-30 for the intra-day market and one a M-5 for the storage system control. This naturally leads to the second issue, which is that the PV power forecasting models must use heterogeneous sources of data in order to have state-of-the-art performance for all required forecast horizons.

The third issue is the gap between individual models performance and overall value generated from PV power. On Fig. 2.4, it is represented by the numerous models that are involved in each decision process, and the fact that each decision relies on the result from the previous decision processes. Besides, decision-aid models can be complex and significantly transform the information given by each of the models they require. Thus, the link between individual models forecast and value of the related decision process is unclear.

Finally, the fourth issue, which is the complexity of the model chain, is represented by the number of required models. Even considering that the PV power forecasting model is seamless, there is still eleven models required (one for PV power forecasting, 7 for market quantities forecasts and three for decision-making).

We identified the issues with the PV power trading value chain that we aim to solve in this thesis. In chapter 3 we will introduce the seamless forecasting model that we developed in order to address the first and second objective of the thesis.

To address the two other objectives, the first step is to introduce a generic notation of the different decision processes so that we can precisely explain how we aim to solve the issues.

2.2.2 Notations

We consider each of the decision processes as an application where a decision $D(X)$ has to be taken conditionally to a set of inputs X. The notation we propose imitates the shape of the decision processes represented in Fig. 2.4, which is always constituted of a set of forecasting models that are combined in a decision-making model. We note as $M_{1,...,n}$ each of these n models and $X_{i,...,n}$. The models can share some of their inputs. Finally, we assume that there is a function T that combines the outputs to obtain the optimal decision. The decision-making process is thus modeled by:

$$D(X_1, ..., X_n) = T(M_1(X_1), ..., M_n(X_n)) \tag{2.5}$$

To completely define each decision process, we propose to add three characteristics:

- A time frame, that is, the time at which the decision must be made and the horizon of the decision.
- The shape of the output, that is the size of the input and output vectors of each process.
- An objective function that can evaluate the reward or penalty obtained from a specific decision.

This notation is generic and can potentially represent any value chain as long as the models M_i and T are defined appropriately. For example, for trading on the French day-ahead market EPEX SPOT without a storage system, the market requires to make a decision everyday at 12 a.m., which is the GCT. Assuming a price taker strategy, the output is a $\mathbb{R}^{24}$ vector corresponding to the offered volume for each hour of the following day. Thus, the decision horizons range from 13 hours to 36 hours. Its objective function is the actual revenue generated from the output defined by equation (2.3). The models M_i are a PV power forecasting model, a positive imbalance price forecasting model and a negative imbalance price forecasting model. The model T is a trading strategy such as the ones proposed in [41] or [42].

The modeling of this value chain with these notations is the first step of the stochastic optimization problem that we have to solve in order to obtain the optimal decision-making function (also called policy). The second step is the design of the policy, that is, how we derive a policy that maximizes the value of the decision. Obtaining efficient policies accounting for uncertainties of the problem is a complex problem for which significant literature exists. Reference [43] proposes an overview of the existing methods to solve such stochastic optimization problems. Recent popular options for stochastic optimization include Reinforcement Learning [44], [45], Approximate Dynamic Programming [46], Robust Optimization (RO) [47], Stochastic Programming [48], or Model Predictive Control (MPC) using a sampled future [**SchildBach2016**].

In this thesis, we will study the participation of a PV power producer in an electricity market. In chapter 4, only the participation in a day-ahead market is considered. In such a case the problem is simple enough that an optimal policy can be derived analytically [41] and so we do not need advanced stochastic optimization methods. We will use either the analytically optimal policy, or a simple Policy Function Approximation (PFA) with a standard ANN to evaluate an alternative modeling of the optimization problem. In a second

case study we will study the participation of a coupled PV/storage system in both an intra-day and a day-ahead market. In this case the policy we want to learn is state-dependent, and so we must use more advanced techniques, that are either MPC with a sampled future or PFA using a Recurrent Neural Network RNN so that the state-dependency can be captured.

In both case studies, the contribution of the thesis is not the stochastic optimization method, since all the methods used are already found in the literature. It is rather in the modeling of the sequential optimization problem that we need to solve. Specifically, we propose two contributions that aim to rely as much as possible on observed data rather than on the problem formulation, and so have data-driven policies.

2.2.3 Reducing the gap between forecast accuracy and value

In the literature, the models involved in a decision process are generally trained to maximize their own performance instead of the value of the related decision. Although some articles studied the link between accuracy and value [49] or proposed indicators taking value into account to evaluate the forecasting performance [50], they did not include the value as an objective during the training phase of the models. In papers proposing data-driven methods with advanced optimization techniques, the actual value of the decision is systematically used to perform the optimization [51], [52], [53]. However, they do not consider how they obtain the forecast state that they use for the optimization method, and so the first step of obtaining the forecast state is not considered in the optimization problem. In this thesis, we propose an alternative training method where we take directly into account the value of the decision during the training, which creates a link between the individual models and the whole decision process. In other words, we include the parametrized function that forecasts the next state in the policy instead of considering only the last step of decision-making as the policy.

To describe this new training approach, we consider that each of the n dedicated models uses a set of parameters $\Theta_{1,\dots,n}$, and we note as $M_i^{\Theta_i}$ the output of the i-th model using the parameters Θ_i.

The standard method where each model is individually trained and the alternative method that we propose in the thesis are represented on figure 2.5.

2.2.3.1 Standard training method

This method, that we call Method 1, consists in separately optimizing the consecutive models M_i. This is the most intuitive approach, as it seems natural that the whole process would perform better if the specific performance of each element of the process were optimized.

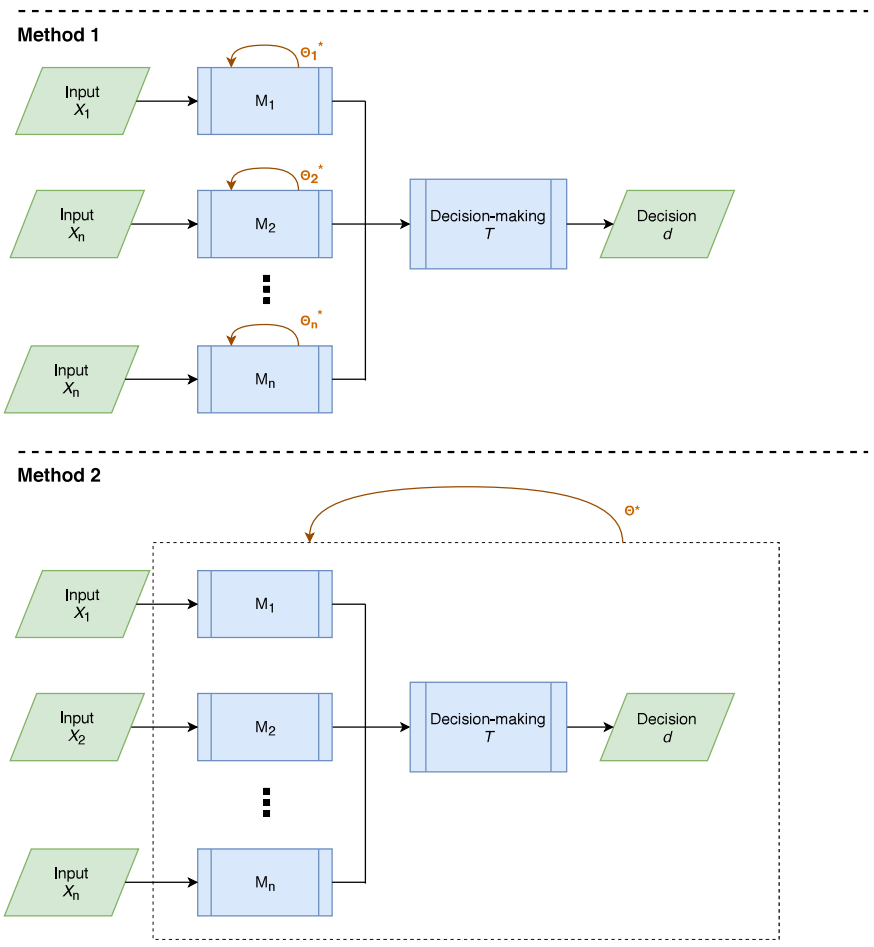

Figure 2.5: Schematic representation of the different methods

To assess the performance of each model M_i, we use the Root Mean Square Error (RMSE) for deterministic quantities and the Continuous Ranked Probability Score (CRPS) for probabilistic quantities. Considering that we have a set of n point forecasts $\hat{x}_i$ or n cumulative distribution function forecasts $\hat{F}_i$, $i \in [1:n]$ of a random variable X, along with their verification values x_i, these criteria are defined as follows:

$$RMSE = \frac{1}{n}\sqrt{\sum_{i=1}^{n}(x_i - \hat{x}_i)^2} \tag{2.6}$$

$$CRPS = \frac{1}{n}\sum_{i=1}^{n}\int_{-\infty}^{\infty}\left(\hat{F}_i(y) - \mathbb{1}(y > x_i)\right)dy \tag{2.7}$$

where function $\mathbb{1}$ outputs 1 if the condition in parenthesis is met, and 0 otherwise. The optimization of the parameters of the whole chain is then performed by identifying

the optimums separately. We note the evaluation function g, which is the RMSE if the evaluated model is deterministic, and the CRPS otherwise. The CRPS and the RMSE are negatively oriented i.e. a lower value indicates a better model.

$$\Theta_i^* = argmin_\theta \left\{ g\left(M_i^\theta \left(X_i \right), Y_i \right) \right\} \tag{2.8}$$

2.2.3.2 Second method: simultaneous optimization

With this method, that we refer to as Method 2, we optimize the whole process globally, using the value of the decision process as the objective function. The rationale behind this optimization is that the individual forecasting models could adapt to each other's forecast errors. For example, if a given model is biased, another model could also acquire a bias to compensate the former. The adaptations that the models could perform on each other are highly dependent on the final objective of the decision process. We assume that we have a function $Eval$ that evaluates the value associated with the decision $D(X_{1,...,n})$.

Noting as $\Theta = \{\Theta_1, ..., \Theta_n\}$ the set of parameters that gathers all of the parameters of the individual models, the optimization problem we must solve in this method is thus:

$$\begin{aligned} \Theta^* &= argmax_{\Theta=[\Theta_i,...,\Theta_n]} \left\{ Eval(D(X_{1,...,n})) \right\} \\ \Theta^* &= argmax_{\Theta=[\Theta_i,...,\Theta_n]} \left\{ Eval\left(T\left(M_1^{\Theta_1}(X_1), ..., M_n^{\Theta_n}(X_n) \right) \right) \right\} \end{aligned} \tag{2.9}$$

2.2.4 Simplifying the model chain

The last objective of the thesis is to simplify the chain value, which involves a lot of models. To do so, we propose an alternative approach for providing the decision. In the literature, the stochastic optimization problems rely on an informed modeling of the decision process, by defining sequential forecasting models that provide a forecast state based on which the policy derives the optimal decision. We propose an alternative modeling where all the sequential models leading to the policy are dropped, and the state used by the policy is directly the union of the inputs used originally by the sequential forecasting models. Instead of using the forecasting models M_i and the decision-aid model T introduced in 2.4, we use a single model M. This model plays both the role of the individual models M_i and the decision-aid T, and so directly provides the decision. In this case, the decision-making is only made based on data, which makes This unique model M should then:

- Use the union of all the inputs X_i as input.

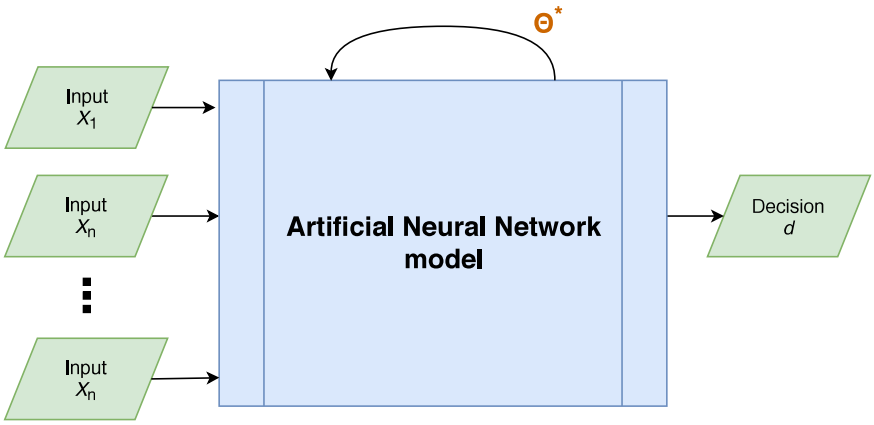

Figure 2.6: Schematic representation of the alternative approach

- Provide a decision with the appropriate shape.
- Be trained using the decision evaluation function *Eval* since it directly provides the decision.

This setup suggests using an ANN as the unique model, since ANNs are very flexible in terms of input and output shape, and can learn any nonlinear function and thus maximize the value of any decision-making process.

Note that in that case, the two proposed training approaches are the same, since the individual model performance is the same as the decision-process value. This is represented on Fig. 2.6 that represents the alternative we propose for trading PV power.

2.3 Summary

In this chapter we gave an overview of the electricity market mechanisms that exist, and identified the ones that are in the scope of this thesis to define the value chain for trading PV power. This value highlighted the systematic issues that we identified in chapter 1 for RES power trading.

The first and second issues are the need for a seamless PV power forecasting model, which will be presented in chapter 3. We proposed some generic notations to precisely explain how we propose to tackle the third and fourth issues, that are a different method for training the forecasting models involved in the decision processes, and an alternative decision-making approach that bypasses the need for individual forecasting models by performing the whole decision-making with an ANN.

Chapter summary in French

Marchés de l'électricité

Comme nous l'avons présenté dans le chapitre précedent, nous étudions la valorisation de l'énergie PV via les marchés de l'électricité. Ce terme génerique désigne plusieurs types de marchés, chacun défini par leurs horaires ou la nature exacte des produits échangés. On peut définir globalement trois types de marchés pour l'énergie : les marchés à terme, les marchés "day-ahead" et les marchés "intra-day". Il existe également des marchés de services système déstinés à échanger de la réserve de puissance.

Les marchés long-termes ne permettent pas à proprement parler d'échanger de l'énergie, mais d'échanger des dérivés financiers indexés sur le prix de l'électricité, permettant de mitiger le risque lié à la variation imprévue du prix de l'électricité. En ce sens, ils ne permettent pas de valoriser la production dans le sens où ils n'autorisent pas à injecter la production, les transactions étant purement financières. Il est néanmoins possible de vendre des contrats long-terme avec obligation de livraison physique, auquel cas le contrat long-terme est simplement traduit automatiquement jour par jour en offre sur le marché day-ahead. Autrement dit, il est équivalent de vendre un contrat long-terme pour un mois donné, ou de vendre jour par jour la quantité équivalente au contrat long-terme sur ce même mois sur le marché day-ahead.

Sur le marché day-ahead, l'électricité est vendue pour le lendemain. C'est un marché organisé, ce qui signifie que les offres de vente et d'achat de tous les participants du marché sont receuillis avant une certaine heure pour construire les courbes d'offre et de demande. L'intersection de ces deux courbes détermine le prix spot. Les offres de vente à un prix inférieur au prix spot et les offres d'achat à un prix supérieur au prix spot sont acceptées, et toutes ces transactions sont effectuées au prix spot. Les participants sont en géneral financièrement responsable de l'écart entre leur production vendue et réalisée. Le prix auquel cet écart est pénalisé est défini par le gestionnaire de réseau en fonctions des moyens d'équilibrage qu'il a du mettre en oeuvre pour compenser les écarts, et ne dépend donc pas du marché.

Finalement, il existe un marché intra-day sur lequel les participants peuvent soumettre des offres de vente ou d'achat d'énergie à tout moment pour la journée en cours, jusqu'à une certaine durée avant l'heure de livraison (30 minutes en France). A la différence du marché day-ahead qui est un marché organisé, le marché intra-day fonctionne en "continous trading" : dès qu'une offre d'achat et de vente se correspondent en termes de volume et de prix, la transaction est acceptée, au prix d'offre.

De façon génerale, le revenu d'un partipant qui a vendu une quantité E_c en day-ahead et une quantité E_{ID} sur le marché intra-day au prix π_{ID} s'écrit :

$$R = \pi_s E + (\pi_s - \pi_{ID})E_{ID} + (E + E_{ID} - E_c)(\pi_B - \pi_s) \tag{2.10}$$

Où π_s est le prix spot calculé par le marché, et π_B le prix de réglement des écarts calculé par le gestionnaire de réseau.

Bien que des marchés de service système existent, il n'existe pas de définition standardisée pour les produits échangés et les horaires. Par conséquent, nous ne les étudions pas dans la thèse, bien que le formalisme proposé pour étudier les autres options se prête également à l'étude de marchés de service système.

Notations

Nous introduisons ici des notations pour expliciter les solutions que nous proposons pour traiter les problèmes strucurels de la chaîne de valorisation identifiés dans l'introduction. De façon génerale, on peut remarquer que chacune des options de valorisation est définie par trois éleménts:

- Un cadre temporel, c'est-à-dire l'heure à laquelle la décision doit être prise et l'horizon de la décision. Par exemple pour la vente en day-ahead, la décision doit être prise à midi le jour précédent, avec un horizon de +12h à +36h selon l'heure de la journée suivante pour laquelle on vend de l'énergie.
- La taille du vecteur de décision d.
- La fonction de valeur de la décision, qui associe à un vecteur d la valeur de la décision $Eval(d)$.

De cette façon, on peut noter chaque processus de prise de décision comme la combinaison d'une série de n modèles prédictifs, de sorte que la sortie ait la taille adéquate. La fonction qui combine la sortie des différents modèles est notée T. Chaque modèle étant paramétré par un ensemble de paramètres Θ, on les note $M_i^{\Theta_i}$, la décision optimale s'obtient depuis les données d'entrée X_i par:

$$d = T(M_1^{\Theta_1}(X_1), M_2^{\Theta_2}(X_2), ..., M_n^{\Theta_n}(X_n)) \tag{2.11}$$

On peut alors expliciter les solutions que nous proposons pour traiter les objectifs de la thèse. La première solution est d'entraîner les modèles individuels pour maximiser la valeur de leur décision au lieu de leur performance de prévision :

$$\Theta^* = argmax_{\Theta=[\Theta_i,\ldots,\Theta_n]} \{Eval(d)\} \tag{2.12}$$

Cette méthode d'entraînement se substitue à la méthode classique qui consiste à maximiser la performance des modèles de prévision individuels :

$$\Theta_i^* = argmin_\theta \left\{ G\left(M_i^\theta \left(X_i \right), Y_i \right) \right\} \tag{2.13}$$

Où G désigne une fonction d'évaluation de performance des modèles de prévision e.g. le RMSE pour les prévisions déterministes ou le CRPS pour les prévisions probabilistes.

La seconde solution que nous proposons dans cette thèse consiste à remplacer les différents modèles de prévision individuels M_i par un unique réseau de neurones artificiel noté M qui prend à la fois le rôle des modèles de prévision individuels et celui du modèle de prise de décision T. Dans ce cas, les deux méthodes d'entraînement sont équivalentes, puisque le modèle donne directement le vecteur de décision d et donc l'entraîner pour sa performance individuelle ou la valeur génerée par sa décision revient au même.

Pour traiter les autres objectifs de la thèse, il est également nécessaire de développer un modèle spécifique de prévision de la production photovoltaïque. Ce modèle est présenté dans le chapitre suivant.

Chapter 3

Seamless PV power forecasting model

Contents

In this chapter we introduce the seamless forecasting model that we developed to tackle the first and second objectives of the thesis. This model can start at any time of the day for any horizon, and thus can be used seamlessly in a chain of decision-making processes for trading PV power. Parts of this chapter were published in article [C] in section 1.7.

3.1 Required properties of the PV power forecasting model

Since the different decision-making processes involved in the PV power trading value chain have different timings, our goal is to have a seamless PV power forecasting model, that is a model that can provide forecasts for several different time frames. More precisely, the model should provide forecasts at any time of the day, for horizons ranging from quasi-real-time to day-ahead, and with any forecast resolution. The algorithm should also be as fast to compute as possible, so that it suffers few operational constraints and thus can be used in any part of the value chain.

Besides, the PV power forecasting model should also reflect the uncertainty of the upcoming PV power in some way, because knowing this uncertainty gives additional information to the decision-aid model and ultimately results in better trading performance, and so forecasts accompanied by uncertainty evaluation is generally recommended [54]. Early examples of trading considering uncertainty can be found in [55] or [56]. Using probabilistic (upcoming PV power as a probability distribution) forecasts rather than deterministic is a convenient way to convey information on the uncertainty. Probabilistic forecasts have more properties than deterministic ones e.g. reliability, sharpness or resolution. Different properties can be required depending on the actual application of the forecasts [57].

The evaluation of probabilistic forecasting models is more complex than deterministic ones, since they have more characteristics and properties. In [58], the authors proposed a first approach for evaluating forecasts with uncertainty. In [59], the authors proposed a paradigm to evaluate probabilistic forecasting models, which is of *"maximizing the sharpness of the predictive distributions subject to calibration"*. Here, calibration refers to a property that is also frequently called "reliability" in the literature. In the remainder of the thesis, we will always use the term "reliability" to refer to this notion. Reliability and sharpness have been extensively studied in the literature (see references [59], [60], [61] or [62]).

Reliability is defined as the consistency between the quantiles obtained from a forecast

distribution and the actual quantiles obtained from the data. For example, if we have a forecast Cumulative Distribution Function (CDF) $\hat{F}$, we can define the $\hat{q}_\alpha$ quantile of level $\alpha \in [0, 1] \subset \mathbb{R}$ as:

$$\hat{q}_\alpha = \hat{F}^{-1}(\alpha) \tag{3.1}$$

Then a probabilistic forecasting model is reliable if the proportion of observations that fall below $\hat{q}_\alpha$ is exactly α given a theoretically infinite set of historical observations.

Sharpness relates to the ability of the model to differ from climatological forecasts. Climatological forecasts provide as forecasts the empirical quantiles, which are observed from an historical set of observations. The need for defining the sharpness characteristic arises from the fact that a climatological forecast is reliable. However, the Probability Distribution Function (PDF) is always the same since the empirical quantiles are always the same given a set of observations. Thus, climatological forecasts convey almost no predictive information.

On the other hand, a sharp model can concentrate the probability information that is uniformly distributed on the set of possible values in a climatological forecast. Thus, a sharp model have smaller Prediction Intervals (PIs) i.e. an interval in which a future observation is expected to fall with a given level of confidence, than a climatological forecast. The sharpness characteristic relates to the size of the PIs of the predictive PDF, which in turn relates to the confidence one can have in a given forecast.

The resolution is another notion used for the evaluation of the forecasts. Resolution refers to the ability of the model to provide different forecasts when the predictors are different. It is easy to see that a climatological forecast has no resolution since the empirical quantiles are not conditioned by any predictors.

It is always possible to recalibrate the forecasting models to be reliable, while sharpness and resolution are inherent properties of the model. Besides, calibration methods to make a model reliable can alter its sharpness and resolution properties. Thus, reliability is often seen as a pre-requisite for probabilistic forecasts, while sharpness and resolution are indicators of the value of the models. In the remainder of the thesis, we will only consider the reliability and sharpness characteristics, following the paradigm of maximizing the sharpness subject to calibration [59].

There are two examples that illustrate the properties of reliability and sharpness fairly well: climatological forecast and deterministic forecasts.

Climatological forecasts provide the empirical quantiles as the forecasts. Empirical quantiles are the quantiles directly estimated from observations. Formally, assuming that

we have a set of n observations $I_1, ..., I_n$ of the solar irradiance, and noting $I_{(1)}, ..., I_{(n)}$ these same observations sorted in ascending order, the quantile of level $\alpha \in [0, 1]$ estimated by the climatological forecast, noted q_α^{clim}, is given by :

$$q_\alpha^{clim} = \begin{cases} I_{(n\alpha)} \text{ if } n\alpha \text{ is an integer} \\ I_{([n\alpha]+1)} \text{ otherwise} \end{cases} \tag{3.2}$$

With $[n\alpha]$ being the integer part of $n\alpha \in \mathbb{R}$. The quantile q_α^{clim} is referred to as the empirical quantile of level α.

Since empirical quantiles converge exponentially with respect to n towards the real quantile of the distribution, this model has excellent reliability when the number of observations is high. However, by definition, climatological predictions have no sharpness.

On the other hand, an unbiased deterministic forecast can be considered as an example of a model with good sharpness but no reliability. We assume that we have forecasts obtained from a regression model as follows:

$$\hat{I} = I + \epsilon \tag{3.3}$$

$$\tag{3.4}$$

Where ϵ denotes the residuals of the model. These forecasts can be considered to also provide predictive distributions with $\hat{f}(x) = \delta(x - \hat{I})$, where δ is the Dirac distribution. The estimated quantiles are therefore all equal to the deterministic forecast $\hat{I}$. For any quantile q_α of level $\alpha \in [0, 1]$, we have:

$$P(I < q_\alpha) = P(I < \hat{I}) = P(\epsilon > 0) \tag{3.5}$$

Since the model is unbiased, the residuals distribution is symmetric around 0, and thus $P(\epsilon > 0) = 0.5$. The reliability of the model is therefore extremely low, since for a reliable model, we must have $P(I < q_\alpha) = \alpha$. However, the sharpness of the model is very high by definition.

3.2 Model choice

The state of the art in solar power forecasting developed rapidly in recent years. It benefited from the wind power forecasting field, which is more mature [63], with a wealth of methods being proposed since the 1980s (see for example [64], [65] or [66]). Wind power and PV

power forecasting shares a lot of methods and algorithms, as they both have close links with meterorology and weather forecasting.

In [67], the authors provide a fairly complete literature review of research in the PV power forecasting field. Generally, the features used as inputs are largely dependent on the forecast horizon. Short-term forecasting (0-6 hours) mostly employs endogenous data, although input from Numerical Weather Predictions (NWP) and meteorological records can be used [68]. Works considering satellite imagery have been appearing for several years, e.g. [69] and[70], while data from neighboring PV plants can be employed in spatio-temporal models [71], [72]. Data from sky imagers are also useful for the very short term (up to a few minutes) [73], but harder to apply as they require significant preprocessing work. For the medium-term (up to few days ahead), forecasts mostly rely on NWPs. However, NWP tend to overestimate solar irradiance, resulting in biased forecasts. Alternative NWP models are sometimes proposed to correct this effect [74]. To produce probabilistic forecasts, an increasing number of papers use ensemble forecasts, that provide several possible weather trajectories by perturbing the initial conditions [75], [76]. The relevance of the different sources of data depending on the temporal and spatial resolution of the forecasts is represented on figure 3.1.

Regarding forecasting techniques, linear auto-regressive models are popular, as they are fast to train, are not computationally intensive, and can issue forecasts at any time of the day without multiplying the number of models [78]. Numerous machine learning models are also used, such as ANNs [78], Support Vector Machines (SVM) [79], or gradient boosting (GB) [80]. Recently, several new methods have emerged. The Extreme Learning Machine (ELM) is a fairly popular variant of ANN [81], [82], [83]. Gaussian Process Regression (GPR) [84] and Markov Chain (MC) [85] models are also becoming more frequent in the literature. Another approach is to combine the output from different forecasting techniques in order to get a more accurate forecast [86]. This usually results in higher accuracy and uncertainty representation, at the cost of a higher computational and maintenance cost to train all the models.

The global forecasting competition GEFCOM 2014 [87] showed that the most efficient algorithms were often non-parametric, such as Quantile Regression Forests (QRF) [88] and GB [89]. This tendency is also observed in [90]. However, [91] performed a comparison of several non-parametric models and found that the performance difference between each other was low. Thus, there are now other criteria than accuracy that matter in the model choice. Among the trending models for both wind and PV power forecasting, we can cite approaches based on analogy that offer a high computational performance [92], [93], hier-

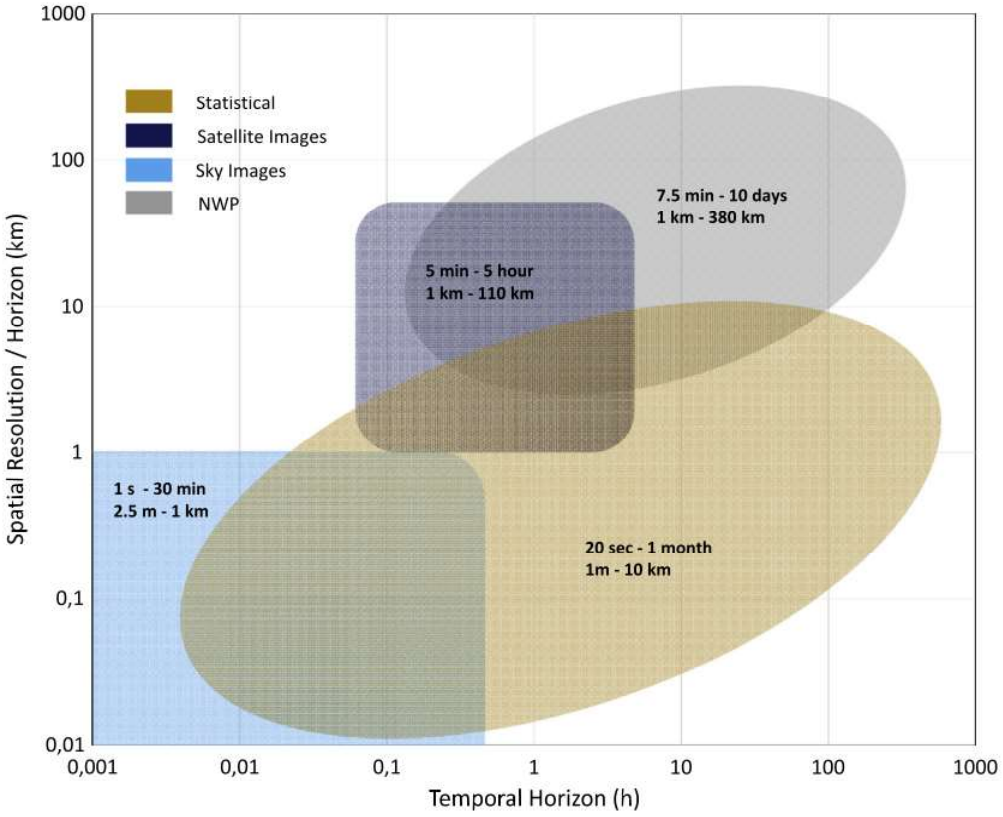

Figure 3.1: Relevance of the different sources of data for PV power forecasting depending on the temporal and spatial resolution of the forecasts.
Source: Antonanzas et al., 2016 [77]

archical forecasting methods that can provide consistent forecasts accross time resolutions [94], [95], and Stochastic Differential Equations (SDE) that offer a high flexibility and adaptative behavior [96], [97], [98].

To achieve our goal of attaining good performance for any time frame, the proposed model must be able to use all of the data mentioned above, depending on the forecast horizon. Regarding the choice of the model, we based our approach on models from the Analog Ensemble (AnEn) family, which have the dual advantage of being lightweight compared to other models and of naturally providing non-parametric probabilistic forecasts.

The baseline AnEn model that is extended in this thesis was described in [99], where past NWPs are used to forecast 10-m wind speed and 2-m temperature. In [100], the authors implemented a model in which they also looked for analogs using NWPs, but applying a different metric than that of [99]. In [101], the authors used the AnEn model to forecast

probabilistic PV power for three large power plants. They emphasized the very low computational time needed to produce the forecasts compared to other models. Several papers have also proposed corrections or adaptations of the AnEn model to obtain better forecasts. In [102], the authors proposed a modification of the Euclidian distance frequently used as a metric to evaluate analogs and used measures along with NWP to search for analogs. This reduced the forecast horizon, making it necessary to run the model multiple times to obtain a complete forecast. In [103], a 20% improvement over the standard AnEn model with a brute-force optimization of the parameters was demonstrated. Several algorithmic variations of the AnEn ensemble, along with a dynamic way of selecting the number of analogs to be retained in the ensemble, and a wrapper method to dynamically optimize the model parameters, were proposed in [104]. In [105], the authors extended the AnEn model with an ANN which significantly improved the forecasts. Finally, [70] proposed an Analog method to produce short-term forecasts of solar irradiance using geostationary satellite images only.

In this thesis, we contribute to the research on AnEn models by addressing several drawbacks of the current implementations. In previous works, most of the time only NWPs are used, and thus forecasts are always the same until a new NWP run is available. It is thus not possible to use state-of-the-art model settings in an intra-day configuration. Besides, although some papers have used data other than NWP in an AnEn setting, no model has used both NWP and other sources of data. Moreover, previous works do not present how they generate probabilistic forecasts from analogs.

3.3 The proposed PV power forecasting model

3.3.1 Model description

The aim of the AnEn model is to generate a set of past observations considered similar to the situation we want to forecast, and use this set to build the forecast density. Initially we generate an N_{An}-member ensemble for a given lead-time by computing a metric between the situation to forecast and all of the past situations. Then we select the N_{An} most similar to past situations and look for the PV power measured at the time of these similar situations. These N_{An} measures constitute the analog ensemble, and each analog can be seen as a sample from the probability density function of the PV power. In the most general formulation of the metric taken from [99], only NWPs were used as inputs. The metric used in this thesis is based on the one defined in [99] but it is adapted to allow different sources of data to be considered. The distance between an instant t for which a forecast is requested and another instant t' in the past is written as follows:

$$D_{AnEn}(\mathbf{X}_t, \mathbf{H}^h_{t'}) = \sum_{i=1}^{N_v} w_i^h \sqrt[p]{\sum_{j=-k}^{0} (\mathbf{X}_{i,t+j} - \mathbf{H}^h_{i,t'+j})^p} \tag{3.6}$$

where N_v is the number of features used as input, h is the forecast horizon (that is, the difference between the time t and the time when the forecasting model is run) and k is a parameter that indicates the length of the time window over which the metric is computed. The parameter p controls the penalization of large differences in the predictors at times t and t'. $\mathbf{H}^h$ and $\mathbf{X}$ are two sets containing the features and input of the model. The set $\mathbf{H}^h$ contains features from NWP and clear-sky data, along with the measures and the satellite data lagged h times. This set is dependent on the horizon of the forecast. When we make a forecast with horizon h, the latest measurements and satellite data were observed h time steps ago, and this should be reflected in the historical data set. Following through, $\mathbf{X}$ contains the NWP for time t and the latest measures and satellite data, observed at time $t-h$. $\mathbf{H}^h$ and $\mathbf{X}$ are scaled and centered, so that each variable contributes to the metric with the same proportion. Thus, only the weights w_i^h can control the relevance of each feature. The weight calculation takes into account the forecast horizon and is presented in the next sub-section.

To our knowledge, previous papers did not present how they generated the PDF from the analogs. In this thesis, the PDF is built with a weighted Kernel Density Estimation (KDE), using the metric value of each member as its weight in the distribution. Given a set of N_{An} AnEn members e_i, which are energy generation observations made at a time when forecasts from the past were similar to the current observations according to the AnEn distance, and their distance values $D_{AnEn,i}$, the PDF $\hat{f_{PV}}$ is estimated by:

$$\begin{aligned}\hat{f}_{PV}(x) = \frac{1}{\sum_{i=1}^{N_{An}} s_i} \sum_{i=1}^{N_{An}} \frac{s_i}{bw} \Bigg[& K\left(\frac{x - e_i}{bw}\right) + K\left(\frac{x + e_i}{bw}\right) \\ & + K\left(\frac{x + e_i - 2E_n}{bw}\right) \Bigg]\end{aligned} \tag{3.7}$$

$$s_i = \left(\frac{\sum_{j=1}^{N_{An}} D_{AnEn,j}}{D_{AnEn,i}} \right)^2 \tag{3.8}$$

$$K(x) = \frac{3}{4}(1 - x^2)\mathbb{1}(|x| <= 1) \tag{3.9}$$

$$bw = \left(\frac{4\hat{\sigma}_e^5}{N_{An}} \right)^{1/5} \tag{3.10}$$

where E_n is the maximal energy generation of the plant over a time step, the s_i terms are similarity measures inversely proportional to the distances, K is the Epanechnikov kernel,

and bw is the bandwidth of the kernels, derived by the Silverman's rule of thumb [106]. $\hat{\sigma}_e$ is the empirical standard deviation of the AnEn members. The first Epanechnikov evaluation corresponds to the kernel centered around the i-th AnEn member value, and the two others are there to ensure that the integral of the distribution is 1 between 0 and E_n. Outside this range, the PDF is set to 0.

As can be seen from Figure 3.1, the different sources of data that must be considered in order to have good performance in both intra-day and day-ahead forecasts are variables from NWP, in situ measurements, clear-sky profile, and spatial data derived from satellite imagery. We should also have used images from sky-imagers but such data was not available. The clear-sky profile is an estimation of the solar irradiance on the ground assuming that there are no clouds. Following these notations, the integration of a clear-sky profile and local measurements is pretty straightforward. However, satellite data is more complex because they have many more features, which require pre-processing in order to reduce their dimension. The required additional processing work will be detailed in Section 3.3.2.

The calculation of the feature-weights is critical. In previous works [103], [107], [104], these were obtained from an off-line optimization for each power plant and remained the same throughout the testing period. In these cases, a measure of the probabilistic performance of the models was used as the optimization objective. In this thesis, we do not use the final performance as a criterion, but we propose a dynamic way to estimate weights based on the most recent data, since the model operates in a sliding window scheme and the weight of the latest measurements will not be the same for a forecast started at noon as for one started at midnight. The criterion used to quantify the weights is Mutual Information (MI), which comes from the information and communication theory [108]. It has been used in machine learning for feature selection [109]. This is a measure of how much the fact of knowing a variable reduces the uncertainty of another variable. The MI between two random variables X and Y, knowing their respective marginal density distributions p_X and p_Y and their joint density distribution $p_{X,Y}$, is:

$$MI(X,Y) = \int\int p_{X,Y}(x,y) log\Big(\frac{p_{X,Y}(x,y)}{p_X(x)p_Y(y)}\Big) dxdy \tag{3.11}$$

The main reason for choosing this criterion rather than simpler ones, e.g. Pearson's correlation, is because it can identify non-linear relationships between random variables. As we are dealing with both features that are strongly and almost linearly correlated to the production (clear-sky profile, last production measurement), and features that are not (temperature from NWP), using a linear correlation criterion would overestimate the weight of the former over the latter. On the other hand, the MI calculation identifies the non

linear information contained in the variables and thus avoids giving significant weights only to variables that are linearly correlated with the PV production such as solar irradiance forecasts.

The weight calculation is carried out in two steps. The first step evaluates the relevance of each variable individually by calculating its MI with the measured power according to (3.11). Computing the MI is not trivial, since it requires formulation of both the marginal and joint distributions of the random variables. We implemented a simple method involving a discretization of the random variables prior to calculating the MI. The discretization algorithm is described in [110]. The MI is finally computed as follows:

- First, discretize the random variables X and Y in n bins, so that each bin has the same number of observations.
- Then, compute the discrete probabilities of the couple of events (A_i, B_j), with the events being defined as A_i: "X is in the i-th bin" and B_j: "Y is in the j-th bin", for all possible values of i and j. These probabilities are simply computed by counting the occurrence of the events.
- Finally, apply the discrete formula for computing the MI:

$$MI(X,Y) = \sum_{i=1}^{n}\sum_{j=1}^{n} p(A_i,B_j) log\left(\frac{p(A_i,B_j)}{p(A_i)p(B_j)})\right) \tag{3.12}$$

The second step sets a limit on the total cumulative weight of each source of data. If such a limit is not set and all the weights are computed independently for each feature, some features are over-represented, because they are highly colinear. In particular, the features from the satellite data are highly redundant. If we compute their weights independently, they all have significant weights. This strongly overestimates the relevance of these features. By reorganizing the features into groups, we can first compute a global weight for each group that will represent the total allowed contribution from this group. Then, the weights computed independently for each feature are normalized so that the cumulated contribution of each group of features does not exceed the global weight for this group.

In a more formal way, the weights are computed as follows. In the first step, intermediate weights $w'_{i,h}$ are obtained by equation (3.13), for each feature i and forecast horizon h. E_{PV} is the time series of energy generation measurements.

Then, the weights are normalized. In practice, the features variables are organized into N_s subsets depending on their source (NWP, measures, satellite data, clear-sky profile). The sets $S_v, v \in \{1, ..., N_s\}$ contain the indexes of the features contained in each of the N_s

sets, corresponding to each data source. A global weight $W_{S_v,h}$ is attributed to each of these sets, and for each horizon. We then obtain the final weights with (3.14).

$$w'_{i,h} = MI(\mathbf{H}_i^h, E_{PV}) \tag{3.13}$$

$$w_{i,h} = \left(\frac{(w'_{i,h})^q}{\sum_{v=1}^{N_s} \mathbb{1}(i \in S_v)(w'_{v,h})^q} \right) \sum_{v=1}^{N_s} \mathbb{1}(i \in S_v) W_{S_{v,h}} \tag{3.14}$$

The parameter q controls the relative contribution of the different weights to the metric and is optimized during the training. The computation of $W_{S_v,h}$ should be done taking into account redundancy between variables from the same source. This is especially important for satellite data where the variables are strongly colinear. We propose to use:

$$W_{S_v,h} = max_{i \in S_v} \{w'_{i,h}\} \tag{3.15}$$

This means that each source of data contributes to the metric as much as the weight of its most informative feature does. As a result, we may underestimate the information conveyed by variables that are not strongly correlated to the PV production, but we will not overestimate the global contribution of a source of data that contains numerous colinear variables, since the individual weights of the redundant features will not add up to more than the weight $W_{S_v,h}$ of their source.

Fig. 3.2 shows the average weights obtained for each type of data and for different time horizons. For every forecast, all features that have non-zero weights for the given forecast horizon are used. The weights represented on Fig. 3.2 are averaged over all starting times but, when observing forecasts always made at the same time as on Fig. 3.3, they are different. For example, when focusing on the forecasts made at 12 a.m. only, the weight given to the latest measurement is near zero, as it is not informative.

The values of the weights of the different sources correspond well with results reported in the literature concerning which source of data is informative for which horizon. The most recent power measurement is very informative for the first few time steps, but its weight decreases quickly. NWPs are always relevant, but even more for day-ahead purposes. For horizons shorter than 4 h, they carry less information than the latest measurements and the satellite data. Satellite data are very useful up to 6 h, even though their value decreases steadily. Equally of interest, the clear-sky profile is useful almost only for the beginning and end of the day, when it becomes the most important feature as can be seen on 3.3. It is not surprising to see that for these instants with very low incoming irradiance even in clear-sky conditions, the amount of solar power is not dominated by the presence of clouds, but by the Sun's path.

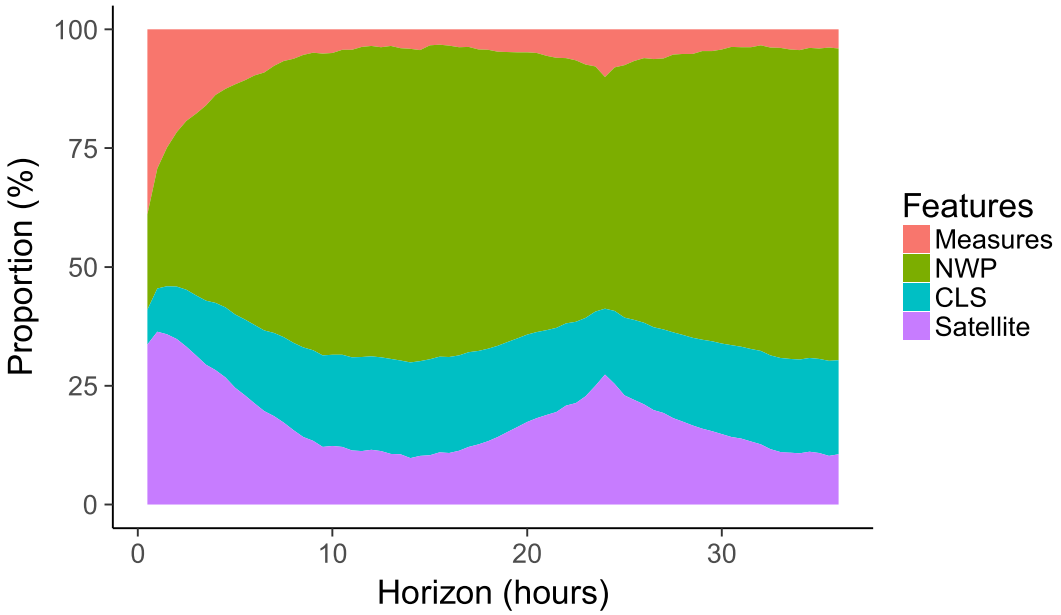

Figure 3.2: Proportion of the different sources of data weights depending on the forecast horizon, averaged over all forecasting times. "CLS" refers to the clear-sky profile.

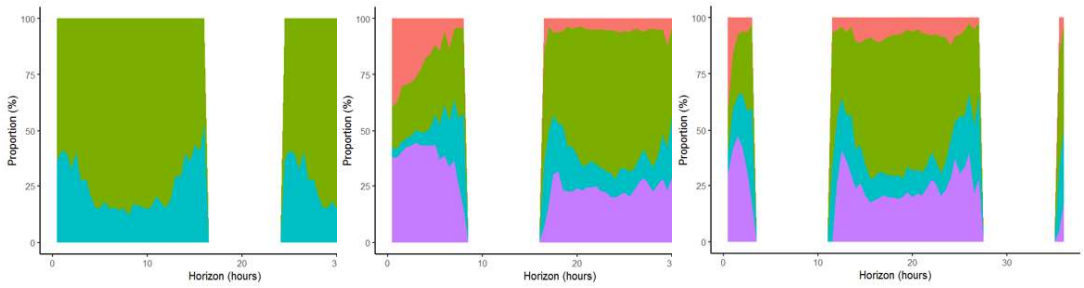

(a) 3 a.m. forecasts (b) 12 a.m. forecasts (c) 17 p.m. forecasts

Figure 3.3: Mutual information between estimated GHI time series and lagged production for different time lags

Also, there is an increase in the proportion of the in situ measurements and satellite data around the horizon +24 hours. This is caused by the fact that the weather has a tendency to remain similar on consecutive days, and thus obtaining some information on the state of the atmosphere by measuring the PV production or getting a satellite image also gives some information on the state of the atmosphere for the following day.

3.3.2 Preprocessing of the satellite images

In the proposed model, estimated GHI time series are derived from the Metosat Second Generation (MSG) satellite images for each pixel using the HelioSat-2 method [111], [112]. We propose to use these time series as conditioning features for the AnEn model when it looks for analogs. Since the model looks for analogs by matching features on several time steps as described by the parameter k from equation (3.6), and since the pixels used to condition the forecasts are in the neighborhood of the plant, we use both the spatial and temporal information from the images. Still, this method is simpler than standard ones e.g. Cloud Motion Vector [113], as it does not try to anticipate the future state of the cloud layer. The choice of taking a purely "data-driven" approach rather than including a preprocessing step for the images to derive cloud motion information is one of the design requirements set here in order to maintain simplicity in the proposed model chain. The mechanism of the AnEn model, where a series of past images is linked to future situations through the analogs, is a process that is expected to reflect the mechanism according to which the temporal variations in the images that reflect cloud motion impact PV production. Section 3.3.3 demonstrates that the inclusion of satellite images as conditioning features is beneficial to the model. This section describes the selection process for the pixels we use to compute the model.

Two parameters must be estimated before including the satellite-estimated GHI. The first one is the maximal distance D_{max} between the power plant and the points for which we use the GHI estimation in the model. Theoretically, the greater this distance, the longer the time horizons for which the estimated GHI time series can be useful. However, increasing D_{max} quadratically increases the number of pixels to be considered. To avoid computational issues, we have to set a limit on this distance D_{max}. The second parameter is the number N_{pix} of pixels we select to derive the features, within the area defined by D_{max}. The selection of a specific pixel from the satellite image results in a GHI time-series from consecutive images. We propose to keep the most informative N_{pix} time-series according to their MI with PV production.

To define D_{max}, we first obtained features estimated from pixels within a 150 km radius

as an upper-bound. Then, for different time horizons h, we computed the MI between the GHI time series derived from each pixel lagged h time and the PV production over one year. We could then visualize the location of the most informative time series for each horizon, as shown in Fig. 3.4. From visualizing the data, we found that for time horizons below 90 min, the global level of the information of the estimated GHI time series is significant compared to other horizons. There is also a significant difference between the most and the least informative time series, the most informative ones being located within a 50 km radius from the plant. On the contrary, for greater horizons, the information is scant. Thus, it does not seem necessary to have a large D_{max} for longer time horizons, or to use satellite data at all. In the end we kept a 50 km value for D_{max}.

In order to further reduce the dimension of this input, we use the averages of GHI estimations over several pixels as features instead of using a single pixel per feature. The initial images are reduced to a grid of 10 $\times$10 equally spaced zones in the latitude/longitude grid, which reduces the 317 pixels contained in the D_{max} radius to 100 features.

We defined the number of features to keep within a D_{max} radius by fitting Least Absolute Shrinkage and Selection Operator (LASSO) models [114] with a 10-fold cross-validation, using all the estimated GHI time series as features to predict the production for horizons ranging from +30 minutes to +36 hours with a half-hourly time step, that is, for 72 different horizons. For a given horizon h, we obtained the LASSO models with:

$$\hat{E}_{PV,t+h} = \hat{\beta}_0^h + \sum_i \hat{\beta}_i^h GHI_{t,i} \tag{3.16}$$

$$\hat{\beta}^h = argmin_\beta \left((E_{PV} - \hat{E}_{PV})^2 + \sum |\beta_i^h| \right) \tag{3.17}$$

where $GHI_{t,i}$ is the estimated GHI for the i-th pixel for time t, and β^h are the parameters of the model.

LASSO models have an intrinsic tendency to produce a sparse feature selection, and to randomly drop features when they are strongly correlated. As our estimated GHI time series are indeed correlated, we took the feature selection performed by the LASSO models as a measure of the redundancy in the time series, instead of actually selecting the most relevant features. We then obtained N_{pix} by averaging the number of features kept by the LASSO models over the 72 forecast horizons:

$$N_{pix} = \frac{1}{72} \sum_{i=1}^{72} \overline{\mathbb{1}(\hat{\beta}_i \neq 0)} \tag{3.18}$$

Finally, we obtain $N_{pix} = 12$ features, which represent roughly 12% of the total number of features considered. This value is retained for the forecasts in Section 3.5. Fig. 3.5 shows

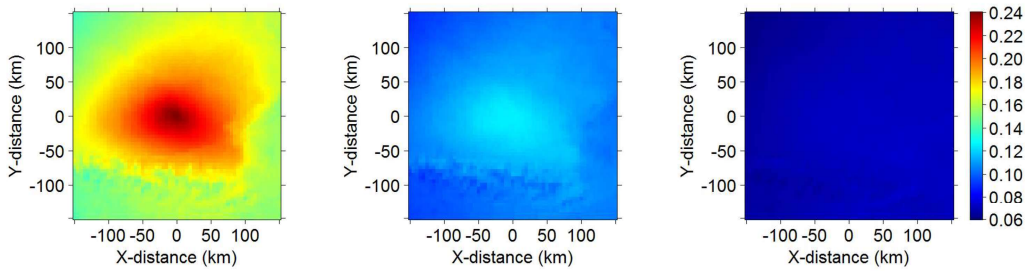

(a) t + 30 minutes (b) t + 90 minutes (c) t + 150 minutes

Figure 3.4: Mutual information between estimated GHI time series and lagged production for different time lags

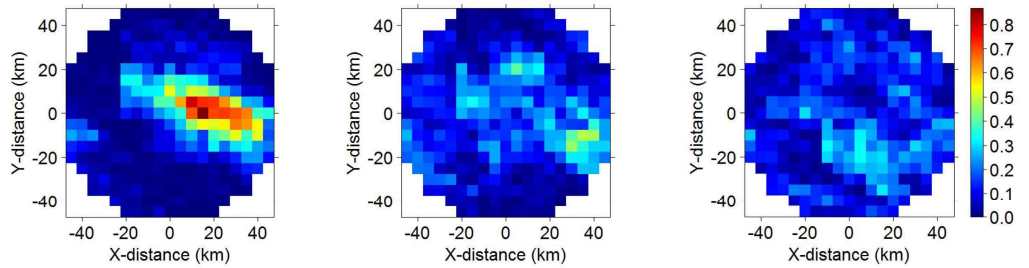

(a) t + 30 minutes (b) t + 90 minutes (c) t + 150 minutes

Figure 3.5: Probability for each pixel to be selected for different forecast horizons using non-averaged satellite images

the average selection probability for each feature within the area defined by D_{max} using non-averaged satellite images, for all forecasts started at 12 p.m. For the 30-minute horizon, the selected pixels are concentrated in an area east of the plant. This suggests that the weather conditions propagate from east to west, which could be explained by the Sun's path, but also by local weather conditions (e.g. a systematic east wind). For the 90-minute forecast, a slight concentration persists to the east of the plant. After this horizon, no recognizable pattern can be found.

3.3.3 Contribution of each source of data

Before performing a thorough evaluation of the AnEn model to other benchmark models, we verified that the different methods we implemented resulted in improved performances. To do so, we evaluated the CRPS introduced in chapter 2 to evaluate whether including the different sources of data had a significant effect on the model performance.

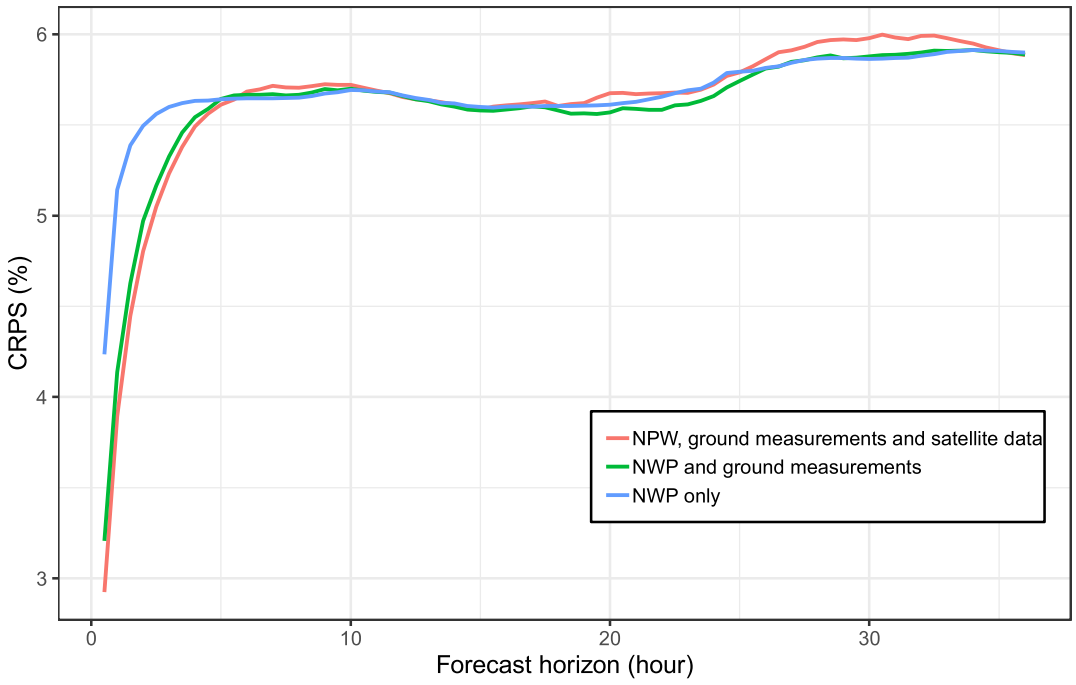

Figure 3.6: Comparison of the performance of the AnEn model depending on the inputs

Figure 3.6 shows how CRPS performance increases when adding incrementally different sources of data. The addition of the last measurement significantly increases performance for time steps up to 5 h. This is self-explanatory, as the last measurement is very informative about the current meteorological situation, but carries little predictive information. The addition of satellite data slightly increases performance up to the 3-hour forecast horizon. This confirms that the added value from satellite data extends up to a few hours, as expected from the literature.

This result is quite interesting, as it shows that the model is able to process both temporal and spatial information from very different sources of data. It could be extended by other features, that are known to improve solar power forecasting, such as measurements from neighboring PV plants or weather stations. However, this would require further work when assigning global weights to each source of data. In our case, using the maximal feature weight as the global weight of the whole source was efficient as the information between each source of data was not redundant. When increasing the sources of data, the chances are higher that two sources of data will carry correlated information. This should be considered for the global weight assignment.

3.3.4 Parameters of the model

In the end, the AnEn model is characterized by few parameters that control the behavior of the metric: p penalizes significant differences between the inputs, while q controls the relative importance of each feature. k is introduced so that an instant t in the morning (resp. evening) cannot be considered similar to an instant t' in the evening (resp. morning).

Finally, two remaining parameters allow us to control the behavior of the model. The first is the number of most similar historical situations N_{An} that we retain for estimating the PDF, and the second is the length L_{PV} of the period preceding the instant to be forecast that we use to search for analogs. Thus, the vector of parameters Θ_1 introduced in 4.1 is constituted of the parameters $[p, q, k, N_{An}, L_{PV}]$.

According to our results, the higher the parameters N_{An} and L_{PV}, the lower the bias of the model. The bias, or Mean Bias Error (MBE) is defined as the average error for a series of n pairs of forecast/verification values $\hat{y}_i, y_i$:

$$MBE = \frac{1}{n} \sum_i (y_i - \hat{y}_i) \tag{3.19}$$

When the time period over which the analogs are searched increases, the model looses some of its conditionality on recent weather conditions, since old data is used. In addition, increasing the number of analogs also has the effect that the model's conditionality on the actual weather forecasts is lost, because as the number of analogs increases, each additional analog used is observed in a situation that is less similar to the actual weather forecasts. Ultimately, as these parameters increase in number, the model tends to produce an unconditional climatological average of the power as a forecast, which would be perfectly reliable, and thus have no bias, but lower sharpness.

Some illustrative probabilistic forecasts for a given plant are reported on Fig. 3.7 along with a quantification of the model's MBE in Table 3.1 with varying N_{An} and L_{PV} values to illustrate this effect. To isolate the effect of these parameters, all the other parameters keep the same value. Each shade of grey represents a PI, with increasing confidence levels from 2% to 98%. Using a longer time period to identify the analogs, or increasing the number of analogs, results in a curve that looks more like the typical "bell" curve of PV production, neglecting the intra-day variability. Ultimately, this results in a lower MBE when using the expectancy of the forecast distributions as deterministic estimates of the production.

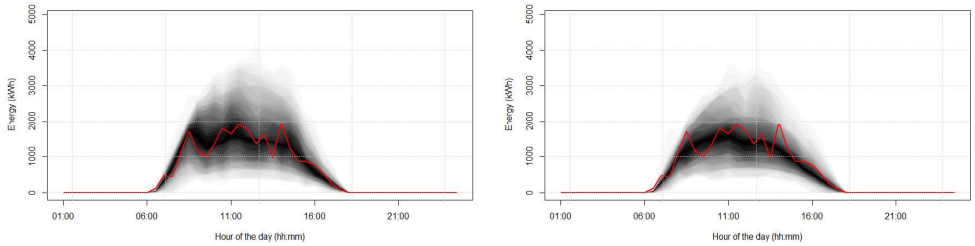

(a) $N_{An} = 240$ analogs, $L_{PV} = 50$ days

(b) $N_{An} = 240$ analogs, $L_{PV} = 150$ days

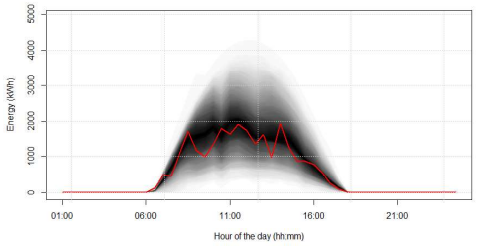

(c) $N_{An} = 720$ analogs, $L_{PV} = 50$ days

Figure 3.7: Example of PV probabilistic forecasts for a given day

Table 3.1: MBE of the PV power forecasting models for varying N_{An} and L_{PV} values

	MBE (%)
$N_{An} = 240$, $L_{PV} = 50$	0.15
$N_{An} = 240$, $L_{PV} = 150$	0.09
$N_{An} = 720$, $L_{PV} = 50$	0.03

3.4 Benchmark models

To compare the AnEn model with the literature, several benchmark models were also implemented depending on the forecast horizon and resolution. The computing times required by the different models, including the AnEn, are reported on table 3.2. These times include the preprocessing of the data.

3.4.1 Persistence

The persistence model is often used as a simple benchmark for PV power forecasting models. In this thesis, we use two variants of the persistence, depending on the forecast horizon. We refer to them as "Persistence 1" and "Persistence 2" in the remainder of the thesis.

The Persistence 1 model simply states that the power forecast $\hat{E}_{PV}$ for all future times is the power E_{PV} observed at the time of the forecast, that is:

$$\hat{E}_{PV,t+h} = E_{PV,t}, \forall h \in \mathbb{N} \tag{3.20}$$

The Persistence 2 model states that the power forecast for a given time is the power observed the day before at the same time:

$$\hat{E}_{PV,t} = E_{PV,t-24h} \tag{3.21}$$

The Persistence 1 model is a benchmark more suited to short-term forecasts, while the Persistence 2 model is a benchmark for day-ahead forecasts.

3.4.2 ARIMA model for short-term forecast

For the 5-minute resolution forecasts, we used an Auto Regressive Integrated Moving Average (ARIMA) model [78], which is best suited to short-term forecasts, using only the production data as input.

For an ARIMA model fitted with order (p_A, d_A, q_A), where p_A is the number of auto-regressive terms, d_A the order of differentiation, and q_A the number of moving average components, a deterministic forecast of the solar output E_{PV} is readily computed as follows:

$$\hat{E}^{d_A}_{PV,t} = a_0 + \sum_{i=1}^{p_A} a_i E^{d_A}_{PV,t-i} + \sum_{j=1}^{q_A} b_j \left(E^{d_A}_{PV,t-j} - \hat{E}^{d_A}_{PV,t-j} \right) \tag{3.22}$$

where $E^{d_A}_{PV}$ is the time series E_{PV} differentiated d_A times:

$$E^{d_A}_{PV,t} = E^{d_A-1}_{PV,t} - E^{d_A-1}_{PV,t-1} \text{ with } E^{0}_{PV,t} = E_{PV,t} \tag{3.23}$$

The vectors of parameters a and b are estimated by maximizing an objective such as the conditional sum of squares of the Akaike Information Criterion (AIC) [115] on the most recent data for each forecast, following a sliding window scheme as for the AnEn.

3.4.3 First state-of-the-art benchmark: quantile regression forests model

The AnEn approach was compared with two state-of-the-art models. The first is the QRF model, because it is widely used and featured several times in the leaderboard of the GEFCOM 2014 [87].

This is a modification of the random forest algorithm [116] that can provide quantile forecasts, and was first proposed by reference [117]. In the original random forest model, a

large number of regression trees are grown over the training set, and the conditional mean of the distribution is obtained by a weighted average of the output of the trees. More specifically, each tree is grown on a random sample with replacement ("bagged version") of the training set, and each split of the trees is done on a random subset of the predictor variables. This prevents the trees from being correlated, and finally avoids overfitting on the training set. For quantile regression, a random forest is grown over the training set, but instead of the conditional mean, the full distribution is estimated from the observations in the output of the trees.

Here, it is trained using the same variables as the AnEn except for the satellite data that caused computational time of the QRF to be too long, along with their one-time-step lagged values. Note that what we call the QRF model is actually a collection of 72 models, each trained to forecast a specific horizon, because the models have to treat the relative importance of the last measurement differently regarding the horizon. This process is automated in the AnEn model, so that there is a single model for all of the horizons. This argument supports the fact that the AnEn model is seamless, as a single model gives consistent forecasts from +5-minute to +36-hour horizons.

3.4.4 Second state-of-the-art benchmark: bayesian ARD model

The second model we used is a Bayesian regression with an Automatic Relevance Determination (ARD) prior [118]. This prior is known to introduce sparsity into the feature selection.

The Bayesian ARD approach models the output E_{PV} as a normal distribution, with the mean being a linear combination of the inputs X, and the precision being a parameter γ:

$$E_{PV} \sim \mathcal{N}(Xw_{ARD},\, \gamma^{-1}) \tag{3.24}$$

The ARD prior on the weights, which introduces sparsity to the approach, models them as centered standard deviations with precisions λ:

$$w_{ARD,i} \sim \mathcal{N}(0,\, \lambda_i^{-1}) \tag{3.25}$$

Then, the parameters γ and λ are obtained by maximizing the likelihood of the data with respect to them. Once they are obtained, the PDF of the output conditionally to the input is entirely defined, and the model can be used with new inputs.

Since this model also provides an automatic derivation of the relevance of each feature similar to the AnEn, and naturally provides a probabilistic output, it is a good comparison model for the AnEn.

Table 3.2: Computation time required for providing PV forecasts for a given horizon, in seconds

	30-minute resolution		5-minute resolution	
	Training	Forecasting	Training	Forecasting
AnEn	-	1.9	-	8.8
Persistence 1	-	5e-3	-	6e-3
Persistence 2	-	5e-3	-	6e-3
ARIMA	9.2e-2	2.5e-7	10e-2	3.7e-3
QRF	4.3	1.3e-2	68.0	4e-2
ARD	10.8	10e-3	154	1e-3

3.5 Evaluation of the AnEn model performance

The proposed AnEn model was used to forecast the power output of twelve PV plants located in southwest France. The plants are noted P1 to P12 and have nominal powers ranging between 2 and 12 MWp. The available measurements cover the period from January 2014 to September 2018. NWPs are obtained from the European Center for Medium-range Weather Forecasts (ECMWF). The ECMWF forecasts are made on a 0.1°×0.1°latitude/longitude grid every 12 hours. The NWP variables used as features are the Surface Solar Radiation Downwards (SSRD), 10-m U- and V-wind speed (10U and 10V), 2-m temperature (2T), Total Cloud Cover (TCC) and Total Precipitations (TP). In situ measurements come from the power plants' monitoring systems. The measurements taken into account are PV power, ambiant temperature, and Global Tilted Irradiance (GTI) i.e. irradiance in the plane of array. The clear-sky profile is computed using the McClear model [22]. Lastly, features obtained from the MSG satellite imagery are computed using the HelioClim-3 database with the HelioSat-2 method [111], [112]. The images are converted into a time series of estimated GHI for each pixel. At the location of the plants, each pixel approximately corresponds to a 5 km×5 km surface.

Since the measurements were available from January 2014 to September 2018, all of the data necessary to perform the simulation were collected for the same period. All of the data were then converted to 30-minute time series to obtain an uniform time-step. The clear-sky profile and in situ measurements have a native 5-minute resolution and the satellite images have a 15-minute resolution. These variables were summed over 30-minute intervals to obtain the 30-minute time series. The NWP have a native 1-hour resolution. All NWP fields were linearly interpolated to obtain the 30-minute time series. However, numerous

applications, such as real-time control of a combined PV and storage power plant, also require short-term forecasts with horizons lower than 30 minutes. Using the exact same model but feeding it with the native 5-minute data, and with 5-minute interpolated NWPs and satellite data, we could provide forecasts with a 5-minute resolution.

The period from May 2016 to April 2017 is used to estimate the structural parameters of the AnEn, QRF and ARD models with an heuristic optimization. The ARIMA order was also obtained by minimizing the AIC on the testing set. Then, to assess the performance of the models, PV power was forecast from May 2017 to April 2018 with the AnEn and QRF models, from 30 minutes to 36 hours ahead with a 30-minute resolution. The forecasts were updated every 30 minutes following a sliding window scheme. For each new forecast, the set $\mathbf{X}$ was updated using the latest in situ measurements, NWP, and satellite-derived GHI estimations. In addition, the set $\mathbf{H}$ was updated with the most recent data available at the time to identify the analogs. We also performed the same evaluation for the ARIMA and AnEn models with the 5-minute resolution forecasts, forecasting from +5-minute to +60-minute horizons, and updating the forecasts every 5 minutes.

Probabilistic forecasts are more complex to evaluate than deterministic ones for which standard procedures are common [119]. Numerous properties are required for predictive densities, while identifying some aspects of the forecasts may fail when using only proper scoring rules. The main required properties are reliability and sharpness as explained in section 3.1. Deterministic criteria are also presented for comparison purposes with results from standard deterministic models in the state of the art.

Since all plants showed similar performance (see Table 3.3), all the figures in the following parts are obtained from a single plant, namely P3. Reliability and sharpness properties of the probabilistic approaches are analyzed, especially when conditioned by the forecast lead-time or horizon.

3.5.1 Reliability

For a perfectly reliable model, the empirical quantile level should be the same as the nominal one, and thus the reliability diagram should be a diagonal line. Figure 3.8 shows the reliability diagram of the three probabilistic models, averaged over all forecast horizons. Consistency bars are also added following [120] to indicate a range within which even a perfectly reliable model could be situated due to the finite size of the testing set with a 90% confidence level. All models fall within the range defined by the consistency bars, and so we cannot reject the hypothesis that they are reliable. Overall, the deviations are limited. For the AnEn and QRF models, the absolute deviations are lower than 2%, which is usually

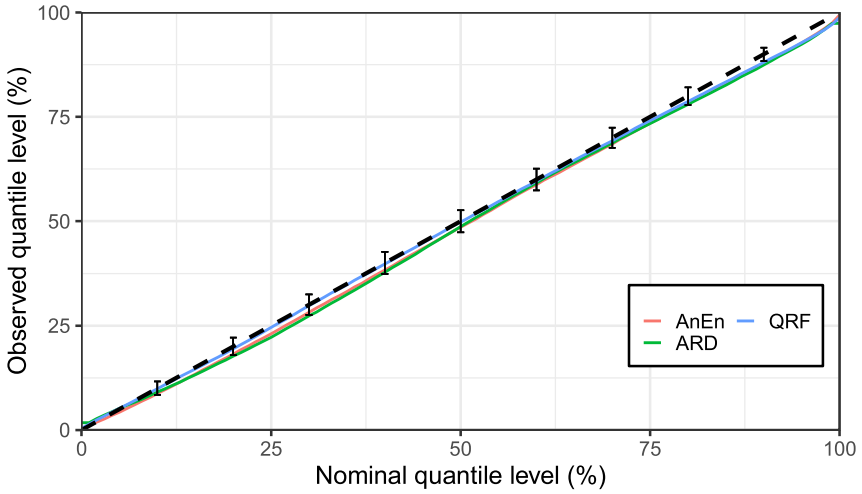

Figure 3.8: Reliability diagram of the three models including consistency bars

considered in the literature as sufficient to have good reliability properties [61]. However, the ARD shows larger deviation from the diagonal compared with the AnEn and QRF models. We explain this by the parametric representation of the uncertainty of PV production. It is difficult to make any assumption on the shape of the distribution of PV power, because it might be skewed and varies over time, thus making the Gaussian assumption from the ARD model highly detrimental to the reliability. In Table 3.3, Reliability (R) reports the mean absolute reliability deviations from the diagonal over several forecast horizons.

However, models should be reliable not only on average over all horizons, but for any subset of the forecasts. Thus, we also studied the reliability conditionally to the forecast horizon and the lead-time. On Figure 3.9, the reliability diagrams are shown individually depending on either their forecast horizon or their lead-time.

The reliability conditional to the horizon is quite good for the three models, rarely exceeding the consistency bars. However, this conditional reliability is difficult to obtain: for several horizons, the reliability exceeds the consistency bars, and so the hypothesis that the model is reliable for this forecast horizon and quantile level must be rejected. Note that the consistency bars are larger since there are a lower number of forecasts when the evaluation is conditional to the forecast horizon. The ARD and AnEn models show larger deviations that were not suggested by the averaged reliability on Figure 3.8. However, it is possible that some of the deviations observed are in fact due to the serial correlation of the data instead of a reliability issue. Using consistency bars that take serial correlation into account such as in [121] could be helpful in identifying this effect.

Besides, the AnEn and QRF have a better reliability conditional to the lead-time of the

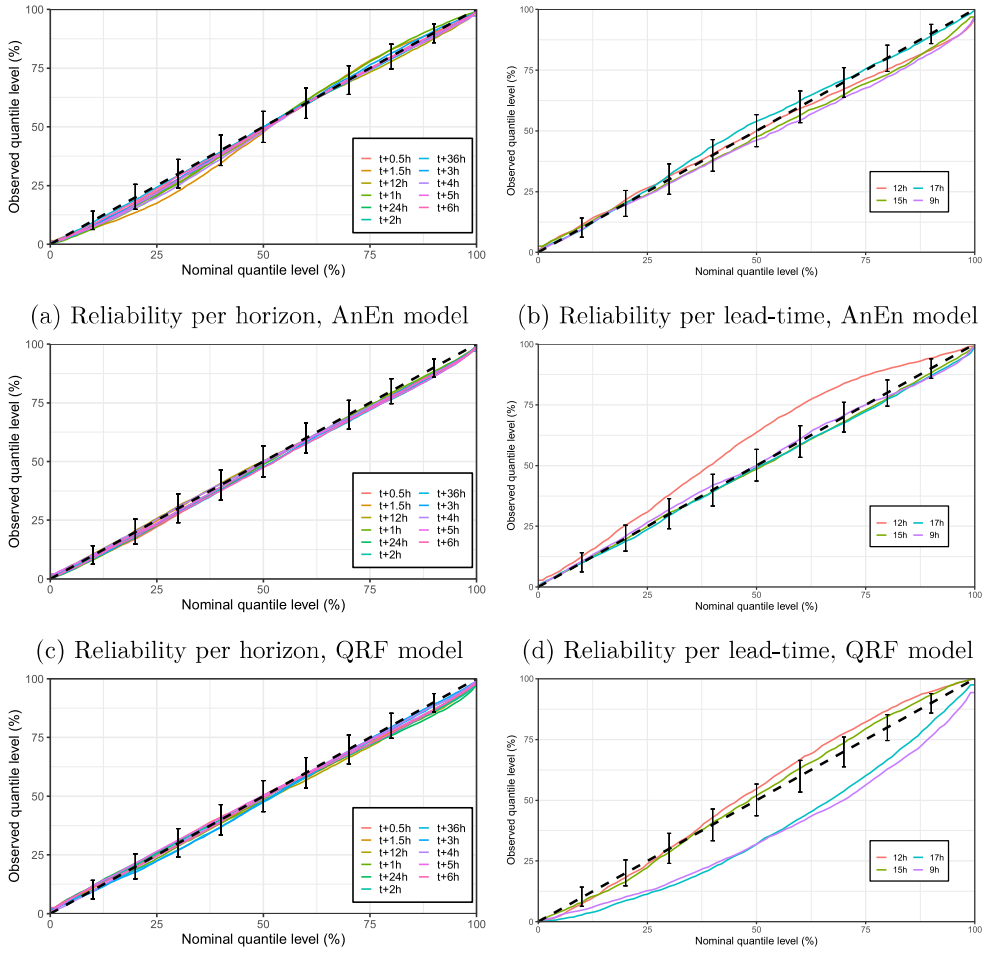

(a) Reliability per horizon, AnEn model

(b) Reliability per lead-time, AnEn model

(c) Reliability per horizon, QRF model

(d) Reliability per lead-time, QRF model

(e) Reliability per horizon, ARD model

(f) Reliability per lead-time, ARD model

Figure 3.9: Conditional reliability of the three probabilistic models

forecast, especially for forecasts that are made early in the evening or late in the afternoon, where the ARD has large deviations.

Globally, even if we cannot say that the models are reliable no matter the subset of the forecasts, the AnEn and QRF models still show good reliability properties, being reliable on average and conditionally to the forecast horizon and lead-time for most quantile levels. The ARD model is not as reliable as the others, but we will still include it in the rest of the evaluation for comparison purposes.

3.5.2 Sharpness

In this thesis, sharpness is assessed using the Prediction Interval Normalized Averaged Width (PINAW) metric. The lower the PINAW, the sharper the model. Noting $I_{i,\alpha}$ the width of the PI with coverage rate α, PINAW can be written as follows:

$$PINAW(\alpha, h) = \frac{\sum_{i=1}^{N} I_{i,\alpha}}{E_n} \tag{3.26}$$

E_n is the maximum amount of energy that can be produced in a time step, taken as the nominal power of the PV plant multiplied by a time step duration. Fig. 3.10 shows the PINAW for different forecast horizons and nominal coverage rates α. Similar to reliability, the PINAW related to the representation of uncertainty is worse for the ARD model. The PINAW are very similar for the AnEn and QRF models, although the AnEn model is slightly sharper.

When looking at the sharpness conditionally to the forecast on Fig. 3.11, it is clear that the AnEn and ARD approaches have a higher sharpness variability depending on the forecast horizon compared to the QRF. The AnEn is especially sharper than the other approaches for forecasts with a 30 minutes horizon. In Table 3.3, Sharpness (S) reports the mean PINAW over all horizons and all nominal coverage values.

Regarding the parameter k from equation (3.6), we found that when using k $>$ 1, the forecast lost considerable sharpness, moving increasingly closer to a climatological forecast. Using $k = 0$ also led to significant errors for short-term forecasts where the model relies heavily on the last observation. Since the generation is the same in the morning or in the evening, past observations in the evening were deemed similar to upcoming situations in the morning and vice-versa. With $k = 1$, the pattern of increasing (for the morning) or decreasing (for the evening) generation is included, and the problematic behavior is prevented without loosing too much sharpness.

3.5.3 CRPS score

At this stage, it is difficult to tell which model performs better, since they show very similar results for both reliability and sharpness. The overall performance of the models is evaluated using the CRPS introduced in 2.

Fig. 3.12 presents the CRPS of the three models depending on the horizon, normalized by the nominal power of the plant. As expected from the reliability and sharpness results, the ARD model performs worse than the two other models for all horizons. The QRF model outperforms for forecast horizons longer than 3 hours. For shorter horizons, the AnEn model performs better. However, as can be seen from Table 3.3, the overall CRPS

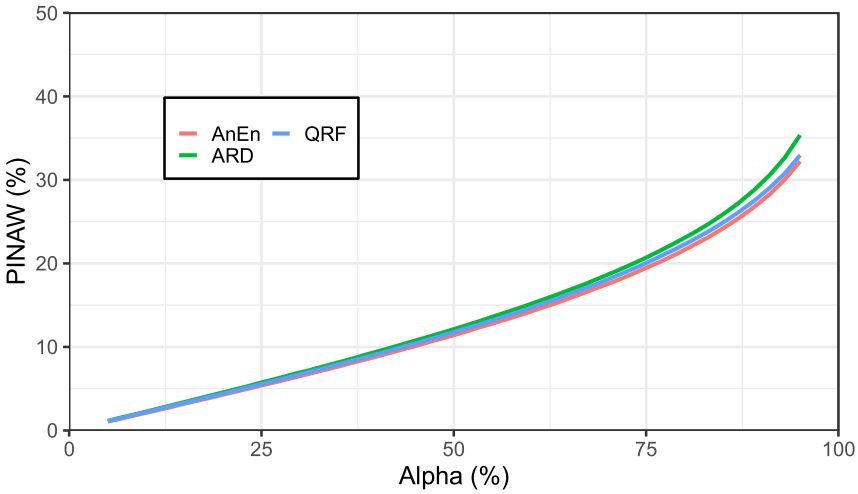

Figure 3.10: PINAW of the three probabilistic approaches averaged over all horizons

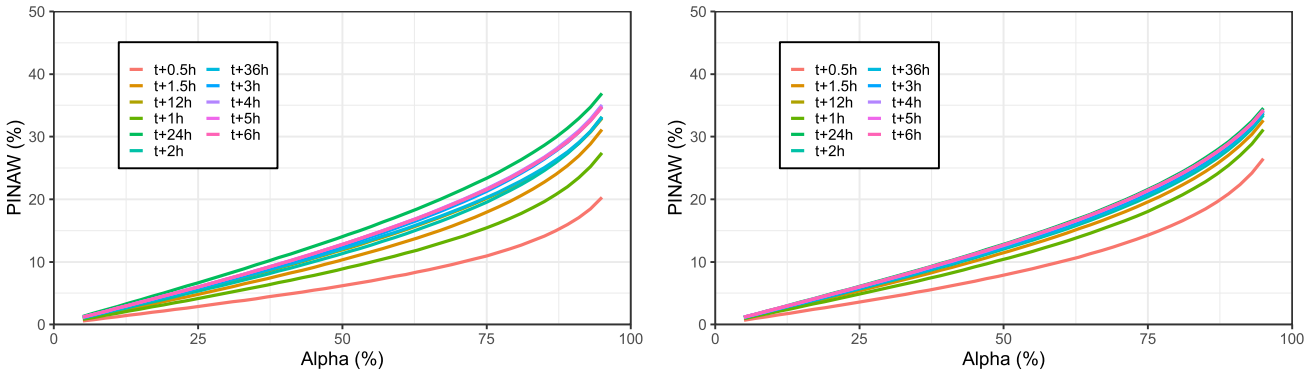

(a) AnEn model

(b) QRF model

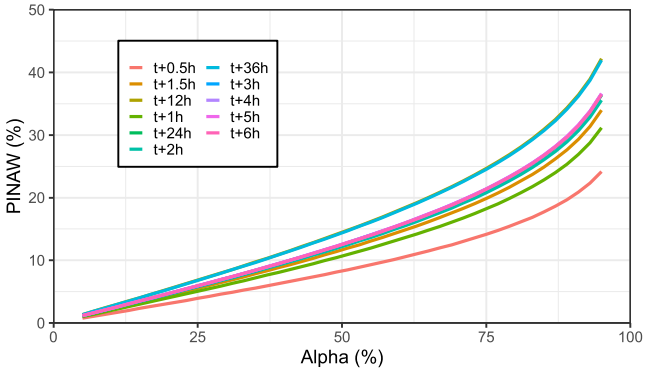

(c) ARD model

Figure 3.11: PINAW of the three probabilistic approaches conitional to forecast horizon

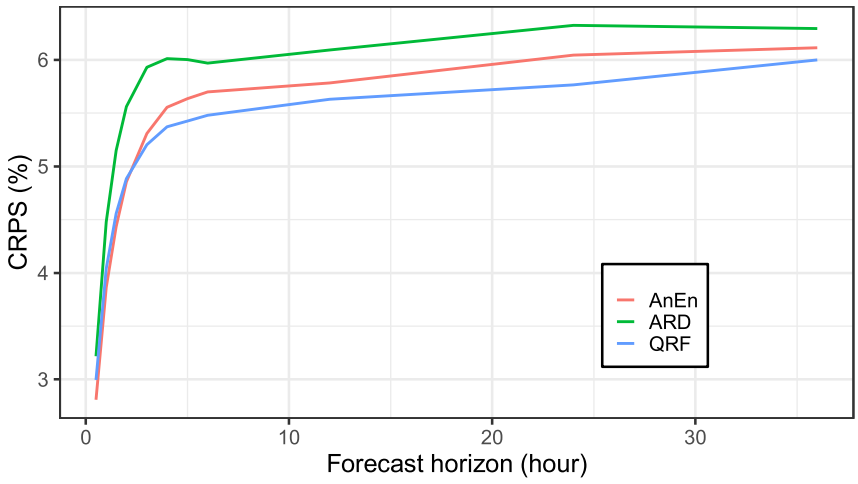

Figure 3.12: CRPS of the three models

differences between the AnEn and QRF models are very low, and they both show state-of-the-art performance.

As the CRPS difference is very low between the QRF and AnEn models, we implemented a Diebold-Mariano (DM) test [122] using the CRPS as the measure of performance, to see if the difference in the forecasts between the models was statistically significant.

Given two sets of forecast CDFs and their matching observations $\{\hat{F}_{PV,1,i}, E_{PV,i}\}$, and $\{\hat{F}_{PV,2,i}, E_{PV,i}\}$, we note the loss differential d:

$$d_i = CRPS(\hat{F}_{PV,2,i}, E_{PV,i}) - CRPS(\hat{F}_{PV,1,i}, E_{PV,i}) \tag{3.27}$$

The Diebold-Mariano test tests the null hypothesis $H_0 : \mathbf{E}(d) = 0$ versus the adverse hypothesis $H_1 : \mathbf{E}(d) \neq 0$. To do so, it can be shown that under the null hypothesis the DM statistic follows the standard normal distribution:

$$DM = \sqrt{(1/n)} \frac{\sum_{i=1}^{n} d_i}{\sqrt{2\pi f_d(0)}} \sim \mathcal{N}(0,\, 1) \tag{3.28}$$

Where $f_d(0)$ is the spectral density of d at frequency 0 which can be approximated from the data, and n is the number of forecast/verification pairs available. On Fig. 3.13 we plot the DM statistic between the AnEn and QRF models for different forecast horizons. We choose a standard 5% significance level, and thus values of the DM statistic lower than the 2.5% quantile or higher than the 97.5% quantile of the normal distribution (respectively -1.96 and +1.96, materialized by horizontal red lines on Fig. 3.13) allow us to reject the null hypothesis.

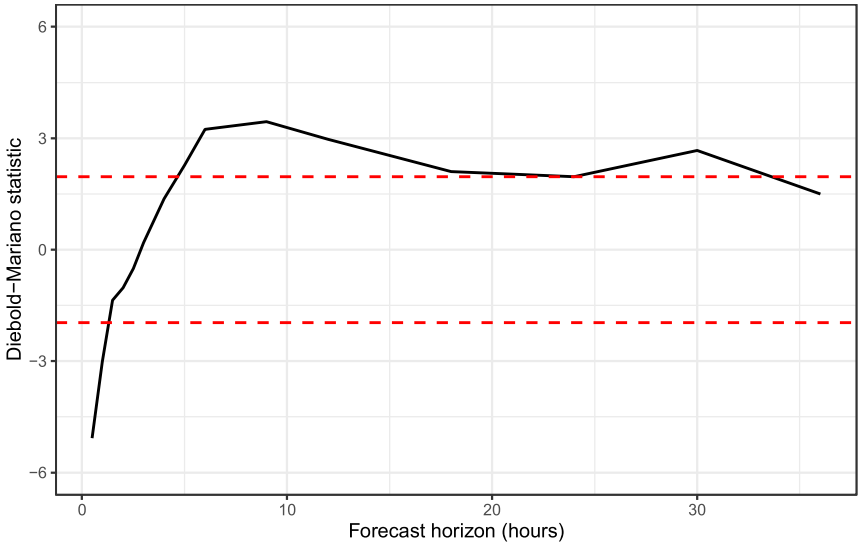

Figure 3.13: DM statistic between the QRF and AnEn model

From Fig. 3.13 we can see that for horizons between 2 and 5 hours, we cannot reject the null hypothesis that the expected value of the CRPS difference between the ANN and QRF models is null, which supports the claim that the two models have similar performance. However, for horizons lower than two hours and higher than 5 hours, the null hypothesis is rejected. Thus, for these horizons, the expected value of the CRPS difference between the model is not null. This supports the claim that the AnEn performs better for short forecast horizons, and that the difference for long forecast horizons is generally slight.

3.5.4 Root mean square error

The RMSE is also computed, taking the densities medians as a deterministic forecasts. This allows us to compare the model with standard deterministic ones. We compared the AnEn and QRF with two variants of the classic persistence models. The first variant, noted Persistence 1, gives the power measurement of the day before at the same time of the day as the forecast. The second, noted Persistence 2, gives the power observed at the starting time of the model as the prediction for all horizons.

The RMSE of the models depending on the forecast horizon is presented on Fig. 3.14. All models consistently outperform Persistence 1 and 2 for all horizons. For the ARD model, although the uncertainty representation is not as good as the AnEn and QRF, as can be seen from the reliability, PINAW and CRPS scores, the deterministic forecasts are good, with RMSE scores similar to the AnEn and QRF. For day-ahead forecasts, the ARD model

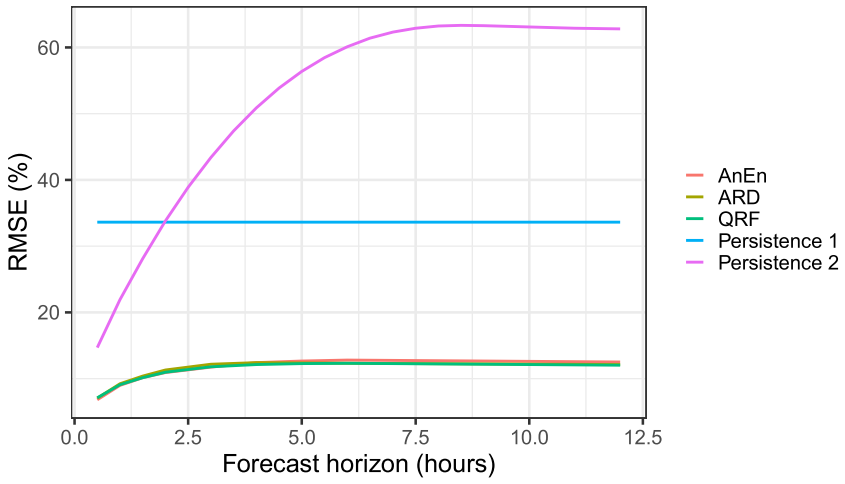

Figure 3.14: RMSE of the models depending on the horizon

is better than the AnEn.

3.5.5 Intra-hourly forecasts

Figure 3.15 shows the average MBE of the three short-term forecasting approaches. The figure shows that the mean forecast error is lower than 0.5% for all models and all horizons. However, the ARIMA model develops a positive bias when the horizon increases, and the AnEn model has a constant positive bias. As expected, the persistence is essentially unbiased.

Figure 3.16 shows the average RMSE conditioned to the forecast horizon for the AnEn, ARIMA and Persistence 2 models for the 5-minute resolution forecasts. The AnEn model is consistently more accurate than the two other models for intra-hourly forecasting. Besides, even though it is not shown with the RMSE criterion, the AnEn provides uncertainty information since it gives a probabilistic estimate of the production.

3.5.6 Overall results

In addition to the previous analyses, overall results are summarized in Table 3.3. Except for the reliability (R) and sharpness (S) scores, which are naturally percentages, all other scores are given in percentage, relative to the installed power of the plant E_n.

The results for intra-hourly forecasts are reported in Table 3.4. Since it is quite long to perform a whole year of 5-minutes forecasts with a rolling window scheme, we only obtained the results for 5-minute forecasts for one plant, P3.

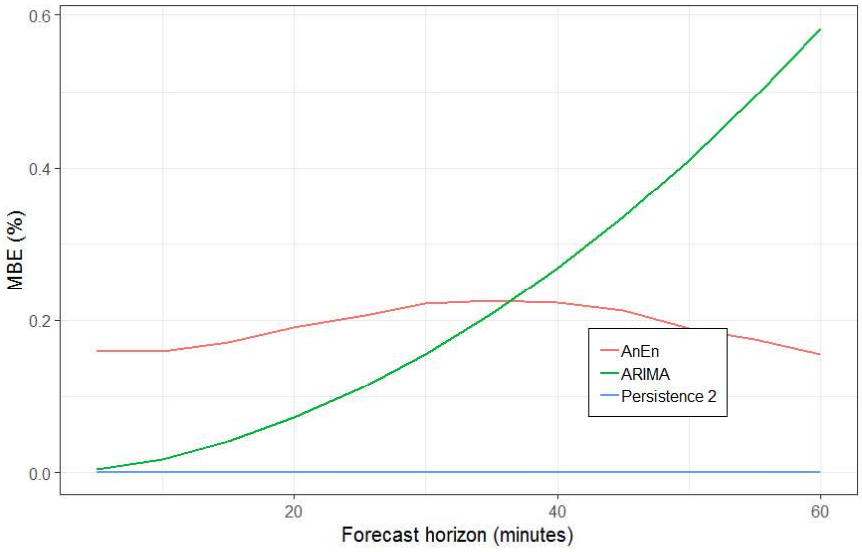

Figure 3.15: MBE of AnEn, ARIMA and Persistence 2 models for intra-hourly forecasts

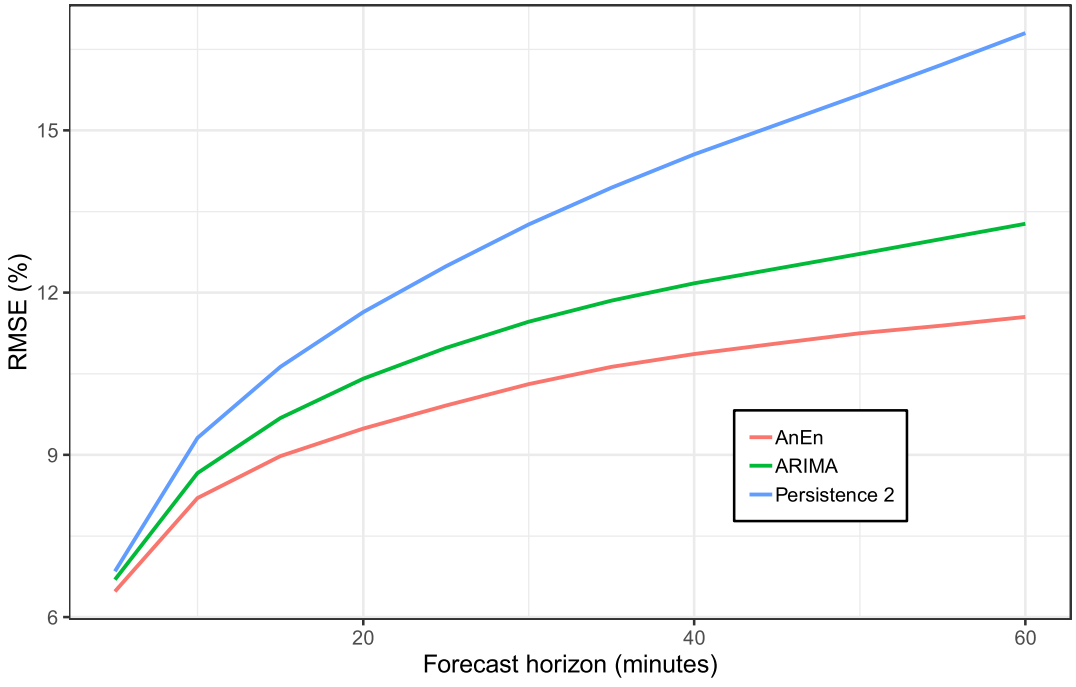

Figure 3.16: RMSE of AnEn, ARIMA and Persistence 2 models for intra-hourly forecasts

Table 3.3: Evaluation Results for 30-minute Resolution Forecasts for 12 PV plants

	AnEn				QRF				ARD				Persistence 1	Persistence 2
Plant	R	S	CRPS	RMSE	R	S	CRPS	RMSE	R	S	CRPS	RMSE	RMSE	RMSE
	%	% of Pn			%	% of Pn			%	% of Pn			% of Pn	% of Pn
P1	1.20	13.47	5.18	11.48	0.95	13.47	5.08	11.29	2.13	15.15	5.59	11.70	19.80	32.70
P2	1.30	14.08	5.81	13.32	1.31	13.89	5.63	12.88	1.96	15.98	6.12	13.03	23.40	35.20
P3	0.52	11.58	4.88	11.78	1.27	11.53	4.57	11.10	3.41	14.89	5.43	11.84	20.40	38.00
P4	1.54	14.06	5.57	12.43	0.68	13.82	5.41	12.12	1.76	14.94	5.70	12.24	20.70	33.30
P5	2.29	15.30	5.93	13.51	2.47	14.83	5.67	12.99	2.97	16.25	6.11	13.38	22.30	33.40
P6	1.02	14.08	5.45	12.17	0.97	14.16	5.36	11.92	2.27	15.28	5.77	12.17	20.90	34.10
P7	0.99	12.88	5.00	11.34	0.64	12.69	4.78	10.90	2.26	13.67	5.19	11.26	19.00	31.60
P8	0.97	14.11	5.74	13.28	0.57	14.00	5.40	12.67	2.02	15.25	5.80	13.04	19.70	31.60
P9	1.29	13.71	5.40	12.27	0.67	13.85	5.28	11.88	1.76	14.82	5.69	12.29	20.20	32.80
P10	2.26	14.74	5.51	12.52	2.22	14.36	5.30	11.90	3.37	15.43	5.83	12.60	21.84	33.43
P11	0.42	13.13	5.25	12.39	0.93	12.93	4.96	11.64	0.91	14.48	5.64	12.24	20.36	33.00
P12	0.63	13.45	5.32	12.13	0.76	13.26	4.99	11.46	1.63	14.32	5.54	11.89	19.10	31.90

Table 3.4: Evaluation results for plant P4 and 5-minute resolution Forecasts
Forecast Horizon from 5 minutes to 1 hour

	AnEn	ARIMA	Persistence 2
	% of Pn	% of Pn	% of Pn
MBE	-0.25	0.27	7.5e-3
MAE	5.68	6.29	7.88
RMSE	9.65	10.8	12.7

3.5.7 Conditional evaluation of the AnEn performance

In this section we focus on the performance of the AnEn conditional to different weather conditions. We propose two studies. In the first, we compare the AnEn model performances conditionally to the season. In the second one, we classify the days in three categories of variability, representing sunny days, cloudy days, and intermediate days. This allows for extrapolating the AnEn model performances to new locations, given that we know the typical weather variability of the new location.

In the evaluation of the AnEn model, we used the CRPS relative to E_n. In this section, we use the CRPS relative to the actual measurements $nCRPS$. For a set of n_f forecast CDFs $\hat{F}_i$ and verification values x_i, this relative CRPS is defined as follows:

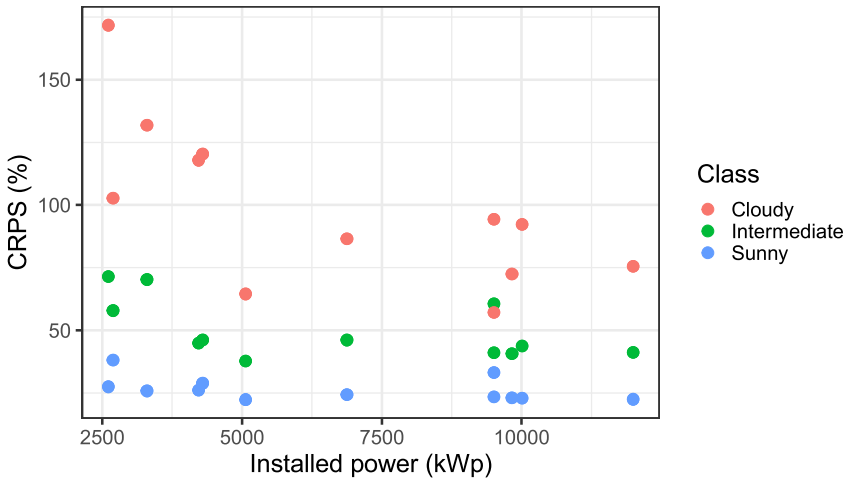

Figure 3.17: CRPS conditional to the production variability

$$nCRPS = \frac{1}{n_f} \sum_{i=1}^{n_f} \frac{1}{x_i} \int_{-\infty}^{\infty} \left(\hat{F}_i(y) - \mathbb{1}(y > x_i) \right) dy \tag{3.29}$$

The cases were $x_i = 0$ are ignored to avoid dividing by zero. The reason for using this indicator is that we will compare the CRPS of the model for different seasons. Since the overall production is different for the different seasons, normalizing by the PV plant installed power which remains the same over the seasons would favor seasons with low production i.e. Autumn and Winter. On the contrary, normalizing by the actual measures follows the seasonal variability of the PV plant production.

3.5.8 Performance conditional to the production variability

We classified the days of the study for each plant in three broad categories: sunny, cloudy, and intermediate. We used the Morphological Clustering Method from [123] to obtain the classifications.

Fig. 3.17 shows the result. As expected, sunny days have lower average CRPS, then intermediate days, and finally cloudy days. It also seems that the nCRPS is lower for bigger plants, at least for cloudy days. This can be explained by a smoothing effect: the larger the plant, the smaller the part of the plant that is affected by a cloud when its shadow area is smaller than the plants' area. Thus, larger plants have a lower variability and ultimately a better performance.

The AnEn model performance has a range between 25 and 175%, which gives conservative upper and lower bounds of the AnEn model performance. To reduce these bounds,

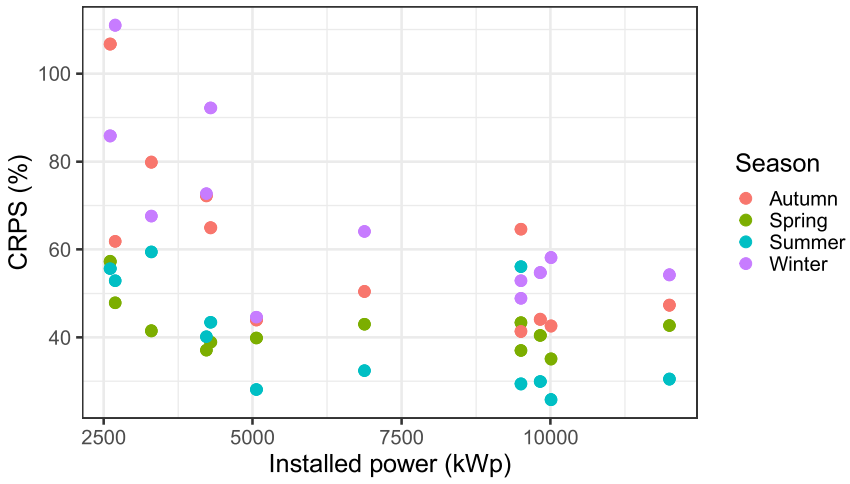

Figure 3.18: CRPS conditional to the season

we propose to also evaluate the performance conditionally to the season, so that we use a real meteorological variability.

3.5.9 Performance conditional to the season

For all the plants, we evaluated the CRPS conditionally to the season. The results are reported on Fig. 3.18. They suggest that the AnEn model typically has better performance during Summer and Spring, while Winter and Autumn have lower performances, which is consistent with France's climate.

The seasonal upper and lower bounds are less conservative in this case, with nCRPS values ranging between 25 and 125%. These values can give an idea of how the model would perform at a different location that has another climate.

3.6 Conclusions

The AnEn model showed similar or better results than all the benchmark models in all forecast ranges. It is slightly less accurate than the QRF model for day-ahead forecasts, but compensates with a lighter computational time, especially for forecasts with a 5-minute temporal resolution. As such, it can be used seamlessly over all time frames. Besides, it shows a better performance regarding computing time than the ARD and QRF models: although the forecasting time is longer, there is no training. The ARD and QRF models require training for each forecast in order to have the same seamless behavior as the AnEn

model. The AnEn showed good performances compared to the ARD and QRF models. Although it has a slightly lower performance for day-ahead forecasts, it has better performance than all benchmark forecasts for the short-term.

Chapter summary in French

Pour répondre aux objectifs identifiés dans l'introduction, le modèle doit être capable de fournir des prévisions à toutes les échelles temporelles possibles le plus rapidement possible. A cela, nous ajoutons la contrainte que les prévisions doivent être sous forme probabiliste, suivant les recommandations de la plupart des publications étudiant la vente d'énergie provenant de sources à production variable. En effet, quantifier l'incertitude associée à une prévision apporte plus d'information, et permet d'utiliser des méthodes de trading avancées prenant en compte la distribution complète de la production d'énergie photovoltaïque, ce qui finalement génère des revenus plus importants en s'exposant à moins de risques.

Une revue de l'état de l'art identifie les modèles issus de la famille des "Analog Ensembles" comme un bon point de départ pour répondre aux contraintes identifiées. En effet, ces modèles fournissent naturellement des prévisions probabilistes avec un temps de calcul faible puisqu'ils s'appuient sur la méthode des plus proches voisins qui a une faible complexité algorithmique i.e. $O(nd)$ avec n le nombre d'échantillons et d la dimension d'un échantillon.

Malgré cela, certaines limitations du modèle AnEn restent à surmonter. Le modèle tel que proposé dans la littérature ne s'appuie que sur des données issues des modèles de prévision météorologiques (Numerical Weather Prediction, NWP), et démarre toujours à heure fixe lorsqu'une nouvelle prévision est disponible. Or, nous souhaitons avoir un modèle qui fonctionne de façon continue et à horizon de prévision variable, ce qui nécessite d'autres données que les NWPs. Pour cela, nous effectons les modifications suivantes :

- Modifier le calcul de la distance entre les échantillons pour pouvoir utiliser de nouveaux types de données pour la prévision à horizon intra-journalier : dernière mesure effectuée, images satellite.

- Implémenter une procédure automatique pour le calcul du poids de chaque variable d'entrée dans la distance, de sorte que l'algorithme identifie les données pertinentes en prenant en compte l'heure de démarrage de l'algorithme et l'horizon de prévision.

Ces deux contributions permettent ainsi d'avoir un modèle de prévision adaptatif capable de fournir des prévisions avec un horizon de prévision allant de quelques minutes à 36 heures. Ces besoins répondent à ceux des marchés de l'électricité.

La modification du calcul de la distance est liée à l'ajout de données d'entrées qui ne sont pas des prévisions comme les NWPs mais plutôt une mesure de l'état actuel comme la dernière mesure de production ou la dernière image satellite. Cela oblige à modifier

l'ensemble d'entraînement selon l'horizon de prévision. Lorsque l'on réalise une prévision à l'instant t pour l'instant $t + 1h$, la variable d'entrée du modèle "dernière mesure" pour l'instant $t + 1h$ correspond à la mesure observée il y a une heure. Par conséquent, dans l'ensemble d'entraînement, la variable "dernière mesure" de chaque échantillon doit correspondre aussi à la mesure observée 1 heure avant. L'ensemble d'entraînement est donc dépendant de l'horizon de prévision, ce qui est traduit dans la nouvelle formulation de la distance. Cette distance entre deux instants t et t' peut alors s'écrire :

$$D_{AnEn}(\mathbf{X}_t, \mathbf{H}^h_{t'}) = \sum_{i=1}^{N_v} w_i^h \sqrt[p]{\sum_{j=-k}^{0} (\mathbf{X}_{i,t+j} - \mathbf{H}^h_{i,t'+j})^p} \tag{3.30}$$

Où N_v est le nombre de variables des données d'entrée, h est l'horizon de prévision et k est un paramètre qui définit la longueur de la fenêtre sur laquelle cette distance est calculée. Puisque l'ensoleillement "clear-sky" calculé (c'est-à-dire en absence de nuages) est utilisé, évaluer la distance sur une fenêtre au lieu d'un point unique permet d'éviter de confondre deuxs instants ayany la même production mais l'un étant le matin (le "clear-sky" augmente) et l'autre étant l'après-midi (le "clear-sky" diminue). Le paramère p contrôle la pénalisation des grandes différences entre les variables d'entrée entre t et t', de même que le RMSE pénalise plus fortement les larges erreurs que la MAE. $\mathbf{H}^h$ and $\mathbf{X}$ sont les deux ensembles qui contiennent les variables d'entrée du modèle à comparer entre les instants t et t'. $\mathbf{H}^h$ et $\mathbf{X}$ sont centrés et réduits, de sorte que la contribution de chaque variable d'entrée à la distance soit uniquement contrôlée par les poids w_i^h.

Le calcul automatique des poids s'appuie sur l'information mutuelle (Mutual Information, MI), qui mesure à quel point la connaissance d'une variable réduit l'incertitude d'une autre variable. Pour deux variables aléatoires X et Y, et leurs lois de probabilités marginales et jointes p_X, p_Y and $p_{X,Y}$, la MI s'écrit :

$$MI(X,Y) = \int\int p_{X,Y}(x,y) log\Big(\frac{p_{X,Y}(x,y)}{p_X(x)p_Y(y)}\Big) dxdy \tag{3.31}$$

Les lois de probabilités sont évaluées empiriquement sur l'historique de données. Le calcul des poids s'effectue en deux temps. Dans un premier temps on calcule la MI de la variable avec la production PV. Les poids sont donc également dépendants de l'horizon de prévision, puisque la variable issue de l'ensemble d'entraînement en dépent aussi comme indiqué précedemment. Seuls les échantillons observés à la même heure de la journée que l'heure pour laquelle on souhaite faire la prévision sont utilisés, de sorte que le calcul des poids soit également dépendant de l'heure de démarrage de l'algorithme. Dans un second temps, un poids maximal est attribué à chaque source de données et les poids sont normalisés

de sorte que la somme des poids issus d'une même source de donnée ne dépasse pas ce poids maximal. Ceci permet de ne pas surestimer les poids des variables issues d'une même source de données et fortement corrélées entre elles e.g. les estimations de rayonnement solaire issues des images satellite.

En outre, nous avons proposé une méthode pour réduire la dimension des images satellites, qui est plus importante que les autres variables et alourdit par conséquent le temps de calcul. Une observation d'image satellite correspond pour notre modèle à l'estimation du rayonnement solaire sur les pixels de l'image qui correspondent à un carré de 300 km de côté centré sur la centrale. Pour réduire cette dimension, nous avons d'abord constaté que la MI entre le rayonnement estimé et la production PV était importante uniquement dans un rayon de 50 km autour de la centrale quelque soit l'horizon de prévision, ce qui réduit le nombre de variables à 317. Cela reste toujours important comparé aux 1 à 6 variables provenant des autres sources. Cette dimension a donc été réduite en utilisant le nombre N de variables retenues par un modèle de type LASSO comme mesure de la redondance des données d'entrée, et pour chaque calcul nous ne gardons qu'un échantillon représentatif de l'image composé des N pixels ayant la plus grande MI avec la production. Ceci permet de réduire le nombre de variables à seulement 12.

Le modèle a été évalué sur un échantillon de douze centrales ayant des puissances installées allant de 2 à 12 MW. Plusieurs modèles de benchmark ont également été développés pour comparer le modèle AnEn à l'état de l'art à la fois en termes de performance et de temps de calcul. Pour les prévisions à court-terme (horizon de +5 minutes à +2 heures), nous avons comparé notre modèle à un modèle auto-regréssif de type ARIMA, spécialisé pour la prévision court-terme, ainsi qu'à la persistance, qui prédit systématiquement la production future comme étant la production observée actuellement. Pour le long-terme (prévisions de +2h à +36h), le modèle AnEn est comparé à deux modèles non-paramétriques issus de l'état de l'art, le Quantile Regression Forest (QRF) et le modèle Automatic Relevance Determination (ARD) model. Les diférents modèles ont été entraînés sur la période couvrant Mai 2016 à Avril 2017, puis ont été évalués sur la période couvrant Mai 2017 à Avril 2018.

Les résultats ont montré que le modèle AnEn a des performances comparables voire supérieures à celle des autres modèles. En terme de temps de calcul, il est comparable pour le long-terme à celui des modèles QRF et ARD, mais bien inférieur à celui de ces mêmes modèles pour les prévisons à résolution 5 minutes. Cependant, le temps de calcul du modèle ARIMA est systématiquement inférieur.

En terme de performances, l'évaluation a été faite selon les recommandations pour les prévisions probabilistes : l'objectif est de minimiser la "sharpness" du modèle sous con-

trainte de conserver sa fiabilité, et par conséquent la fiabilité est d'abord vérifiée avant de mesurer la "sharpness". La fiabilité traduit la calibration du modèle : pour un modèle parfaitement fiable, la grandeur prédite est inférieure au quantile de niveau α exactement α % du temps. Cette propriété est fondamentale pour les prévisions probabilistes. La "sharpness" représente à quel point la distribution de probabilité est concentrée : une distribution très large et uniforme apporte peu d'information sur la situation à venir, tandis qu'une distribution concentrée porte plus d'information.

Les modèles AnEn, QRF et ARD ont des propriétés de fiabilité satisfaisantes en moyenne. Cependant, lorsque nous évaluons la fiabilité des modèles conditionnellement à l'horizon de prévision ou l'heure de la prévision, tous les modèles présentent des déviations de fiabilité. Malgré cela, les déviations restent cohérentes : nous avons calculé l'amplitude des déviations causées par la taille finie de l'échantillon d'évaluation pour un modèle parfaitement fiable. Dans la plupart des cas, les modèles restent dans cette plage d'amplitude. Il y a cependant une exception pour l'évaluation de la fiabilité conditionnellement à l'heure de prévision pour les heures autour du lever et du coucher du soleil, et particulièrement pour les modèles QRF et ARD.

Le modèle ARD a par ailleurs une moins bonne "sharpness" que AnEn et QRF qui ont une "sharpness" comparable. Cependant, le modèle AnEn a une meilleure "sharpness" pour les prévisions à court-terme, tandis que le modèle QRF est meilleur à long-terme. A niveau de fiabilité comparable, cela suggère que le modèle AnEn est plus performant à court-terme.

Pour comparer les modèles QRF et AnEn de façon plus précise, nous utilisons également le CRPS, qui est un score probabiliste qui prend en compte à la fois la fiabilité et la sharpness. Le CRPS confirme que le modèle AnEn est plus précis à court-terme tandis que le modèle QRF est meilleur à long-terme. Le modèle ARD, comme les scores de fiabilité et "sharpness" le laissaient présager, a un moins bon CRPS quelque soit l'horizon. Selon nous, ceci est dû à l'hypothèse faite par le modèle ARD que la distribution de la production est paramétrique, et plus précisément gaussienne. Cette hypothèse est très discutable, parce que la production photovoltaïque est bornée et asymétrique, contrairement à une distribution gaussienne.

Pour les prévisions de court-terme à résolution 5 minutes, l'évaluation a été faite de façon déterministe car les modèles de benchmark n'offraient pas de prévisions probabilistes. Les résultats montrent que le modèle ARIMA et AnEn ont de bien meilleurs performances que la persistance. D'autre part le modèle présente de meilleures performances que le modèle ARIMA.

Finalement, concernant les temps de calculs, le modèle AnEn est avantageux. Le modèle AnEn suit le paradigme dit de "lazy learning", c'est-à-dire que tous les calculs du modèle sont

effectués à chaque requête de prévision. Le temps de prévision du modèle AnEn est donc plus long que celui des modèles QRF et ARD, mais il ne nécessite pas d'entraînement. En outre, pour obtenir un comportement adaptatif similaire à celui du modèle AnEn, les modèles ARD et QRF doivent être entraînés pour chaque prévision, de façon à s'adapter à l'horizon de prévision et l'heure de démarrage du modèle. Pour les prévisions à résolution 30 minutes, le temps d'entraînement+prévision des modèles ARD et QRF est comparable à celui de prévision du modèle AnEn. Cependant, pour les prévisions à résolution cinq minutes, les modèles ARD et QRF sont longs à entraîner, ce qui rend leur utilisation opérationnelle impossible. Au contraire, le modèle AnEn conserve un temps de calcul raisonnable.

Pour les prévisions à court-terme, le modèle AnEn est cependant plus long à calculer que la persistance, qui ne fait que consulter l'historique de données, et le modèle ARIMA. Le gain de performance reste justifie cependant cette augmentation du temps de calcul qui ne remet pas en cause son utilisation opérationnelle.

Le modèle AnEn est donc une bonne option pour concentrer tous les besoins de prévision de la chaîne de valorisation de l'énergie photovoltaïque en un seul modèle. Bien qu'il souffre d'une performance légèrement moindre que le QRF pour la prévision à horizon J+1, cela est compensé par ses avantages opérationnels, c'est-a-dire son temps de calcul faible et son absence d'entraînement.

Chapter 4

Trading of PV power on the French EPEX SPOT market

Contents

In this chapter we apply the solutions we proposed to tackle the systematic issues of the PV power trading value chain in a simplified case where the PV producer participates in a day-ahead market only. This simplified value chain does not consider intra-day markets and hedging with storage systems, and thus is only a proof of concept of the different approaches we introduced. However, analysis of the results on this simplified value chains already

highlights some comparative results on the different approaches and trading methods. Parts of this chapter were published in article [A] in section 1.7.

4.1 Description of the case study and the trading approaches

4.1.1 Case study

In this case study, we study the participation of a PV power plant as a BRP on a day-ahead market with a dual-pricing balancing mechanism, using the generic notations of the PV power value chain described in chapter 2. This market structure describes several European markets such as EPEX SPOT in France or NordPool in Northern Europe. The market structure assumed is:

- A day-ahead market where each participant has to submit buying or selling orders the day before delivery.
- A balancing mechanism where each BRP has to take financial responsibility for its imbalances.

These two markets are sequential, as explained in 2. First, the producer submits its bids for the next day. Then after delivery, the producer, which is also a BRP, pays the TSO for its imbalances through the balancing market. Intra-day markets that can correct the producer's position during the delivery day are not considered at this stage but will be studied in chapter 4.

A dual-pricing electricity market refers to the case where imbalances are settled through two different prices depending on their sign. Usually, if the producer produces more energy than it has sold, then the excess energy is sold at a price lower than the spot prices for this market time unit. On the contrary, when the producer produces less than it has sold, it has to buy the lacking energy at a price higher than the spot price for this market time unit.

This case study is well known and several papers propose solutions for trading in such a market structure. In [124] and [125], the authors proposed to minimize the expected balancing costs based on scenarios of wind power generation and imbalance prices. In [41], the authors propose a closed-form solution to the optimal bidding problem, assuming that the spot price is independent from the bids. Some refinements over this methodology were proposed in [126] and [127]. More recently, authors considered also game theory [128] or strategic reserve purchase [129] to improve the revenue, however in this case study we restrict ourselves to a day-ahead electricity market only. In this thesis, as explained in chapter 1, we do not aim to improve the trading strategy but rather to improve the revenue by addressing

two issues. The first is the gap between the accuracy of the individual forecasting models and the actual value of their forecasts, and the second is the overall complexity of the value chain. Therefore, we use this case study to show how using the value function to train the models and replacing the complex series of forecasting models by a single ANN can lead to different bidding behaviors and improved revenue.

Under the assumed market structure, the revenue of a producer for a given market time unit is obtained with equation (2.3):

$$R(E_c) = \pi_s E_c + \begin{cases} \pi_+(E - E_c) \text{ if } E > E_c \\ \pi_-(E - E_c) \text{ if } E < E_c \end{cases} \tag{4.1}$$

where E_c is the energy sold by the producer, E is the actual delivered energy, π_s is the spot price that is given by the market clearing after the bids from all market participants have been submitted, and π_+ and π_- are the imbalance prices for positive and negative imbalances, computed by the TSO, depending on the cost it had to meet to compensate the producer's imbalances.

We propose two approaches for trading the PV power as depicted in Fig. 4.1.

4.1.2 First approach

In this approach, we keep the standard model chain for RES energy trading on electricity markets, where RES power and market quantity forecasts are first produced, then used by a trading strategy that estimates the optimal bids. However, we propose a global optimization loop that optimizes the whole model chain using the revenue generated on the electricity market as the objective function following the Method 2 for training the models introduced in chapter 2. This approach is called A1-M2, and it is compared to the standard approach called A1-M1, where we optimize the models separately to maximize their performance following the training method Method 1, then inject their forecasts into the trading strategy.

In this test case, following the notations from section 2.2, we have four individual models:

- $M_1^{\Theta_1}$, which forecasts the PV power with parameters Θ_1
- $M_2^{\Theta_2}$, which forecasts the spot price with parameters Θ_2
- $M_3^{\Theta_3}$, which forecasts the imbalance price for negative errors with parameters Θ_3
- $M_4^{\Theta_4}$, which forecasts the imbalance price for positive errors with parameters Θ_4

Approach 1 is the most frequent approach in the literature. In most cases, deterministic or probabilistic forecast of the variable resource and electricity market prices are produced,

an then an optimal bid is derived. To perform this approach, numerous works focused on the three required components that are intermittent resources forecasts, electricity price forecasts, and deriving optimal bids.

4.1.3 Second approach

The second approach that we propose is called Approach 2. It consists in bypassing the individual forecasting models, and replace them with a unique ANN model that directly provides the decision, as shown in Fig. 2.5. The inputs and outputs of this unique model are the same as the inputs and outputs of the global decision-making process.

In this case, the only way of training the model is to use directly the loss function i.e. the revenue on the electricity markets, since there are no intermediary models. Thus, Methods 1 and 2 for training the models are equivalent. To our knowledge, no work proposed similar approaches, that allow participating in electricity markets without required production forecasts.

We also compare the three approaches with an even simpler one referred to as A0, where the bids on the electricity market are simply the expectation of the PV power generation. Approaches A1-M1, A1-M2 and A2 are represented on Fig. 4.1.

4.2 Approach 1: dedicated forecasting models

4.2.1 PV power forecasting model

In this chapter as in the remainder of the thesis, we always use the seamless forecasting model presented in chapter 3 to obtain the PV power forecasts.

4.2.2 Trading strategy

Along with PV power forecasts, a trading strategy that requires price forecasts is also required to perform the approach A1. The strategy we used is described in [41]. It relies on the hypothesis that the RES producers' bids have no influence on the spot price ("price taker" hypothesis). This hypothesis is true at the national level when the penetration of price takers is low. However, since increasing numbers of RESs are participating in electricity markets, usually following a price-taker strategy, the influence of RES bids on the spot price can become significant. However, since we deal with individual power plants, their output is small compared to the volume of electricity traded on the market and thus we neglect this effect.

Based on equation (4.1), we can rewrite the revenue of a producer as follows:

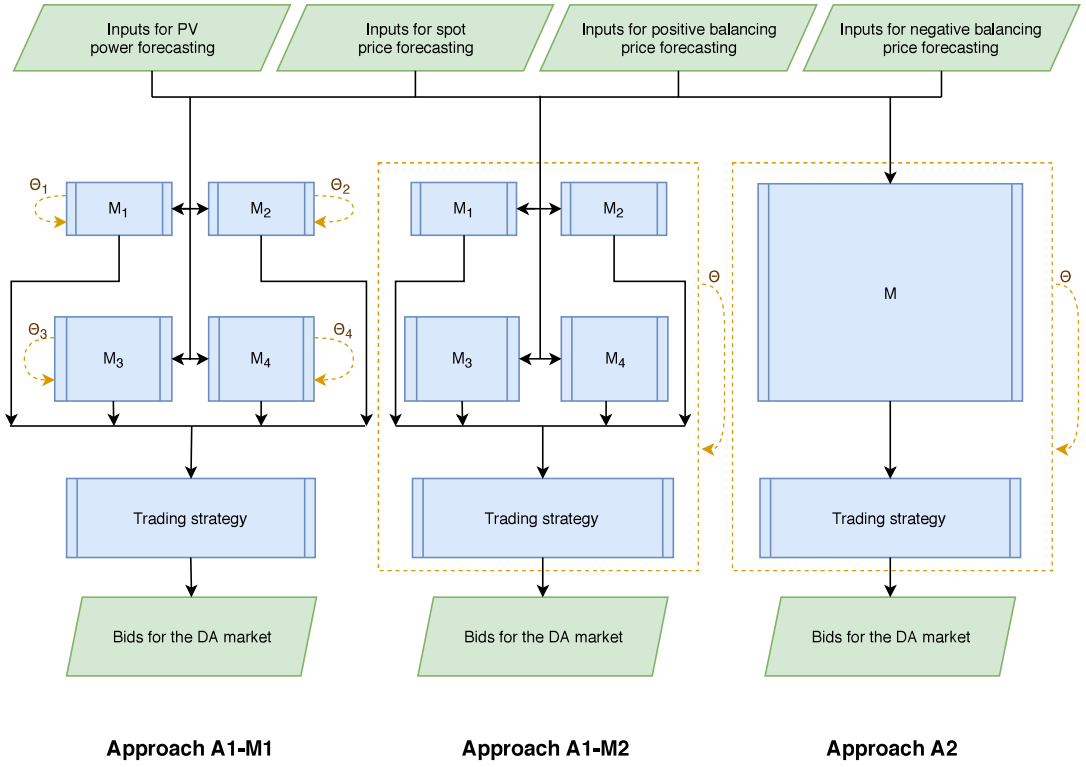

Figure 4.1: Flowchart of the different approaches

$$R(E_c) = \pi_s E_{PV} - (\pi_s - \pi_B)(E_{PV} - E_c) \tag{4.2}$$

$$\pi_B = \begin{cases} \pi_+ \text{ if } E_{PV} > E_c \\ \pi_- \text{ if } E_{PV} < E_c \end{cases} \tag{4.3}$$

With this formulation, we can see that the first term in (4.2) is independent from the bid, as the price-taker hypothesis states that π_s is independent from E_c, and so is the actual energy produced by the PV plant E_{PV}. Thus, maximizing the revenue is equivalent to minimizing the penalty function $Pen(E_{PV}, E_c) = (\pi_s - \pi_B)(E_{PV} - E_c)$. Generally, the prices π_+ and π_- are bounded by the spot price π_s so that the penalty term is always positive. The optimization problem that gives the optimal bid E_c^* is then:

$$E_c^* = argmin_{E_c \in [0, E_n]} \{\mathbb{E}[Pen(E_{PV}, E_c)]\} \tag{4.4}$$

$$E_c^* = argmin_{E_c \in [0, E_n]} \left\{ \int_0^{E_n} Pen(x, E_c) f_{PV}(x) dx \right\} \tag{4.5}$$

Replacing $Pen(E_{PV}, E_c)$ by its actual value, we obtain:

$$E_c^* = argmin_{E_c \in [0, E_n]} \left\{ \int_0^{E_n} (\pi_s - \pi_B)(x - E_c) f_{PV}(x) dx \right\} \tag{4.6}$$

This problem is known as the newsvendor optimization problem. The exact solution is given by [41]:

$$E_c^* = F_{PV}^{-1} \left(\frac{\pi_s - \pi_+}{\pi_- - \pi_+} \right) \tag{4.7}$$

where F_{PV} is a forecast CDF of the energy production of the plant. The application of this strategy for an RES power plant then requires input from a probabilistic RES power forecasting model, and from spot and imbalance price forecasting models.

4.2.2.1 Forecasting market quantities

At the time of the bids, we are not yet aware of the three prices π_s, π_+ and π_-. Therefore, we have to implement a forecasting model for these three market quantities.

We use Support Vector Regression (SVR) to obtain a deterministic estimate of the spot price, using as inputs the day of the week, time of day, a forecast of the national energy demand provided by the TSO, and the spot price observed the day before at the same time. SVR models are a machine learning technique commonly used for energy price forecasting [130]. The SVR model uses a radial kernel with a parameter γ and we use a parameter C to penalize the constraint violations.

The other prices π_+ and π_- are forecast with a simple k-Nearest Neighbor (kNN) estimator, using the predicted spot price as a feature. The only parameters we use are then n, the number of neighbors we retain, and L_{Price} the length of the period over which we look for neighbors. Depending on whether these parameters relate to the positive or negative imbalance price-forecasting model, they are noted $\{n_+, L_{Price_+}\}$ or $\{n_-, L_{Price_-}\}$. As for the AnEn model, these parameters allow us to control the bias-variance trade-off.

In many electricity markets, the rules for deriving the imbalance prices are also dependent on the state of the power grid. For example in the Nord Pool electricity market, the imbalance prices are equal to the spot price depending on whether the power grid is in excess or in shortage of electricity at the national level. For example, if the grid is in shortage of electricity at the national level, the price for positive imbalances is equal to the spot price. For an independent producer in positive imbalance, everything happens as if it had no imbalance: its excess energy is paid at the spot price. In the first case study in France, there are no such rules under the French TSO rules and so we do not consider

forecasting the power grid state. For the second test case in Danemark, these rules exist, but for consistency with the method used in the first test case, we do not consider forecasting the power grid state. Besides, many TSOs are planning to move to single-pricing schemes for balancing energy. In such cases, the prices π_+ and π_- and the forecast of the power grid state is implicit depending on whether the forecast imbalance price is higher or lower than the forecast spot price, and so it should not be detrimental to not consider explicitly forecasting the state of the power grid.

4.3 Approach 2 : direct bidding through neural networks

With approach A2, we do not use any intermediary model as with A1. We use a single model M whose output is directly the decision for each decision process. Thus, according to the notations from 2, the decision model T is simply the identity.

For each decision process, the model M that we use to provide the decision is an ANN. Models from the ANN family are generally trained using the backpropagation algorithm. This algorithm makes the training of the network very efficient. However, it can only be used when the objective function of the network is differentiable. This is not usually the case in this thesis since the network is trained using an arbitrary function to derive the value of the decision e.g. the revenue generated from the bids. However, in most parts of the value chain, the objective function is a multiplication of the forecast error by the penalty price, which is easily differentiable with respect to the bid. There is sometime a non-linearity caused by the dual-pricing rule. In that case, the objective function is dependent on the sign of the forecast error which adds a sign check in the objective function. However, the gradient of such an operation is easily defined outside of 0, which allows implementing an ANN without much complications.

The main risk with this model is overfitting. Since the typical number of parameters of ANNs is significant, they can easily memorize the entries from the training set to achieve high accuracy on the training without developing the ability to generalize. However, many machine-learning techniques exist to limit the overfitting of these models such as cross-validation, regularization or dropout layers.

4.4 Trading results from the two approaches

4.4.1 Overall trading results

We present results from the two proposed approaches for the participation of twelve PV power plants located in France. In-situ measurements of power injected into the grid, local temperature, and solar irradiance are available for the twelve plants from January 2014 to January 2018.

For approaches A1-M1 and A1-M2, the model chain is optimized by solving the optimization problems formulated in Section 2.2 over the training set. Then, the optimal chain is used to obtain bids for the testing set. For approach A2, we used the machine learning library *PyTorch* [131] to implement and train an ANN for each of the plants considered in the study. The ANN models use as input the union of the inputs of the AnEn power forecasting model (i.e. measurements, NWPs and clear-sky profile) and the price quantities forecasting models (i.e. TSO forecasts of the national demand and RES power generation, and spot price observed the day before at the same time). This represents a total of eleven input features. The ANN model uses a single hidden layer of 20 artificial neurons, and an output layer of one neuron since only a single value is expected from the ANN. The models were trained using a 10-fold cross-validation on the period from May 2015 to May 2016 with the Adam optimizer [132] on 100 epochs, a learning rate of 0.001 and a batch size of 16. The trading evaluation was made for the period from May 2016 to May 2017.

Fig. 4.2 shows the results from the different approaches for a given trading day. This specific day is chosen for illustrative purposes. Approach A2 is much more conservative than the other ones. This results in a negative MBE that will be studied in Section 4.4.3. Besides, it is interesting to note that approaches A1-M1 and A1-M2, which use a PV power forecast model, tend to produce bids that are more volatile, while A2 tends to produce smoother bids. Finally, while A1-M1 and A1-M2 both use market information and thus do not only rely on PV power forecasts, A2 proposes bids that deviate comparatively more from the PV power expectancy, because of its revenue-focused optimization.

4.4.2 Evaluation of the trading approaches

The whole results are summarized in table 4.1. The performances of the different approaches for the different plants are compared on Fig. 4.3. The strategy that generates the best revenue varies considerably between all of the plants studied, although all approaches seem to generate very similar revenues.

On the 12 plants, none obtained the best revenue with approaches A0 or A1-M1, 7 with

Table 4.1: Complete results

Plant	Approach	Imbalance	Penalties	Net revenue	Penalty per imbalance
		%	€	€	€/MWh
	A0	**30.59**	2.23	41.87	7.30
P1:	A1-M1	30.97	2.25	41.86	7.26
9 828 kWp	A1-M2	31.20	**2.11**	**41.97**	**6.77**
	A2	33.69	2.44	41.64	7.24
	A0	27.57	1.99	40.37	7.21
P2:	A1-M1	27.72	1.96	40.39	7.08
2 694 kWp	A1-M2	**27.44**	1.84	40.52	6.70
	A2	30.39	**1.76**	**40.61**	**5.79**
	A0	**22.88**	1.82	41.25	7.94
P3	A1-M1	22.91	1.77	41.30	7.72
10 009 kWp	A1-M2	22.95	1.61	41.44	7.00
	A2	25.80	**1.43**	**41.66**	**5.54**
	A0	**28.18**	2.01	39.07	7.12
P4:	A1-M1	28.66	2.02	39.06	7.05
6 876 kWp	A1-M2	28.44	**1.87**	**39.20**	6.59
	A2	30.04	1.96	39.12	**6.52**
	A0	**31.53**	2.28	36.98	7.23
P5:	A1-M1	32.08	2.29	36.96	7.15
4 296 kWp	A1-M2	31.83	**2.16**	**37.09**	6.80
	A2	34.78	2.33	36.93	**6.69**
	A0	**30.70**	2.14	39.37	6.97
P6:	A1-M1	31.06	2.16	39.35	6.96
11 994 kWp	A1-M2	31.18	**2.04**	**39.48**	6.53
	A2	33.35	2.56	38.96	**6.45**
	A0	**28.56**	1.83	38.84	6.41
P7:	A1-M1	28.99	1.86	38.81	6.42
5 064 kWp	A1-M2	29.02	**1.73**	**38.94**	**5.97**
	A2	31.72	1.90	38.77	5.98
	A0	**32.26**	2.20	37.37	6.82
P8:	A1-M1	32.30	2.17	37.40	6.72
9 504 kWp	A1-M2	32.81	2.10	37.46	6.41
	A2	39.94	**1.89**	**37.68**	**4.74**
	A0	**29.58**	2.18	39.35	7.37
P9:	A1-M1	30.03	2.19	39.34	7.29
9 504 kWp	A1-M2	29.85	**2.06**	**39.47**	6.89
	A2	32.97	2.17	39.35	**6.59**
	A0	**28.09**	1.88	38.49	6.68
P10:	A1-M1	28.38	1.87	38.50	6.58
4 224 kWp	A1-M2	28.32	1.76	38.61	6.21
	A2	31.94	**1.73**	**38.64**	**5.41**
	A0	**28.68**	1.84	36.81	6.42
P11:	A1-M1	28.84	1.80	36.85	6.25
3 300 kWp	A1-M2	28.82	**1.69**	**36.96**	5.86
	A2	33.41	1.90	36.75	**5.69**
	A0	28.94	1.83	36.88	6.31
P12:	A1-M1	**28.92**	1.81	36.90	6.24
2 610 kWp	A1-M2	29.31	**1.74**	**36.97**	5.93
	A2	31.17	**1.74**	**36.97**	**5.58**
	A0	**17.46**	1.44	40.41	8.26
Aggregation:	A1-M1	17.9	1.44	40.41	8.06
79 903 kWp	A1-M2	18.78	**1.23**	40.59	6.69
	A2	21.83	1.43	**40.69**	**6.56**

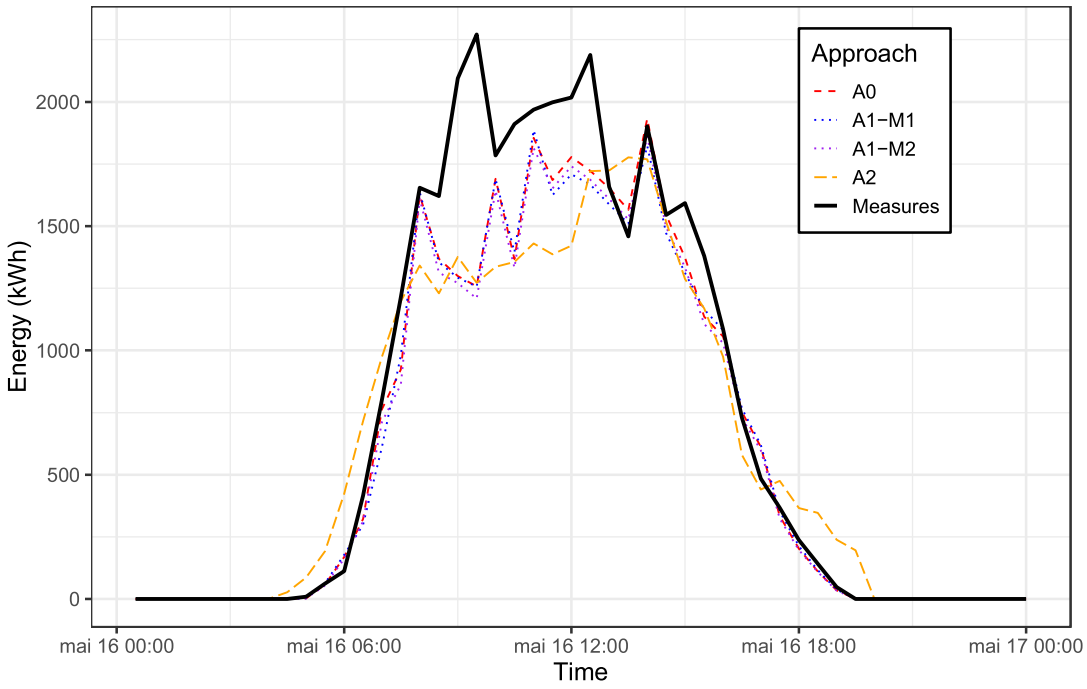

Figure 4.2: Example bids from the approaches A0, A1-M1, A1-M2 and A2 for day 2016-05-16

approach A1-M2, and 4 with approach A2, and approaches A1-M2 and A2 tied on the last plant. No approach stands out significantly from the others in terms of net revenue. A1-M2 and A2 produced the best results for all plants, which suggests that it is worth using revenue as the objective function.

Overall, method A1-M1 seems more efficient. However, it is interesting that approach A2 systematically causes the highest imbalances, yet produces the lowest penalty per imbalance. Thus, it seems that the ANN model involved in this approach focuses more on reducing errors when the imbalance prices are significant than on reducing the total amount of errors.

More generally, the more market information the approaches include, the more imbalances they generate, but with fewer penalties per imbalance as can be seen from Fig. 4.3 and table 4.1. A1-M1 generates a low error but a high penalty per imbalance. When using A1-M2 instead of A1-M1, and thus incorporating market information in the PV power forecasting model, the imbalances increase but the penalties per imbalance decrease. Finally, A2 results in the most imbalances but the lowest penalties per imbalance.

The participation of the 12 aggregated plants is also studied and represented on Fig. 4.3. It is clear from the figure that the aggregation of the 12 plants has a better predictability

Table 4.2: Comparison of the revenue generated from the aggregation and the average revenue of the individual plants weighted by their nominal power (€/MWh)

	A0	A1-M2	A1-M2	A2
Weighted average revenue	39.28	39.29	39.41	40.69
Aggregation	40.41	40.41	40.59	39.3

thanks to the smoothing effect, as it achieves the lowest relative amount of imbalances and penalties. However, it seems that the penalties decrease less than the imbalances, since the average penalties per imbalance is high compared to individual plants. In the end, it is still beneficial to operate the 12 plants together: table 4.2 shows that for all approaches, the revenue of the aggregation is approximately 3% higher than the mean revenue of the individual plants weighted by their nominal power.

4.4.3 Behavior of trading strategies

To understand the reason why the different approaches perform differently, we analyze the bidding behavior of the different approaches. First, we analyze the MBE in the bids to understand how the different approaches use the market information. Table 4.3 shows the average MBE of the approaches over all of the N_p plants.

$$MBE = \frac{1}{N_p} \sum_{i=1}^{N_p} \overline{\frac{(E_{PV} - E_c)}{E_{n,i}}} \tag{4.8}$$

From the bids' error statistics, we can see that adding market information to PV power forecasts without considering the value creates a significant MBE, because the bids are not the expected outcome of the distribution, but a given quantile that depends on market information. Depending on how often positive or negative errors are penalized, the bids can then show a tendency to prefer positive or negative errors. In general, positive errors were more often penalized than negative errors during our testing period. However, the negative errors were penalized by 21.2 €/MWh on average, while the positive errors were penalized by only 10.3 €/MWh. This is consistent with the fact that the power grid is more often in excess of energy since the TSO has to hedge against worst cases of production, but the impact of a negative error when the power grid is in shortage of energy has a higher impact. Approach A1-M1 uses this first effect to propose aggressive bids, while A1-M2 prefers the second effect to have conservative bids. For approach A2 however, the bids acquire a small positive MBE, which suggests that it has a slightly conservative bidding policy.

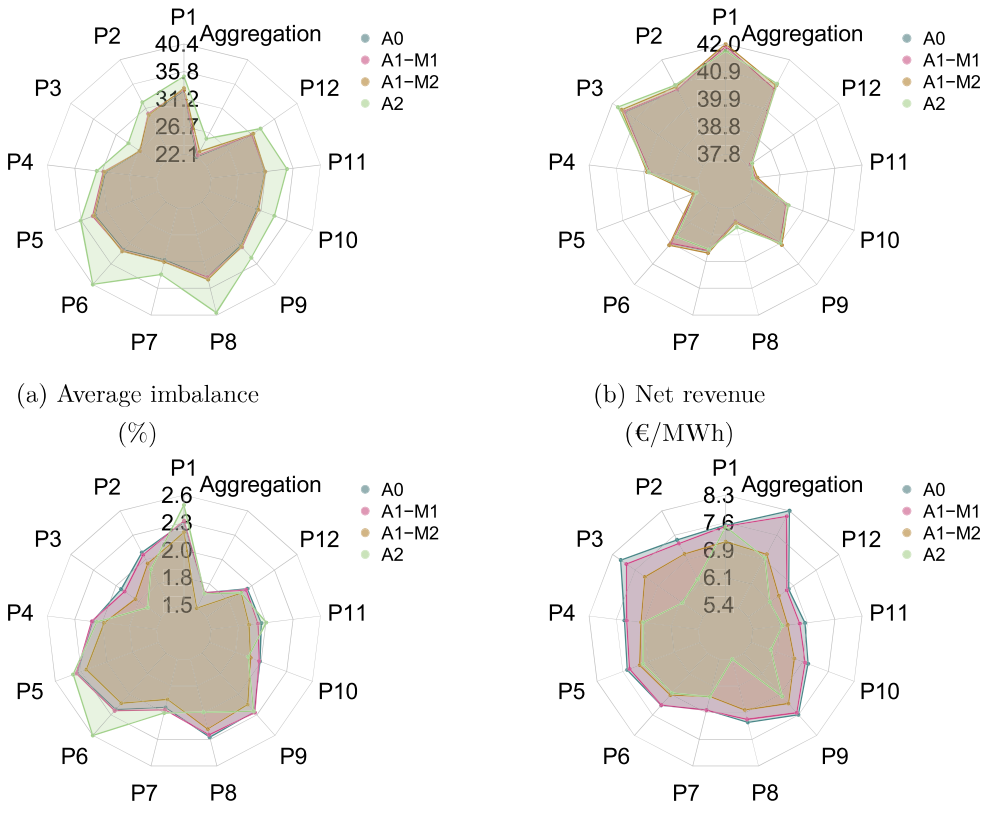

(a) Average imbalance (%)

(b) Net revenue (€/MWh)

(c) Average penalties (€/MWh)

(d) Average penalty per imbalance (€/MWh)

Figure 4.3: Results comparison of the different approaches

Table 4.3: Average MBE of the different trading approaches

	A0	A1-M2	A1-M2	A2
MBE (%)	-0.09	-0.15	0.22	0.04

Table 4.4: Trading results on the testing period (Jan 2009 - October 2009)

		Forecast RMSE	Absolute Bids Error	Penalties	Net Revenue	Penalty per Imbalance
		%	MWh	DKK	DKK	DKK/MWh
P1	A0	14.0	654	14 969	334 704	22.4
	A2	-	657	14 317	335 357	21.8
P2	A0	15.6	746	17 896	379 988	22.9
	A2	-	775	17645	380 239	22.8
P3	A0	15.0	705	15 303	323 179	21.2
	A2	-	720	14 874	323 608	20.7
P4	A0	16.6	785	17 279	367 804	22.2
	A2	-	757	16 841	368 242	22.3
P5	A0	16.3	764	18 681	365 797	23.8
	A2	-	797	18 784	365 695	23.6
P6	A0	19.0	946	22 711	438 805	23.2
	A2	-	970	21 043	440 473	21.7
P7	A0	16.5	774	19 055	358 754	23.2
	A2	-	814	18 322	359 487	22.5
P8	A0	15.6	752	15 473	386 620	21.6
	A2	-	751	15 193	386 900	20.2
P9	A0	16.1	757	17 082	352 124	22.3
	A2	-	762	17 279	351 928	22.7

Another effect can also be identified when looking at the evaluation results. We looked at the spread of the errors over the magnitude of the imbalance prices for both positive and negative imbalances, in order to understand how the second approach could generate lower penalties with higher imbalances. The results are shown on Fig. 4.4 for plant P4 as an illustration, and show that the errors with approach A2 are concentrated on low penalty levels, especially for negative errors. So even if approach A2 generates more imbalance, it is better at understanding at what time the imbalance prices are high, and so can still be competitive regarding the actual penalties.

4.5 Extension to wind power in the NordPool market

In this section, we aim to illustrate the fact that the solutions we propose for solving the systematic issues of PV power trading can be used in a large variety of settings, since they are generic. Here we apply them to the participation of a wind producer in the electricity market NordPool. This test case is intended to illustrate the common case of a RES producer that does not have the means to produce its own forecast, and thus buys forecasts from a

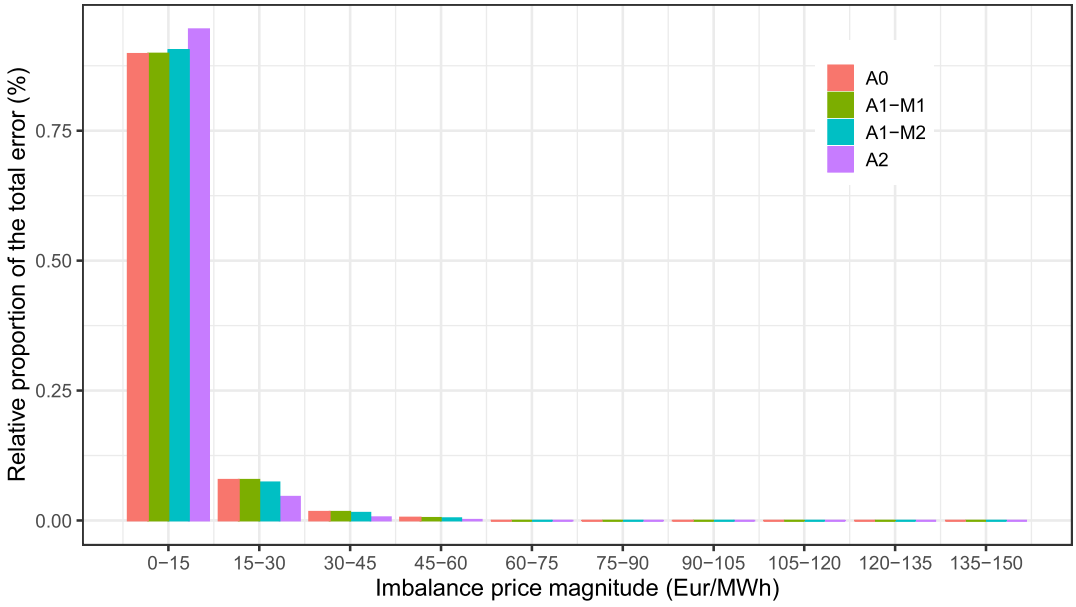

(a) Positive errors

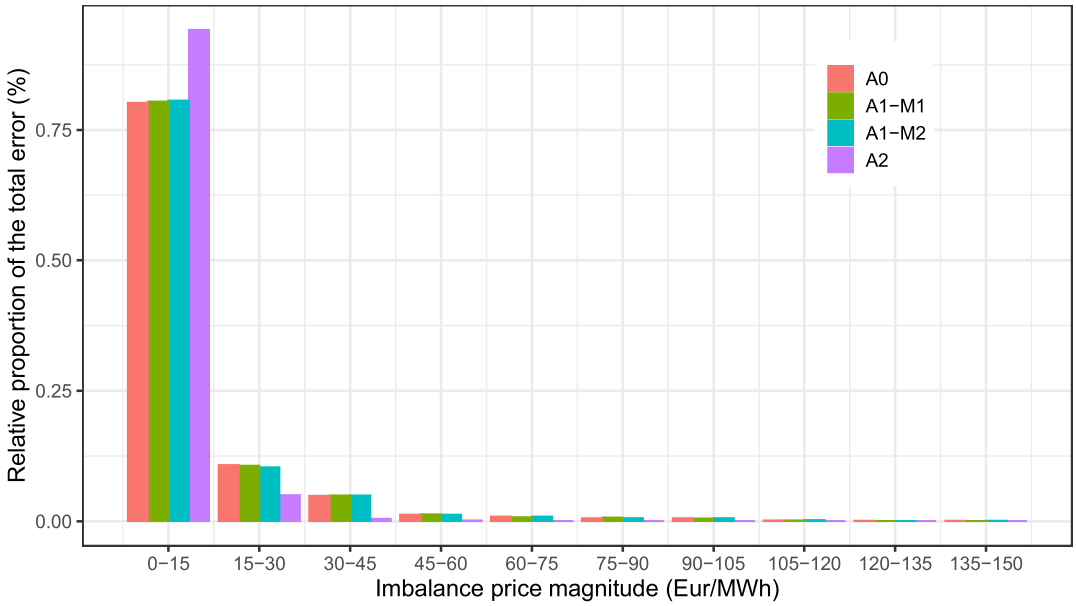

(b) Negative errors

Figure 4.4: Cumulated errors depending on imbalance price magnitude

third party. The goal is to show that even with limited input, the replacement of the chain of models by a single ANN can improve the energy value.

All data relative to the wind power come from [133]. The forecasts are obtained using regression forests and are deterministic. Therefore, in the following methodology, the CDF of the wind power forecasts F_w are considered to be a Heaviside function centered on the deterministic forecast E_w:

$$F_w(x) = 1 \text{ if } x > E_w, \text{ 0 otherwise} \tag{4.9}$$

Note that in this case, market quantity forecasts cannot be used since they are used to derive an optimal quantile of the CDF to bid on the electricity market, which will always reduce to the deterministic forecast of the wind power.

Besides, since we do not dispose of our own forecast model, we cannot apply the different training methods since there are no models to train. Thus, only two strategies can be evaluated: strategy A0, where the deterministic wind power forecast is bid on the electricity market, and strategy A2, where the deterministic wind power forecasts are used as inputs for the ANN.

We study the output from nine wind power plants located in Denmark. In situ measurements of energy generation are available from January 2008 to October 2009. The year 2008 was used as the training period, and the period from January to October 2009 as the test period.

Approach A0 is implemented by bidding the deterministic wind power forecasts. For Approach A2, the ANN uses only the deterministic wind power forecasts as inputs. Results from the two approaches are summarized in Table 4.4. In this study, Approach 2 consistently produces more imbalances again, however it almost always outperforms the benchmark.

This study consolidates the fact that the second approach produces bids that cause more imbalances, but lowers the average amount of penalties paid for any imbalance. With PV power on EPEX SPOT, this did not systematically generate a higher revenue, however with wind power in NordPool, the revenue was higher with the second approach for 7 out of the 9 plants.

4.6 Conclusions

Overall, the models adapt in different ways to minimize revenue. A1-M2 tends to re-calibrate the bidding process after incorporating market information. A2 behaves differently, as it tends to offer lower bids than the expected production. This is because negative errors are

usually penalized more heavily than positive ones. This approach is also much better at identifying instants when the imbalance prices are high, with most of its errors occurring when the imbalance price is low. However, since it does not rely on PV power forecasts, it creates more imbalances than A1-M2.

The difference between approaches A1-M1 and A2-M2 highlights the impact of training the individual models for value instead of accuracy. This difference is similar to the difference between A1-M2 and A2: model A1-M2 usually generates more imbalance than A1-M1 but less penalties, which ultimately generates a better revenue.

The choice of a given approach depends highly on the context. The difference in revenue is not significant and should not be a sufficient incentive for the energy producer to choose one approach rather than another. However, the actual bidding behavior could be relevant for choosing an approach. In a system where the difference between imbalance prices and spot prices can be very large, A2 would be preferable, since it concentrates the imbalances when this difference is low. On the other hand, when this difference is almost always low, any of the other approaches would be more beneficial: all approaches would try to bid the exact forecast, but approaches A1 seem to be more efficient at this. If the imbalance prices correctly translate the most preferable approach for the grid, the amount of penalties would be a sufficient criterion to decide on the best approach, because in that case, the approach that is the most supportive of the grid would also be subject to fewer penalties.

Chapter summary in French

Description du cas d'étude

Dans ce chapitre, nous présentons l'étude d'un premier cas d'étude en appliquant les solutions proposées pour traiter les problèmes structurels de la chaîne de valorisation de la production PV présentées dans les chapitres précedents. Ce cas d'étude est celui d'un producteur PV vendant son énergie dans un marché day-ahead tout en étant financièrement responsable de ses écarts auprès du gestionnaire de réseau.

La règle de pénalisation des écarts est celle du "dual-pricing", c'est-à-dire qu'il y a deux prix de réglèment des écarts : un pour les écarts positifs (la production est supérieure à la quantité vendue) et un pour les écarts négatifs (la production est inférieure). Cette règle est par exemple celle du gestionnaire de réseau français RTE et de nombreux gestionnaires de réseau en Europe du nord comme Statnett en Norvège ou Energinet au Danemark.

Ce cas d'étude a été étudié à de nombreuses reprises dans la littérature. Dans cette thèse, il sert à évaluer la capacité d'amélioration du revenu des solutions que nous proposons dans une chaîne de valorisation simplifiée. Ces solutions comprennent :

- L'utilisation du modèle AnEn présenté au chapitre 3 pour obtenir les prévision PV.
- L'implémentation de deux approches pour obtenir les offres pour le marché de l'électricité. La première notée A1 conserve la chaîne classique de modèles de prévisions de prix et de production individuels, la deuxième notée A2 utilise un réseau de neurones artificiels de façon à simplifier la chaîne de valorisation.
- L'implémentation de deux méthodes d'entraînement pour les modèles, la première notée M1 visant à maximiser leur performance de prévision individuelle, la deuxième notée M2 visant à maximiser la valeur de la décision associée sur le marché de l'électricité.

On obtient finalement quatre possibilités selon qu'on utilise l'approche A1 ou A2, et la méthode d'entraînement M1 ou M2. En pratique, les deux méthodes d'entraînement sont identiques pour l'approche A2 puisque il n'y a qu'un seul modèle, dont la sortie est directement la décision optimale, ce qui laisse finalement les possibilité A1-M1, A1-M2 et A2. Par ailleurs, nous comparerons également ces possibilités avec un solution de réference A0, pour laquelle l'offre soumise au marché de l'électricité est simplement la meilleure estimation de la production PV.

Approche 1

Pour l'implémentation de cette approche, quatre modèles sont nécessaires:

- $M_1^{\Theta_1}$ qui prévoit la production PV
- $M_2^{\Theta_2}$ qui prévoit le prix spot de l'électricité
- $M_3^{\Theta_3}$ qui prévoit le prix de réglement des écarts négatifs
- $M_4^{\Theta_4}$ qui prévoit le prix de réglement des écarts positifs

Les bonnes propriétés du modèle AnEn en terme de performance comme de coût de calcul nous ont incité à le garder comme modèle pour effectuer la simulation de la participation de la centrale PV au marché de l'électricité. Les prévisions de prix spot ont été réalisées par un modèle de type SVM fréquemment utilisé, en exploitant en données d'entrée des prévisions de consommation nationale et de production d'énergie intermittente réalisées par le gestionnaire de réseau. Le prix de réglement des écarts a été calculé par une approche des k plus proches voisins. Finalement, la combinaison de la sortie des différents modèles a été calculée en utilisant un résultat de la littérature qui montre que l'offre de vente optimale dans le sens où elle minimise les pénalités est donnée par:

$$E_c^* = F^{-1}\left(\frac{\pi_s - \pi_+}{\pi_- - \pi_+}\right) \tag{4.10}$$

Où F est la fonction de répartition de la production PV, π_s le prix spot et π_- et π_+ les prix de réglement des écarts négatifs et positifs.

Approche 2

L'approche A2 consiste à utiliser directement un modèle ANN pour obtenir les offres de vente d'énergie. Il n'y a donc qu'un seul modèle M^Θ impliqué. Le réseau a été entraîné pour maximiser le revenu géneré sur le marché day-ahead. Pour cela il dispose en données d'entrée des mêmes variables que pour la prévisions de production PV et de prix utilisées dans l'approche A1.

L'objectif est que le modèle apprenne par la fonction de revenu les tendances systématiques du marché et parvienne à offrir des offres de vente stratégiques, conditionnelles à la prévision de la situation en termes de production PV et de consommation et production intermittente nationale.

Résultats

Les deux approches on été effectuées sur la période allant de Mai 2016 à Mai 2017. La différence entre les approaches A1-M1 et A1-M2 sont assez faibles, tant en terme de comportement que de résultats. L'approche A2 au contraire présente un comportement assez différent en développant un biais assez marqué comparé aux autres approches, ce qui génère des offres de ventes conservatrices.

Ceci s'explique par le fait que le prix moyen de pénalisation des écarts négatifs est plus élevé que celui des écarts positifs. L'approche A2 semble avoir appris cette tendance et propose donc des offres conservatrices pour éviter d'être en situation d'écart négatif. Cela génère naturellement un volume d'écart plus important mais un montant de pénalités plus faible. Cela devient encore plus évident lorsque l'on regarde le montant moyen de pénalités par volume d'écart : l'approche A2 est sytématiquement celle ayant le montant moyen le plus bas. A l'inverse les approches A1-M1 et A1-M2 génèrent un volume moyen d'écart plus faible, mais ont un montant de pénalités similaire et paient en moyenne plus de pénalités pour chaque volume d'écarts.

Au final, le meilleur revenu a été obtenu avec l'approche A1-M2 pour 7 des 12 centrales, avec l'approche A2 pour 4 centrales et les deux approches A1-M2 et A2ont obtenu le même résultat pour la dernière centrale. Les différences de résultat sont assez faibles, ce qui rend difficile le choix d'une approche par rapport à l'autre. Il est cependant rassurant de constater que toutes les approches exploitant des informations de prix génèrent de meilleurs revenus que l'approche de benchmark A0. Finalement, le choix de l'approche doit être guidé par le comportement que l'on souhaite favoriser. Si l'on souhaite minimiser les erreurs de production PV dans un contexte ou les erreurs sont pénalisées uniformément e.g. l'appel d'offres AO CRE ZNI 3 en France [24], l'approche A1 semble plus pertinente. Si au contraire on est dans un contexte où les variations de prix sont importantes et qu'on s'attend à ce que les informations de marché soient plus déterminantes que les informations météorologiques, il peut être judicieux de choisir l'approche A2.

Remarquons finalement qu'avec une règle de pénalisation des écarts idéale, les comportements bénéfiques pour le réseau (offrir le montant le plus proche de l'estimation de la prévision PV) devraient être ceux qui sont les plus incités financièrement pour le producteur PV, et donc que les deux approches A1 et A2 devraient converger vers le même comportement.

Chapter 5

Trading with a storage system

Contents

In this chapter we apply the solutions we proposed in chapter 2 to the whole PV power value chain. We do not restrict ourselves to the bidding phase as in chapter 4, but we also consider the operation phase with both intra-day trading and hedging with a storage system. Parts of this chapter were published in article [B] in section 1.7.

We trained all individual models with method M2 i.e. by maximizing the value of the related decision-making process. Thus, we do not compare the two training methods M1 and M2 introduced in chapter 2, since the study from 4 suggested that training method M2

was more efficient regarding revenue. Therefore, we only study the difference between the approaches based on individual forecasting models (approach 1) and ANNs (approach 2).

5.1 Description of the case study

In this chapter, we propose to extend the case study from chapter 4 by also considering the operation phase that was described in chapter 2. To have more degrees of freedom in the operation phase, we consider the addition of a Battery Energy Storage System (BESS) coupled with the PV power plant. This choice is also motivated by the fact that such systems are expected to play a big role for power grids, since they can balance forecast errors from uncertain energy generation sources and TSOs are forbidden to own or manage storage facilities for this purpose [134]. We evaluate through this case study the profitability of PV/BESS systems in current market conditions.

The market structure considered in this section is an extension of the case study from chapter 4. We still have a day-ahead market where each participant has to submit buying or selling orders the day before delivery and a balancing market where each BRP has to take responsibility for its imbalances, but we also consider an intra-day market in the operation phase.

On the intra-day market, each participant can submit an offer up to 30 minutes before delivery in order to compensate its imbalance. As described in chapter 2, intra-day markets usually follow a continuous trading paradigm. That is, a selling (resp. buying) offer is accepted whenever a matching buying (resp. selling) offer is submitted by another party. This generates additional uncertainty on the revenue, since there is no way to know for sure if an offer would have been accepted when simulating using past time series. This was not the case with the day-ahead market where the price taker hypothesis could guarantee that the offers were accepted. As a result, the simulation of the intra-day market participation requires modeling the acceptation or rejection of the intra-day offers.

In the end, there are three consecutive decisions to make:

- How much energy to offer on the day-ahead market at D-1, 12 a.m.
- How much energy to offer on the intra-day market at M-30.
- How much energy to charge/discharge from the BESS. This decision should be taken as close to real-time as possible. Given the available data, we can run simulations with a 5-minute time step and thus this decision is taken at M-5.

Given the market structure of this case study, we can derive the revenue of a producer. As explained previously, the revenue of a producer that participates in a day-ahead and intra-day market with a dual-pricing balancing mechanism follows equation (2.4). We reformulate it by differentiating the part of the production E that comes from the PV panels E_{PV} and the part that comes from the BESS E_{BESS}.

We also introduce a term $C(E_{BESS})$, that reflects the cost due to the ageing of the BESS when used to deliver the amount of energy E_{BESS}. This cost is obtained with the rainflow counting algorithm [135], [136]. The ageing of the BESS can be divided into two components: cycling ageing which is caused by the actual usage of the BESS and calendar ageing, which is the degradation caused by time. In the remainder of the thesis, we will focus on the cycling ageing of the BESS and consider its calendar ageing as a given life time. The end-of-life of the BESS is thus defined as the minimum life time given by the cycling and calendar ageing. As an example, if the calendar ageing gives a life time of 20 years, and the cycling ageing a life time of 50 years, we consider that the actual life time of the BESS is 20 years. We penalize the revenue with the cost associated with the life-loss of the BESS. Note that the penalized revenue R' is not an actual cash flow, and that the cost associated with the life-loss is only here to make the control of the BESS more conservative regarding the life time. The penalized revenue R' then writes:

$$\begin{aligned} R' = \pi_s(E_{PV} + E_{BESS}) - (E_{PV} + E_{BESS} + E_{ID} - E_c)(\pi_s - \pi_B) + (\pi_s - \pi_{ID})E_{ID} \\ - C(E_{BESS}) \end{aligned} \tag{5.1}$$

Regarding the day-ahead participation of the PV/BESS, works based on stochastic programming are frequent, for example in [137], [138], [139] or [140]. In [141], the authors propose to control the risk-aversion of the operator using the conditional-value-at-risk. With such stochastic control, it is very important to use a representation of the uncertainty based on production scenarios, derived from the forecasts. Using a sequence of forecast distributions fails to account for the temporal correlation of the forecast errors, which is critical to the good operation of a storage system. Robust Optimization (RO) is also a popular choice for such applications [142], [143].

Some authors also propose an MPC approach to bid on intra-day market auctions [144], [145]. However, in our setting the intra-day market is a continuous trading market, which complicates the modeling of the participation. In reference [146], the authors proposed a systematic way to trade on such continuous market, using real historical data on which offers were available on the intra-day market at each time. In [45], the authors proposed a

method based on the same inputs but using Reinforcement Learning (RL). However, in this thesis we did not have such data.

Many works use Model Predictive Control (MPC) for real-time control of PV/BESS. This consists in optimizing the control of the BESS on a receding horizon, in order to take into account the forecast future state of the system when optimizing the next time step. Different objective functions can be optimized on the receding horizon. In most cases, the optimized function is either the producer's profit [147], [148] or the energy imbalance [149], without considering profit. However, in many cases the uncertainty of the upcoming PV production is overlooked in MPC approaches, that is, the future is not considered based on sampled scenarios but rather on deterministic forecasts. Alternatively, in [150], the authors propose to use linear rules for the real-time operation of the PV/BESS, considering the uncertainty with scenarios. In [143], the real-time operation of the BESS is performed using RO for computational simplicity. Recently, some authors proposed to use RL to control single storage systems that perform energy arbitrage [151], [152], [153].

In this thesis, we use different strategies for the control of the PV/BESS. For the day-ahead participation we use stochastic programming, and for the real-time control of the BESS we use either a MPC approach with sampled scenarios as representation of the uncertainty, or analytical solutions based on simplifying assumptions of the problem. For the participation on the continuous intra-day market, we propose a novel method for offering intra-day bids in the absence of an history of available bids, which is mandatory in the literature. However, it is difficult to evaluate the quality of this method since we do not dispose of this history to confront it with our intra-day bidding strategy. Deterministic forecasts of both day-ahead and imbalance prices are performed with the same models as in chapter 4, along with probabilistic forecasts of the PV power production using the AnEn model. In Approach 2, we use ANN at every stage to perform directly a Policy Function Approximation. The literature suggests that using a RL paradigm could be more efficient for this task. However, the contribution of the thesis is not in the models developed for performing the approaches, but in the proposal of an alternative combination and training of existing elements in order to obtain data-driven and value-oriented tools.

5.2 Approach 1: dedicated models and MPC controller

Following the revenue formulation from equation (5.1), PV power and price forecasting models are required again. We also need decision-making models for each of the three consecutive decisions. Using the first approach with dedicated models, the workflow can be summarized as in Fig. 5.1.

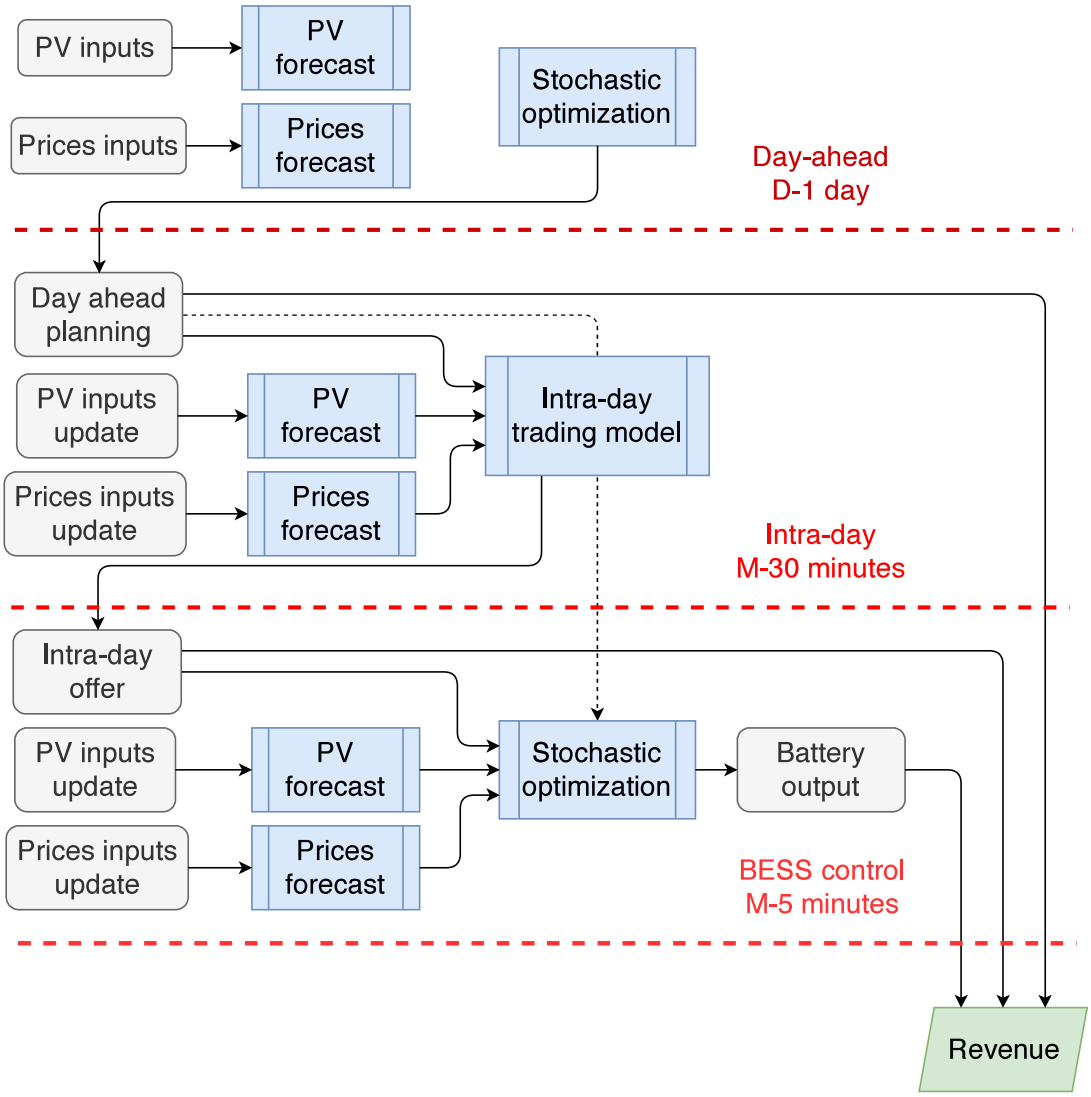

Figure 5.1: Flowchart of approach A1

Different MPC controllers are required for day-ahead bidding of the PV/BESS, for intra-day market participation and for real-time control of the system. In the following sections we present the different algorithms we compared.

5.2.1 Day-ahead offering strategy

The aim of the day-ahead controller is to provide the bids of the combined PV/BESS for the forthcoming day. We propose a first benchmark where the BESS is not used at the day-ahead level, and a second where the BESS is considered along with its usage cost. In all the day-ahead algorithms, the PV/BESS is considered as a price taker.

5.2.1.1 Benchmark: No BESS in the day-ahead planning (DA0)

For the benchmark, we do not use the BESS at the day-ahead level, and thus, all the terms related to the BESS are ignored. To derive the optimal bids E_c^*, we must then solve:

$$E_c^* = argmax_{E_c \in \mathbb{R}^{N_{MTU}}} \sum_{i=1}^{N_{MTU}} \pi_{s,i} E_i - (\pi_{B,i} - \pi_{s,i})(E_i - E_{c,i}) \tag{5.2}$$

where N_{MTU} is the number of market time units in a day. In these conditions, the optimal bids that minimize the penalties for the producer are given by [41] as already mentioned in chapter 4:

$$E_{c,i}^* = F_{PV,i}^{-1} \left(\frac{\pi_{s,i} - \pi_{+,i}}{\pi_{-,i} - \pi_{+,i}} \right) \tag{5.3}$$

where $F_{PV,i}$ is a forecast CDF of the energy production of the plant for the i-th market time unit. This benchmark strategy is referred to as strategy DA0 in the remainder of the thesis.

5.2.1.2 Optimal bidding using the BESS (DA1)

When the BESS is used at both the day-ahead and real-time levels, then the entire formulation of the revenue from equation (5.1) is optimized. Once again, we separate the bids into a first part accompanied by uncertainty from the PV plant $E_{c,PV}$, and the output from the battery $E_{c,BESS}$ which has no uncertainty: since the BESS is controllable, we assume that the actual output of the BESS E_{BESS} is always equal to the amount of the bid $E_{c,BESS}$.

This assumption allows us to avoid formulating a second-stage problem optimizing the real-time control of the BESS once the day-ahead schedule is set based on scenarios of PV production to perform stochastic programming. Thus, this approach might give sub-optimal

solutions for the day-ahead planning. However, since we will perform the real-control of the BESS during the simulation, we will still consider the opportunity to deviate from the day-ahead schedule, and so we do not expect that neglecting it at the day-ahead stage will negatively affect the revenue.

With these assumptions, the optimization problem that needs to be solved to derive the optimal bids is:

$$E^*_{c,PV}, E^*_{c,BESS} = argmax_{\left[E_{c,PV}\in\mathbb{R}^{N_{MTU}}, E_{c,BESS}\in\mathbb{R}^{N_{MTU}}\right]} \mathbb{E}\left(\sum_{i=1}^{N_{MTU}} \begin{bmatrix} \pi_{s,i}(E_{PV,i}+E_{c,BESS,i}) - (\pi_{s,i}-\pi_{B,i})(E_{PV,i}-E_{c,PV,i}) \\ - C(E_{c,BESS,i}) \end{bmatrix}\right) \tag{5.4}$$

However, to ensure that we can assume that $E_{BESS} = E_{c,BESS}$, and to correctly simulate the operation of a BESS, we must add the three following constraints where SOC (State of Charge) is the amount of energy in the battery at a given time step, relative to its full capacity Cap in MWh.

$$-\frac{1}{\eta_{Ch}} Cap(1 - SOC_i) < E_{c,BESS,i+1} < \eta_{Dis} Cap SOC_i \tag{5.5}$$

$$-E_{c,BESS} < E_{PV} \tag{5.6}$$

$$Cap|SOC_i - SOC_{i-1}| \leq E_m \tag{5.7}$$

$$SOC_{i+1} - SOC_i = -\frac{E_{C,BESS,i+1}}{\eta_{Dis} Cap} \text{ if } E_{C,BESS,i+1} > 0, \ \frac{\eta_{Ch} E_{C,BESS,i+1}}{\eta_{Dis} Cap} \text{otherwise} \tag{5.8}$$

The first constraint ensures that the energy in the BESS is never lower than 0 or higher than the capacity of the battery Cap, taking into account the charge and discharge efficiencies of the BESS, respectively η_{Ch} and η_{Dis}. The second constraint ensures that the BESS can only be charged from the PV plant, and not from the grid. Finally, the third constraint is a limitation on the power rating of the BESS, defined by the parameter E_m, that is the maximum energy that can that the BESS can charge or discharge during consecutive time steps. This method is referred to as method DA1. The last constraint states that the variation of the SOC is the power flow of the BESS divided by its capacity.

5.2.2 Intra-day offering strategy

5.2.2.1 Intra-day market model

As stated before, the intra-day market allows buying or selling additional energy up to 30 minutes before the time of delivery. At the intra-day stage, the bids E_c and the spot prices

π_s are already known, thus the decision that the energy producer must take is the amount of energy to buy or sell and for what price.

The intra-day market follows a continuous bidding scheme. This means that whenever a matching buying and selling offer are submitted to the intra-day market, the transaction is accepted at the price of the offer. Thus, when simulating the operation of the intra-day market, the only way to know if a given offer would have been accepted is to have a complete list of the intra-day offers, along with their time of submission and acceptation if they were accepted. Then, one can check if a given offer would have found a counterpart in the historical offers data.

However, we did not have access to such data in this thesis. Thus we propose a participation strategy based only on price and power production forecasts, by modeling continuous trading mechanism of the intra-day market. Without access to historical data of accepted and rejected intra-day offers, it is impossible to compare the model to reality and thus to validate it. Still, we propose to base the behavior of the intra-day market on real market considerations, so that the intra-day market model is consistent with the economy of electricity markets.

As we are not acting on the BESS at this stage, we drop the distinction between E_{PV} and E_{BESS} and only consider the total amount of production E, except for the ageing cost of the BESS which only depends on E_{BESS}. Using equation (2.4), the penalized revenue at the intra-day stage writes:

$$R'_{ID} = \pi_s E + (\pi_s - \pi_{ID})E_{ID} - (E + E_{ID} - E_c)(\pi_s - \pi_{B,ID}) - C(E_{BESS}) \tag{5.9}$$

Where $\pi_{B,ID}$ is the imbalance price considering that a bid of volume E_{ID} was accepted:

$$\pi_{B,ID} = \begin{cases} \pi_+ \text{ if } E + E_{ID} > E_c \\ \pi_- \text{ if } E + E_{ID} < E_c \end{cases} \tag{5.10}$$

So the goal of the intra-day participation is to maximize the difference ΔR between the revenue with the intra-day bid and the revenue without:

$$\Delta R = (\pi_{B,ID} - \pi_{ID})E_{ID} + (\pi_{B,ID} - \pi_B)(E - E_c) \tag{5.11}$$

We propose to define a probability p_{ID} that the offer is accepted. We assume that the intra-day market is liquid enough so that the probability of acceptation of the offer p_{ID} only depends of the price π_{ID}. In other words, if an offer is economically interesting based on its price π_{ID}, then it will find a counterpart no matter its volume E_{ID}. We propose to define p_{ID} as follows:

$$p_{ID} = \begin{cases} \dfrac{\pi_{ID} - \pi_+}{\pi_- - \pi_+} \text{ if } E_{ID} > 0 \\ \dfrac{\pi_- - \pi_{ID}}{\pi_- - \pi_+} \text{ if } E_{ID} < 0 \end{cases} \tag{5.12}$$

Consider for example the case when one wants to buy energy $E_{ID} > 0$. No one should be willing to sell energy at a lower price than π_+ since it is the price given by the TSO for excess energy. Thus, the probability of acceptation for a buying offer with price π_+ should be 0. Besides, anyone would be willing to sell at a price higher than π_-, since the benefit from selling would more than compensate the penalty for missing energy given by the TSO. Thus, the probability of acceptation with price π_- should be 1. Then, the probability p_{ID} is linearly interpolated between π_+ and π_-. The same rationale is used to derive the probability when selling energy i.e. $E_{ID} < 0$.

To keep π_{ID} independent from the volume E_{ID}, we will always treat separately the case $E_{ID} > 0$ and $E_{ID} < 0$. Thus, the acceptation of the offer is a Bernoulli trial with probability p_{ID}. We can then rewrite ΔR as:

$$\Delta R = B\left[(\pi_{B,ID} - \pi_{ID})E_{ID} + (E - E_c)(\pi_{B,ID} - \pi_B)\right] \tag{5.13}$$

Where B is a Bernoulli trial with success probability p_{ID}, that is a random variable that takes the value $B = 1$ (the offer is accepted) with probability p_{ID} and $B = 0$ (the offer is not accepted) with probability $(1 - p_{ID})$.

5.2.2.2 Offering strategy

The objective of the offering strategy is to maximize the expectation of ΔR, which is a function of π_{ID} and E_{ID}. This expectation can be written as follows:

$$E[\Delta R] = \sum_{i \in \{0,1\}} \int_{e=0}^{E_n} \Delta R_{|B=i,E=e} f_{PV}(e) p_i de \tag{5.14}$$

with:

$$p_i = p(B = i) = \begin{cases} p_{ID} \text{ if } i = 1 \\ 1 - p_{ID} \text{ if } i = 0 \end{cases} \tag{5.15}$$

When the offer is rejected, $\Delta R = 0$, and thus:

$$E[\Delta R] = \int_{e=0}^{E_n} p_{ID} \Delta R_{|B=1,E=e} f_{PV}(e) de \tag{5.16}$$

$$= p_{ID} \int_{e=0}^{E_n} \left[(\pi_{B,ID} - \pi_{ID}) E_{ID} + (e - E_c)(\pi_{B,ID} - \pi_B) \right] f_{PV}(e) de \tag{5.17}$$

If $E_{ID} > 0$, when $e < E_c - E_{ID}$ we have $\pi_{B,ID} = \pi_B = \pi_-$. Similarly when $e > E_c$ we have $\pi_{B,ID} = \pi_B = \pi_+$. Otherwise, $\pi_{B,ID} = \pi_+$ and $\pi_B = \pi_-$. Thus:

$$E[\Delta R] = p_{ID} \left\{ \begin{array}{l} E_{ID}(\pi_- - \pi_{ID}) \int_{e=0}^{E_c - E_{ID}} f_{PV}(e) de + ... \\ E_{ID}(\pi_+ - \pi_{ID}) \int_{e=E_c}^{E_n} f_{PV}(e) de + ... \\ \int_{e=E_c - E_{ID}}^{E_c} \left[(e - E_c)(\pi_+ - \pi_-) + E_{ID}(\pi_+ - \pi_{ID}) \right] f_{PV}(e) de \end{array} \right\} \tag{5.18}$$

Using $\int_{e=0}^{x} f_E(e) de = F_{PV}(x)$ and $F(E_n) = 1$ where F_{PV} is the CDF of the energy production:

$$E[\Delta R] = p_{ID} \left\{ \begin{array}{l} E_{ID} \left((\pi_- - \pi_+) F_{PV}(E_c - E_{ID}) + (\pi_+ - \pi_{ID}) \right) + ... \\ (\pi_+ - \pi_-) \int_{e=E_c - E_{ID}}^{E_c} (e - E_c) f_{PV}(e) de \end{array} \right\} \tag{5.19}$$

Using the same calculation method, we find exactly the same result when $E_{ID} < 0$. To simplify the equations we note:

$$G(\pi_{ID}, E_{ID}) = E_{ID} \left((\pi_- - \pi_+) F_{PV}(E_c - E_{ID}) + (\pi_+ - \pi_{ID}) \right) \tag{5.20}$$

$$+ (\pi_+ - \pi_-) \int_{e=E_c - E_{ID}}^{E_c} (e - E_c) f_{PV}(e) de \tag{5.21}$$

And so:

$$E[\Delta R] = p_{ID} G(\pi_{ID}, E_{ID}) \tag{5.22}$$

Where p_{ID} is a function of π_{ID} only and G a function of both π_{ID} and E_{ID}. Now to identify a possible maximum of the additional revenue, we have to perform a second partial derivative test. Using the Leibniz rule for derivation under the integral sign, we get:

$$\frac{\partial E[\Delta R]}{\partial \pi_{ID}} = \frac{dp_{ID}}{d\pi_{ID}} G(\pi_{ID}, E_{ID}) - p_{ID} E_{ID} \tag{5.23}$$

$$\frac{\partial E[\Delta R]}{\partial E_{ID}} = p_{ID} (F_{PV}(E_c - E_{ID})(\pi_- - \pi_+) + (\pi_+ - \pi_{ID})) \tag{5.24}$$

$$\tag{5.25}$$

And the second derivatives are given by:

$$\frac{\partial^2 E[\Delta R]}{\partial \pi_{ID}^2} = \frac{d^2 p_{ID}}{d\pi_{ID}^2} G(\pi_{ID}, E_{ID}) - 2E_{ID} \frac{dp_{ID}}{d\pi_{ID}} \tag{5.26}$$

$$\frac{\partial^2 E[\Delta R]}{\partial E_{ID}^2} = -p_{ID}(\pi_- - \pi_+) f_{PV}(E_c - E_{ID}) \tag{5.27}$$

$$\frac{\partial^2 E[\Delta R]}{\partial \pi_{ID} E_{ID}} = \frac{\partial^2 E[\Delta R]}{\partial E_{ID} \pi_{ID}} = \frac{dp_{ID}}{d\pi_{ID}} (F_{PV}(E_c - E_{ID})(\pi_- - \pi_+) + (\pi_+ - \pi_{ID})) - p_{ID} \tag{5.28}$$

These expressions are independent on the actual model for the probability p_{ID} and could thus be used to perform this test for various possible models, as long as they are independent on the volume E_{ID}. However, given the model we proposed in section 5.2.2.1, we can simplify it to find possible critical points. All the following calculations are made with $E_{ID} > 0$, $p_{ID} = \dfrac{\pi_{ID} - \pi_+}{\pi_- - \pi_+}$. The calculations are similar for the other case. We have:

$$\frac{\partial E[\Delta R]}{\partial E_{ID}} = 0 \implies \pi_{ID}^* = \pi_+ \text{ or } E_{ID}^* = E_c - F_{PV}^{-1}\left(\frac{\pi_{ID} - \pi_+}{\pi_- - \pi_+}\right) \tag{5.29}$$

The determinant $Det(\pi_{ID}, E_{ID})$ of the Hessian matrix of $E[\Delta R]$ is given by:

$$Det(\pi_{ID}, E_{ID}) = 2E_{ID} \frac{\pi_{ID} - \pi_+}{\pi_- - \pi_+} f_{PV}(E_c - E_{ID}) - F_{PV}(E_c - E_{ID})^2 \tag{5.30}$$

For the possible critical point at $\pi_{ID}^* = \pi_+$, we have:

$$Det(\pi_+, E_{ID}) = -F_{PV}(E_c - E_{ID})^2 < 0 \tag{5.31}$$

The critical point, if it exists, can only be a saddle point i.e. a maximum for one variable and a minimum for the other. Therefore, we only focus on the second possible critical point to find a maximum. We already have:

$$\frac{\partial^2 E[\Delta R]}{\partial \pi_{ID}^2} = -\frac{2E_{ID}}{\pi_- - \pi_+} < 0 \tag{5.32}$$

So to prove that the critical point at E_{ID}^* equals to $E_c - F_{PV}^{-1}\left(\dfrac{\pi_{ID} - \pi_+}{\pi_- - \pi_+}\right)$, we still have to prove that the determinant D is positive at this critical point. At this critical point, the determinant writes:

$$Det(\pi_{ID}^*, E_{ID}^*) = F_{PV}(E_c - E_{ID})(2E_{ID} f_{PV}(E_c - E_{ID}) - F_{PV}(E_c - E_{ID})) \tag{5.33}$$

Given that F_{PV} is a CDF and thus always positive, we must show that:

$$2E_{ID} f_{PV}(E_c - E_{ID}) - F_{PV}(E_c - E_{ID}) > 0 \tag{5.34}$$

Without more assumptions on f_{PV}, it is difficult to show that this critical point is a local maximum. To simplify the control of the PV/BESS for the intra-day market, we simplify it by stating that $\pi_{ID} = \pi_s$, so that any accepted trade is at best beneficial for the revenue, at worst neutral, as long as it reduces the imbalance. In such a case, the additional revenue is a function of E_{ID} only. By replacing π_{ID} by π_s, we get:

$$\frac{dE[\Delta R]}{dE_{ID}} = 0 \implies E^*_{ID} = E_c - F^{-1}_{PV}\left(\frac{\pi_s - \pi_+}{\pi_- - \pi_+}\right) \tag{5.35}$$

$$\frac{d^2E[\Delta R]}{dE^2_{ID}} = -(\pi_s - \pi_+) f_{PV}(E_c - E_{ID}) \tag{5.36}$$

The second derivative is negative when $\pi_s > \pi_+$. As stated in chapter 2, this is usually the case, otherwise positive imbalances could generate revenue through negative penalties. In this chapter's test case, the market structure is the same as in 4 where negative penalties did not appear. However, the training and testing period are more recent, and so positive imbalance prices higher than the spot price or negative imbalance prices lower than the spot price appear. In these cases, the optimal intra-day offer E_{ID} becomes a local minimum of ΔR. However, these cases remain less frequent than the usual case where $\pi_+ \leq \pi_s \leq \pi_-$, and so we expect that the critical point $E^*_{ID} = E_c - F^{-1}_{PV}\left(\frac{\pi_s - \pi_+}{\pi_- - \pi_+}\right)$ generates additional revenue on average. Therefore the offering strategy is to offer the volume E^*_{ID} given at equation (5.35) at the price π_s.

5.2.3 Real-time control

In real-time control of the PV/BESS, the day-ahead prices and energy sold on the day-ahead and intra-day market are known, and the only sources of uncertainty come from the PV power generation and imbalance prices. Following the offering strategy for the intra-day market, the price π_{ID} is set at π_s and thus everything happens as if the energy sold at the day-ahead stage was $E_c - E_{ID}$, whether E_{ID} is positive, negative, or null. Thus, in this section, E_c designs the sum of the volumes sold in the day-ahead and real-time electricity market instead of the day-ahead market only.

Along with the benchmark strategy, which is not to use the BESS at all, we define two additional real-time control strategies. The first one is purely analytical and tries to minimize the penalties for the next market time unit, without taking into account the BESS ageing cost or the near future after the next market time unit. In contrast, the second strategy takes all of these factors into account.

5.2.3.1 First strategy: analytical solution (RT1)

The first algorithm minimizes the term arising from imbalances between the bids and PV/BESS production. Since we are in real time, the bids E_c have already been submitted and the market has been cleared. Thus, the day-ahead prices π_s are known and the only design variable is the BESS output E_{BESS}. The BESS is allowed to deviate from its planning $E_{c,BESS}$ to compensate deviations coming from the PV power forecast error, thus we do not necessarily have $E_{BESS} = E_{c,BESS}$ anymore. At this stage, the only design variable is the amount of energy we charge or discharge from the BESS E_{BESS}. In this case, we can write the real-time penalized revenue R'_{RT} as a function of E_{BESS} only and get:

$$\begin{aligned} R'_{RT}(E_{BESS}) =& E_{PV}\pi_s - (E_{PV} + E_{BESS} - E_c)(\pi_s - \pi_B) \\ &+ E_{BESS}\pi_s - C(E_{BESS}) \end{aligned} \tag{5.37}$$

For the first method, we focus on reducing the penalties, so we do not consider the term $E_{PV}\pi_s$ and we neglect the terms $\pi_s E_{BESS}$ and the BESS usage costs $C(E_{BESS})$. The first neglected term represents a profit that can be obtained from the difference in day-ahead prices during the day. However, this profit is supposed to have already been realized at the day-ahead level. Besides, the profit alternates between positive and negative values depending on the charge or discharge of the BESS. Its impact should thus be reduced when summed over several time steps. On the other hand, the penalty term $Pen = (E_{PV} + E_{BESS} - E_c)(\pi_s - \pi_B)$ is generally positive. Finally, neglecting the BESS usage costs allows us to propose a closed-form solution to the revenue maximization problem. The expectation of the penalty term Pen for the next time step writes:

$$\mathbb{E}(Pen) = \int_0^{E_n} (p + E_{BESS} - E_c)(\pi_s - \pi_B) f_{PV}(p) dp \tag{5.38}$$

Since π_B is dependent on the sign of the imbalance, the expectation of the penalty term must be rewritten:

$$\begin{aligned} \mathbb{E}(Pen) = & \int_0^{E_c - E_{BESS}} (p + E_{BESS} - E_c)(\pi_s - \pi_-) f_{PV}(p) dp \\ & + \int_{E_c - E_{BESS}}^{E_n} (p + E_{BESS} - E_c)(\pi_s - \pi_+) f_{PV}(p) dp \end{aligned} \tag{5.39}$$

As mentioned before, in our test case the penalties can be negative. In order to avoid a divergent solution, we bound the imbalance prices by the spot prices, so that the algorithm

can not try to seize revenue by increasing a supposedly remunerated imbalance. In other words, if the grid is short (resp. in excess of) energy, the positive (resp. negative) imbalance price is at maximum (resp. minimum) equal to the spot price, so that positive (resp. negative) imbalances are not remunerated. This assumption is used to derive the strategy, however it is of course not enforced when evaluating the strategy on the testing period.

which gives:

$$\begin{aligned}\mathbb{E}(Pen) = (\pi_s - \pi_-) &\int_0^{E_c - E_{BESS}} (p + E_{BESS} - E_c) f_{PV}(p) dp \\ + (\pi_s - \pi_+) &\int_{E_c - E_{BESS}}^{E_n} (p + E_{BESS} - E_c) f_{PV}(p) dp \end{aligned} \tag{5.40}$$

Using the variable change $x = p - E_c$, we get:

$$\begin{aligned}\mathbb{E}(Pen) = (\pi_s - \pi_-) &\int_0^{-E_{BESS}} (x + E_{BESS}) f_{PV}(x + E_c) dx \\ + (\pi_s - \pi_+) &\int_{-E_{BESS}}^{E_n - E_c} (x + E_{BESS}) f_{PV}(x + E_c) dx \end{aligned} \tag{5.41}$$

Finally, using the Leibniz rule for differentiating under the integral sign, we obtain:

$$\begin{aligned}\frac{d\mathbb{E}(Pen)}{dE_{BESS}} =& (\pi_s - \pi_-) F_{PV}(E_c - E_{BESS}) \\ &+ (\pi_s - \pi_+)(1 - F_{PV}(E_c - E_{BESS}) \end{aligned} \tag{5.42}$$

The second derivative is:

$$\begin{aligned}\frac{d^2\mathbb{E}(Pen)}{dE_{BESS}^2} =& - (\pi_s - \pi_-) f_{PV}(E_c - E_{BESS}) \\ &+ (\pi_s - \pi_+) f_{PV}(E_c - E_{BESS}) \end{aligned} \tag{5.43}$$

This second derivative is negative provided that $\pi_+ \leq \pi_s \leq \pi_-$. As discussed before, this is not always the case, but given that it is the most frequent case we expect this strategy to generate additional revenue. Thus, by making the first derivative equal to 0, we find the minimum:

$$E_{BESS}^* = E_c - F_{PV}^{-1}\left(\frac{\pi_s - \pi_+}{\pi_- - \pi_+}\right) \tag{5.44}$$

The first method thus consists in computing a forecast distribution of the PV power, deterministic forecasts of the imbalance prices, and to inject them into this optimal solution. Although the solution is in a closed form, the BESS constraints prevent the use of this solution more than one time step ahead, and the BESS usage cost is neglected. This is referred to hereafter as the RT1 method.

5.2.3.2 Second strategy: numerical optimization (RT2)

The second method is very similar to the offering strategy including the BESS from section 5.2.1.2, however it is performed using a MPC approach, to adapt it to the real time. This means that the whole revenue formulation is maximized over the N_{MPC} next time steps, then the result of the optimization from the first time step is used as the command for the BESS for the next market time unit. This allows us to take into account the future forecast state of the system in the real-time control.

Since we are in a real-time setting, the day-ahead prices and bids are known, as for the first real-time strategy. As a result, the only design variable is the BESS command. Therefore, the optimization problem to solve for each time step is:

$$\begin{aligned} &E^*_{BESS} = argmax_{E_{BESS} \in \mathbb{R}^{N_{MPC}}} \\ &\mathbb{E}\left(\left[\sum_{i=1}^{N_{MPC}} \begin{array}{c} (E_{PV,i} + E_{BESS,i})\pi_{s,i} - (E_{PV,i} + E_{BESS,i} - E_{c,i})\,(\pi_{s,i} - \pi_{B,i}) \\ - C(E_{BESS,i}) \end{array}\right]\right) \end{aligned} \tag{5.45}$$

subject to the same constraints as in section 5.2.1.2.

We change N_{MPC} at each time step, depending on the time of day, so that all of the remaining day is included in the optimization. This is especially important because day-ahead planning often results in full discharge of the BESS in the evening when day-ahead prices are usually high due to high demand. As such, the whole day must be included in the optimization loop. If N_{MPC} is too low, the BESS could discharge itself entirely during the day to compensate forecast errors, and thus be unable to provide the energy in the evening. This second method is referred to as RT2.

5.2.4 Forecasting and optimization tools

To implement these different algorithms, we use the same forecasting models as in chapter 4.

5.2.5 Optimizer

To solve the different optimization problems that appear in DA1 and RT2, we decide to employ stochastic optimization. It is important to use scenarios to represent the uncertainty because of the temporal dimension of the PV/BESS management problem [154]. This temporal dimension can be seen from the second constraint formulated in equation (5.6). One of the essential characteristics of PV power forecasts is the positive correlation between the forecast errors at consecutive time steps. In other words, if a forecast error is positive (resp. negative) for a given time step, the forecast error for the following time step is also likely to be positive (resp. negative). This is a problem for BESSs, because since a BESS can compensate forecast errors, a significant error present on several consecutive time steps would quickly either charge the BESS to its maximum or discharge it to its minimum, depending on the sign of the error. Due to the temporal correlation of the errors, this worst-case scenario is much more likely than the consecutive distributions might suggest if they were considered independent. During the simulation, the energy remaining in the BESS is tracked to ensure that the second constraint from equation (5.6) is respected.

A large number of PV production scenarios are generated following [155]. The scenarios are then reduced using a Partitioning Around Medoids (PAM) algorithm, and the median of the objective over the scenarios is optimized. The resulting non-linear optimization problem is solved using the COBYLA algorithm [156].

The PAM algorithm reduce the scenarios by partitioning the whole set of scenarios in a fixed number of classes n_C. The algorithm can be summarised as follows:

- Compute the distance between each pairs of scenarios. We used the sum of the euclidean distances between the realizations as the distance. In other words, given two scenarios $E_{1,\dots,N_{MPC}}$ and $E'_{1,\dots,N_{MPC}}$, the distance between the scenarios is given by $\sum_{t=1}^{N_{MPC}} \sqrt{(E_t - E'_t)^2}$

- Find n_C scenarios that are representative of the whole scenarios, called medoids. To do so, the sum of the distances between each scenario and its closest medoid is minimized using an heuristic optimization algorithm.

- Associate each scenario to its closest medoid.

Then, the medoids are used as probable scenarios, and the probability of each medoid is estimated by the number of scenarios populating this medoid's class compared to the total number of scenarios.

5.2.6 Results

A simulation of the control of the aggregated PV/BESS made from the twelve plants is performed for four months (January to May 2018). We used this period because these months correspond to the times when the forecasting algorithm performance is lower, and thus there are more opportunities for the BESS to reduce the uncertainty and add value to the PV power. The total peak power of the aggregated plant is 91 897 kWp.

For each time step of the simulation, the PV power and market quantity forecasts are updated based on the inputs known at the time. Then, if the day-ahead market closes for the considered time step, bids are submitted for the next day using one of the two methods from section 5.2.1 i.e. either with or without considering a BESS. Then, the optimal offer for the intra-day market is derived. The control set-point for the BESS for the next time step is obtained using one of the two methods from section 5.2.3 i.e. either with an exact solution to the simplified problem or a numerical optimization for the whole problem. Then, the process goes to the next time step, updates the SOC, the PV power, and market quantities forecast, and continues the algorithm until the final time step. A flowchart of the algorithm is represented on Fig. 5.2.

The NWPs required for the AnEn model are obtained from the ECMWF, along with measurements and satellite data to improve short-term forecasts as in chapter 3. Forecasts of the national demand and renewable energy generation required for the day-ahead price forecasts are provided by RTE, the French TSO.

The BESS considered in the test case is a lithium-ion storage system, since it is an already mature technology, and also because the investment costs of this technology are expected to decrease in the coming years. However, both the operational and economical values of the storage system are parameters, and studying any other battery storage technology is possible by changing these parameters.

Ageing parameters for the rainflow counting algorithm are taken from [157] and [158]. Regarding costs, prospective values for the year 2030 from [158] are used in the base case, that is a 200 €/kWh investment cost. Besides, in all simulations, we set the parameter E_m from equation (5.7), which controls the power rating of the BESS so that the BESS can fully charge or discharge in two hours. This is to simulate a BESS with a power rating of 0.5C, which is common in commercial lithium-ion storage systems. We used a BESS with a 91 897 kWh storage capacity, which corresponds to a 1:1 ratio with the installed peak power.

The simulation is performed using the software R along with the packages *e1071* [159] for the SVR model and *nloptr* [160] for the implementation of the COBYLA algorithm.

Different combinations of day-ahead and real-time methods are evaluated. The sensit-

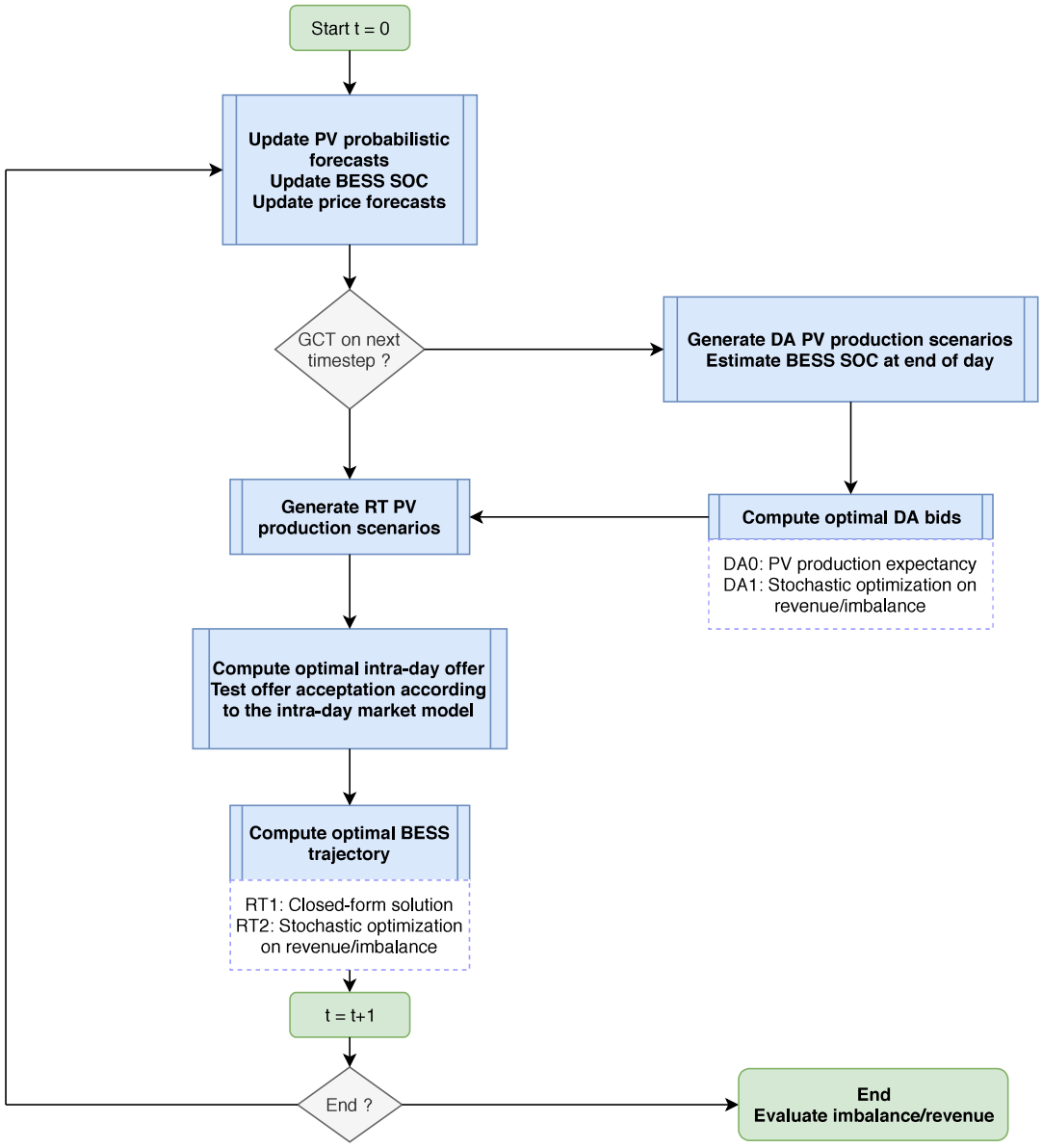

Figure 5.2: Flowchart of the MPC controller

Table 5.1: Evaluated strategies for imbalance minimization

Strategy	Overall objective	Intra-day participation	Control methods
I0 (benchmark)	Imbalance	No	DA0/RT0
I1	Imbalance	No	DA1/RT1
I2	Imbalance	No	DA1/RT2
I3	Imbalance	Yes	DA1/RT1
I4	Imbalance	Yes	DA1/RT2

Table 5.2: Evaluated strategies for revenue maximization

Strategy	Overall objective	Intra-day participation	Control methods
R0 (benchmark)	Revenue	No	DA0/RT0
R1	Revenue	No	DA1/RT1
R2	Revenue	No	DA1/RT2
R3	Revenue	Yes	DA1/RT1
R4	Revenue	Yes	DA1/RT2

ivity of the results to the installed capacity of the BESS and electricity market prices is studied, providing guidelines on the sizing of the BESS for trading in electricity markets. The different method combinations tested are summarized in tables 5.1 and 5.2.

Examples of the typical output of the different strategies are represented on Fig. 5.3 (imbalance minimization) and 5.4 (revenue maximization). We can see that when using market information, the benchmark for revenue maximization R0 is more variable than for imbalance minimization I0. Besides, when only minimizing imbalance, the BESS is not used in the day-ahead planning in strategies I0 to I4, while it is used with strategies R0 to R4 with spikes at times when the spot price is higher. For strategies I0 to I4, the intra-day market participation modifies the bids, but it is unclear on the figure whether it actually contributes to reducing the imbalance. Its effect on revenue maximization is also hard to understand without knowing the forecast imbalance and spot prices at the time. However, results reported in table 5.3 reveal that the intra-day market participation contributes to reducing the imbalance or maximizing the revenue over the testing period.

Regarding the control methods, there are not much differences between methods RT1 and RT2 for imbalance minimization or revenue maximization. The main difference is that sometimes strategy RT2 prefers not to compensate a forecast error in order to be more

Table 5.3: Trading results

	Imbalance reduction				
	I0	I1	I2	I3	I4
Total imbalance (MWh)	5 033	3 266	3 252	3 166	**1 412**
Penalties (€)	39 060	23 678	23 846	17 920	**11 684**
Revenue (€)	1 048 830	1 056 133	1 055 865	1 060 827	**1 063 120**
BESS life loss (%)	0	3.1e-2	3.1e-2	**1.7e-2**	2.6e-2
Monetized BESS life loss (€)	0	5 698	5 698	**3 125**	4 779
	Revenue maximization				
	R0	R1	R2	R3	R4
Total imbalance (MWh)	7 054	4 641	4 860	4 239	**3 403**
Penalties (€)	33 100	33 095	23 760	21 720	**18 861**
Revenue (€)	1 054 789	1 074 126	1 074 593	**1 085 190**	1 080 152
BESS life loss (%)	0	0.40	**0.35**	0.40	0.36
Monetized BESS life loss (€)	0	73 518	**64 328**	73 518	66 166

efficient later: compare for example R1 and R2. In the displayed afternoon, with strategy R2, the BESS does not discharge even if there is a forecast error in order to keep some charge for the evening.

5.2.6.1 Test case results

The results of the study are shown on table 5.3. The results presented feature actual cash flows which means that the revenue indicated in the table does not include the cost associated with the BESS life loss. The purpose of this cost is only to help the algorithms controlling the BESS in a more conservative way.

We can see from the results that all strategies contribute to reducing the imbalance. As expected, strategies I0 to I4 achieve better results than strategies R0 to R4 for imbalance minimization. In the best case, that is strategy I4, the relative imbalance reduction is 72%.

With strategies R0 to R4, the total imbalance is higher. This is another illustration of the fact that reducing the imbalance does not systematically contribute to revenue, since there are times when imbalances are not penalized if they help the power grid at the national level. In some cases, they can even be rewarded. Besides, since the BESS is used in day-ahead trading, its available capacity to compensate imbalances is decreased. For example, if the forecasts overestimate the PV power generation and the BESS is scheduled to discharge

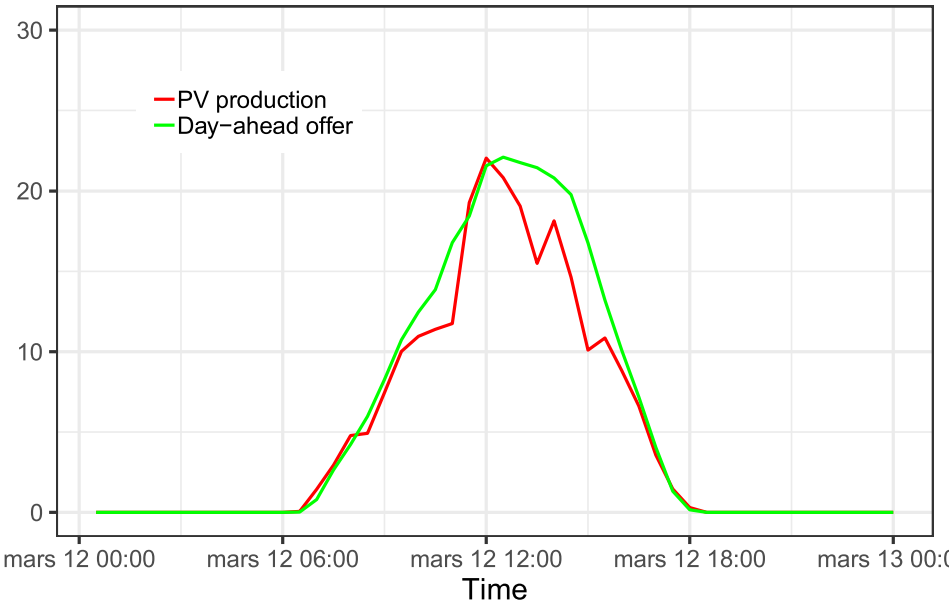

(a) Strategy I0

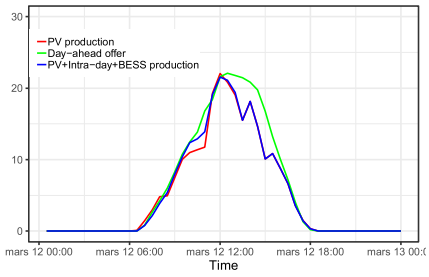

(b) Strategy I1

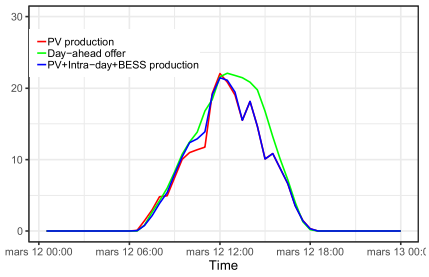

(c) Strategy I2

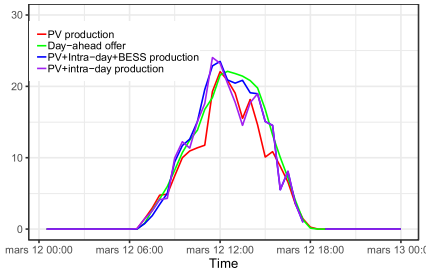

(d) Strategy I3

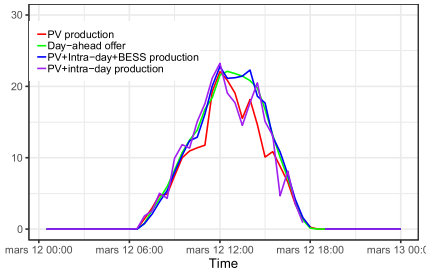

(e) Strategy I4

Figure 5.3: Example outputs from the four strategies minimizing imbalance, for day 2018-02-09

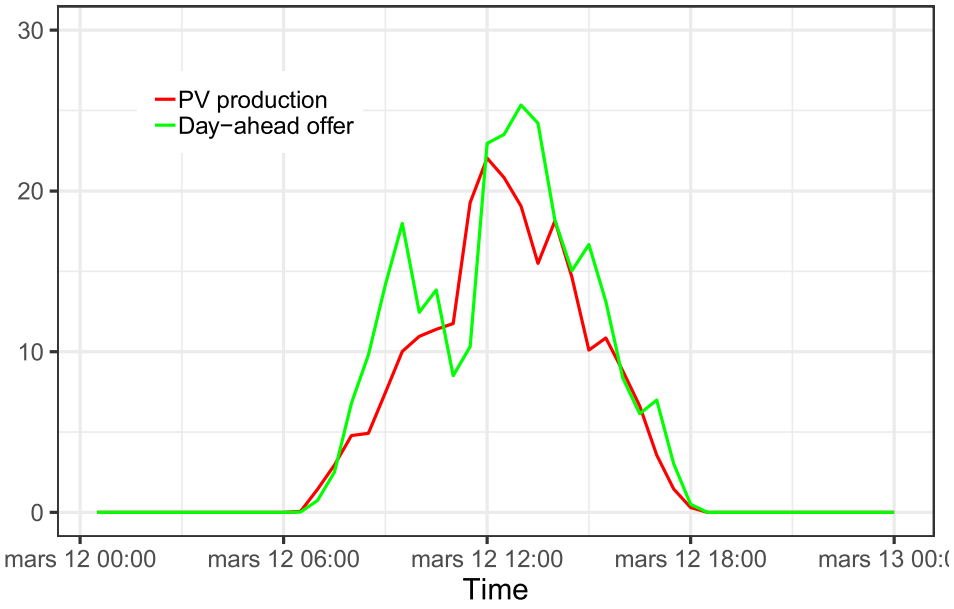

(a) Strategy R0

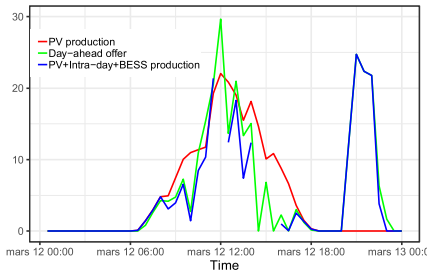

(b) Strategy R1

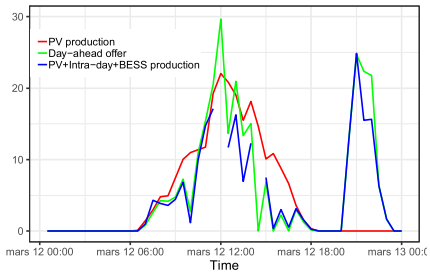

(c) Strategy R2

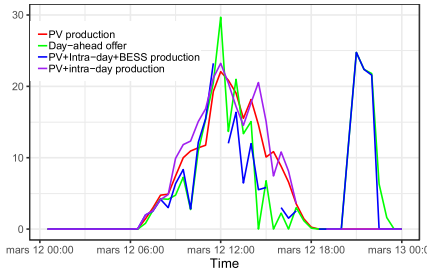

(d) Strategy R3

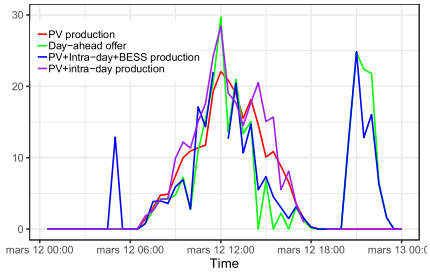

(e) Strategy R4

Figure 5.4: Example outputs from the four strategies maximizing revenue, for day 2018-02-09

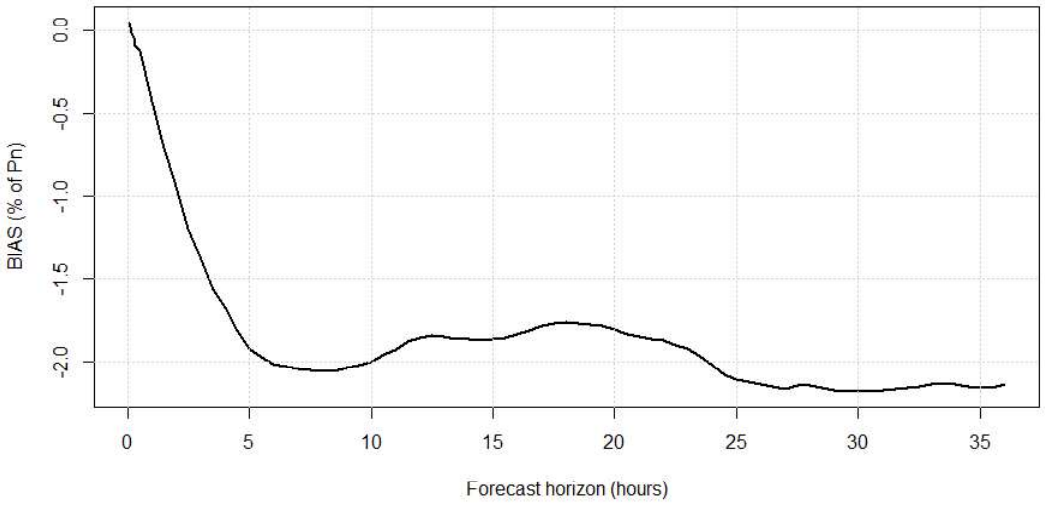

Figure 5.5: MBE of the AnEn forecasts over the testing period

entirely in the evening, the lower amount of PV production prevents the BESS from realizing its commitment unless it charges more than expected during the day. This ultimately results in a higher imbalance, since the BESS had to charge and could not correct the imbalances. Since the PV power forecasting model has a tendency to overestimate production according to figure 5.5, this is a common scenario.

Still, strategies I1 to I4 can increase revenue but not to the same extent as R1 to R4. This is because the latter strategies profit from the differences in day-ahead price at different times of the day. With strategies I0 to I4, shifting the production at times where the spot prices are higher does not contribute to reduce the imbalance, and so this effect does not occur. The revenue stream from this source of profit is much more reliable than from the compensation of imbalances, because the day-ahead price behavior is much less volatile, and it has a strong daily pattern featuring higher prices in the morning and evening when energy demand is high.

The control strategy and the participation to intra-day market improve the objective in most cases. The strategy obtaining the best results is put in bold in table 5.3. In almost all cases and for all criteria except the BESS life loss, the strategy that performs the best is the one using both the intra-day market and the MPC control of the BESS. There are two notable exceptions. For revenue maximization, strategy R3 (analytical solution) performed better than R4 (numerical optimization). We found it surprising, because since there is no

MPC control with the method RT1 used in R3, there are no theoretical reasons that the BESS could be able to deliver the energy sold in the day-ahead market at times when there is no production but the spot prices are high. Still, we can understand that since we are optimizing for penalties in that case, not every imbalance is compensated, and it could be that there are not enough penalties to correct, which ultimately could prevent the BESS to perform its day-ahead planning. Another explanation could be that the MPC controller used in R4 preserves the BESS life loss compared to R3, which is probably at the cost of preventing some additional revenue is some cases. Overall, it seems that using strategy R4 is more reliable, as the MPC controller provides more guarantees that the BESS controller can perform its day-ahead planning, but this choice is ultimately up to the PV power plant operator.

An important remark is that the BESS degradation is low for all strategies, although greater for strategies R0 to R4 where deep charging and discharging cycles are performed. Overall, BESS life loss is very low. In the worst case, the BESS life loss is 0.4% over the 4 months of the testing period, which means that the BESS would last around 75 years considering only the cycling life loss. In practice, calendar ageing will reduce the life time of the BESS and will cause its end of life much earlier, typically after 10-20 years of usage [161]. This suggest that the cycling ageing of the BESS can be neglected at least in the operational phase of the BESS, since more aggressive control methods do not reduce the actual life time of the BESS.

5.2.7 Sensitivity analysis

In this section, we discuss the sensitivity of the results to different parameters of the simulation. To perform the sensitivity analysis, we extrapolated the raw results from the initial simulations. We used different methods depending on the strategy and the parameter for which we evaluate the sensitivity.

5.2.7.1 Sensitivity to the BESS size

This analysis was based on the observation that BESS life loss from cycling ageing is very low compared to the calendar ageing. Therefore, we neglected the BESS ageing in the objective function from equation (5.1). Following this, we noticed that both the objective function and the constraints were linear with respect to the BESS capacity. Therefore, for the optimization problems of the day-ahead bids, we assumed that reducing the BESS bids E_{BESS} by the same factor as the BESS size reduction would provide a good estimate of the optimal bids, while still respecting the constraints. The real-time control of the BESS

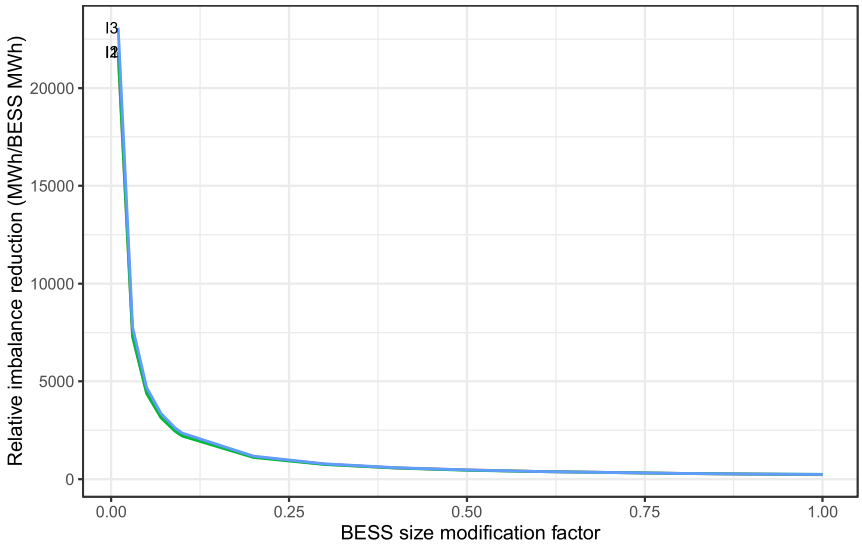

Figure 5.6: Imbalance reduction per installed BESS capacity

follows the same linear optimization problem and we can make the same assumption for the real-time control of the BESS, assuming there is no intra-day participation . With intra-day markets, the problem remains linear but since the intra-day offers are dependent on E_{BESS}, we can not use the results from the initial simulation who had different intra-day offers. Besides, this approach is only valid for BESS sizes lower than the size of the initial simulation, so that the constraint from equation (5.6) remains true for lower bids. If the BESS size and thus the BESS optimal bids increase, this constraint could be strongly violated.

For the benchmark algorithms and the control method RT0, the decisions regarding the control of the BESS are independent from the BESS size. Thus we can easily estimate the output of the simulation for different BESS sizes by using the same command as in the original simulation, then ensuring that the constraints are respected to show the saturation effects from the BESS.

In the end, we performed this analysis for strategies with control method RT0 and strategies with control method RT1 and no intra-day market participation, that is strategies I1 to I3 and R1 to R3.

The sensitivity of the results to the BESS size is reported on Fig. 5.6 and 5.7. Because relative revenue, imbalance and penalties increase almost linearly with the installed capacity, we depict the revenue increase or the imbalance reduction relative to the installed BESS capacity to better reflect the efficiency of the different approaches.

For the strategies minimizing imbalance, there are not much differences in the sensitivity of each strategy to the BESS size. All strategies perform better with smaller BESS sizes. This seems reasonable, because with smaller sizes, the output of the BESS is limited and thus there is less risk of overcompensating a forecast error, and thus create an error in the other direction. For example, consider the case when the forecast production is 10 MWh, and the day-ahead bid is 12 MWh. The command would be to output 2 MWh of the BESS. If the BESS size is 10 MWh, this command can be performed. However with a smaller BESS size (1 MWh), the BESS output would be limited to 1 MWh. If the actual realization is higher than 10 MWh, the larger BESS output will overcompensate the error, creating an imbalance in the other direction. On the other hand, the smaller BESS will still reduce the imbalance. For small BESS sizes, an error on the exact amount of imbalance is not necessarily harmful if the sign of the forecast error is correct, which gives another reason why the MBE of the forecast model is its most important characteristic for the PV/BESS control.

Still, larger BESS sizes correct more imbalances, even if each installed BESS MWh is less efficient. An operator would have to set an optimal cost-efficiency point to correct the most possible imbalances for the lowest possible installation costs.

For strategies maximizing the revenue, the behavior is very different when there is an intra-day market participation (R3) or not (R1 and R2). Strategies R1 and R2 have a similar behavior, although strategy R2 seems to better manage small BESS sizes, thanks to the MPC controller that takes into account the SOC of the BESS when deriving the output, and thus limits saturation effects. Strategy R3 performs much better than the two others for lower BESS sizes. We think that since the intra-day market already compensates a significant part of the forecast errors, the BESS size can be more devoted to generating revenue on the day-ahead market. Then the same effect as for minimizing imbalances appears: for small BESS sizes, the BESS outputs are smaller, thus limiting the risk of having significant losses on a given BESS output.

Overall, it appears from the results that taking BESS life loss into account does not generate a significant improvement in control strategies. Besides, taking the near future into account with a MPC used in method RT2 when managing a BESS is only useful when the ratio of BESS capacity compared to PV capacity is low (that is, $\leq$ 25%). For higher ratios, the saturation effects are less frequent and thus a simpler algorithm can be used.

Finally, it is clear that the market conditions of the test case are not favorable to PV/BESS. Compared to the 200 €/kWh we used as the installation price of a BESS, gaining at most 90,000 €over the course of the test period (4 months) for that 91 897 kW portfolio

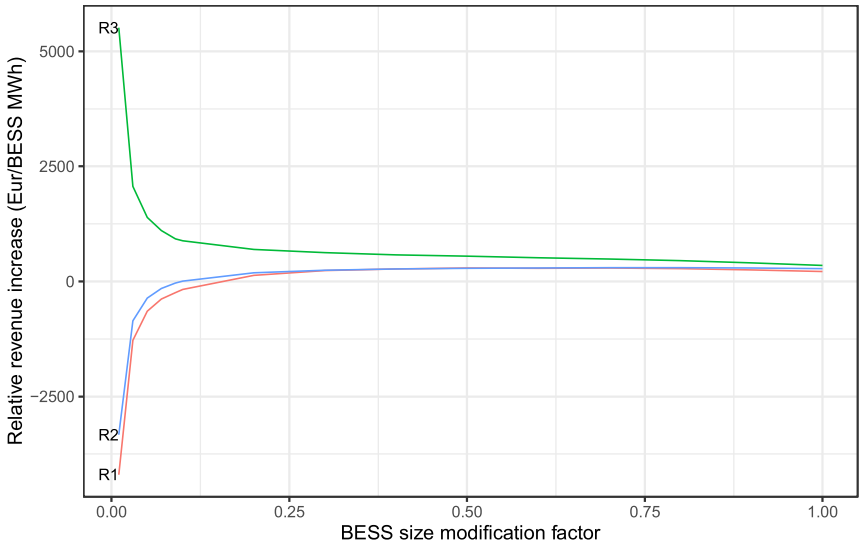

Figure 5.7: Revenue increase per installed BESS capacity

leads to an extremely long return on investment in France.

5.2.7.2 Sensitivity to market conditions

The market conditions are of particular importance for analyzing the results, and so we also performed a sensitivity analysis on the market prices. Namely, we compared the difference in results when the day-ahead prices are higher than the actual prices used in the initial simulation, and also when the magnitude between the day-ahead prices and imbalance prices is higher than the actual ones.

We assumed that the controlling algorithms' output was the same after modifying the price signals. This assumption is true only for strategies using the control RT1, if we keep the same relative magnitude between the day-ahead and imbalance prices, so that the perception of the financial risk of being in imbalance, i.e. the ratio $\frac{\pi_s - \pi_+}{\pi_- - \pi_+}$, is the same. For strategies using the control method RT2, the control algorithm depends on other quantities than this ratio, and thus it is not possible to modify the price signals without modifying the control of the BESS.

We tested the strategies on two variations of the price signals. The results are represented on Fig. 5.8 and 5.9. The first variation we tested involved multiplying the day-ahead prices by a given factor, maintaining the same difference between the day-ahead and imbalance prices ("Spot only"). The second variation was to multiply the difference between the imbalance prices and the day-ahead prices by a given factor, keeping the same day-ahead

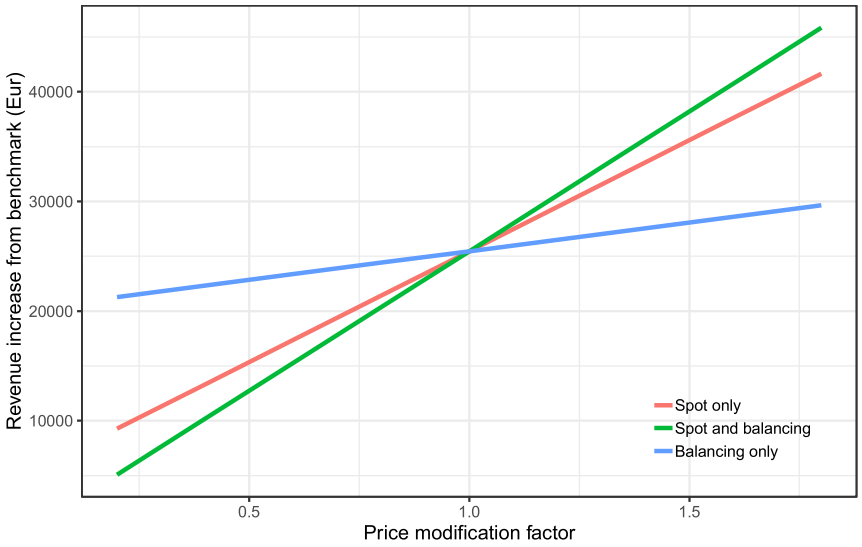

Figure 5.8: Sensitivity of the revenue to market conditions for strategy R1

signal ("Balancing only"). Finally, we also multiplied both signals ("Spot and balancing"); the multiplication factors must remain the same so that the relative difference between day-ahead and imbalance prices remains the same.

For both strategies, the revenue increase is directly proportional to the market prices. Since it is also directly proportional to the BESS installation cost, the return on investment time of a PV/BESS could be significantly reduced if both the BESS installation cost reduces and the market prices increase. The results are much more sensitive to the spot price than the imbalance price variations. This is another illustration of the fact that the benefits from reducing the imbalances are low and uncertain, while the benefits from shifting the production to times with higher spot prices are much more reliable.

5.3 Approach 2: direct bidding with neural networks

This approach consists again in dropping the intermediate models to take each of the consecutive decisions with a single ANN that consider all the inputs. However, the decisions to take are more complex than in the first test case of chapter 4. Since we operate a BESS, we must take into account its operational constraints. Since the state of the BESS depends on the history of its usage, the ANN must consider this history in addition to its inputs. In practice, there are two main consequences for the ANN design and training:

- Since the behavior of intra-day markets and day-ahead markets with BESS is more

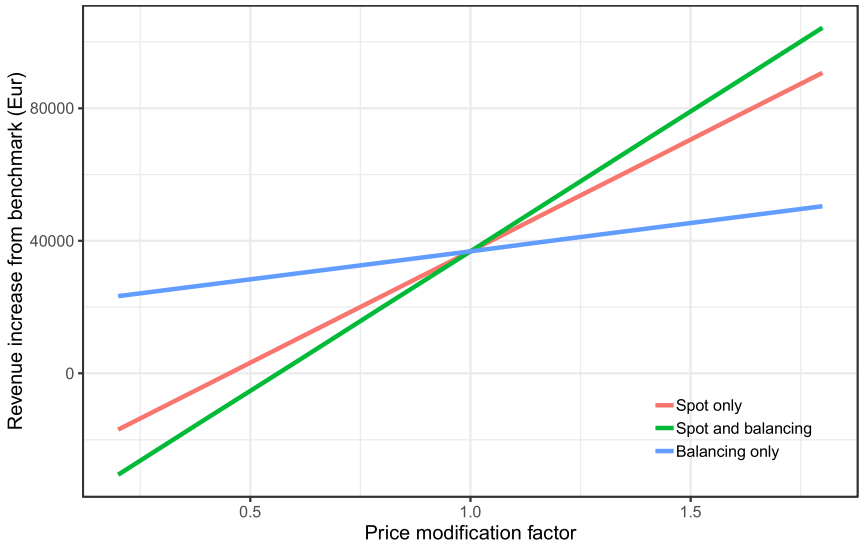

Figure 5.9: Sensitivity of the revenue to market conditions for strategy R3

complex and more design variables are involved, the ANN must also have more complexity, which means more parameters. Therefore, their training is more difficult.

- Since the ANN must consider the history of the BESS usage in addition to the inputs, we use a specific design of ANNs called Recurrent Neural Network (RNN).

For the control of the PV/BESS with operational constraints, we must use RNNs. For the intra-day control, the BESS is not involved, and we can use standard ANNs; however the randomness of the intra-day market must be taken into account using the intra-day market model. Therefore, using approach 2, the workflow simplifies as represented on Fig. 5.10.

5.3.1 Day-ahead bidding

For the day-ahead bidding, the operational constraints of the BESS prevent the use of a standard ANN. These constraints are the ones already presented in 5.2.1.2 in equations (5.5) to (5.7).

Although there are ways to directly constrain the output of a neural network, these constraints are difficult to enforce, most notably because the constraints for time step i require knowing the output for time step $i-1$. However, all the outputs must be calculated at the same time, which is the GCT of the day-ahead electricity market. Therefore, we choose to train an unconstrained neural network, and to perform modifications of the

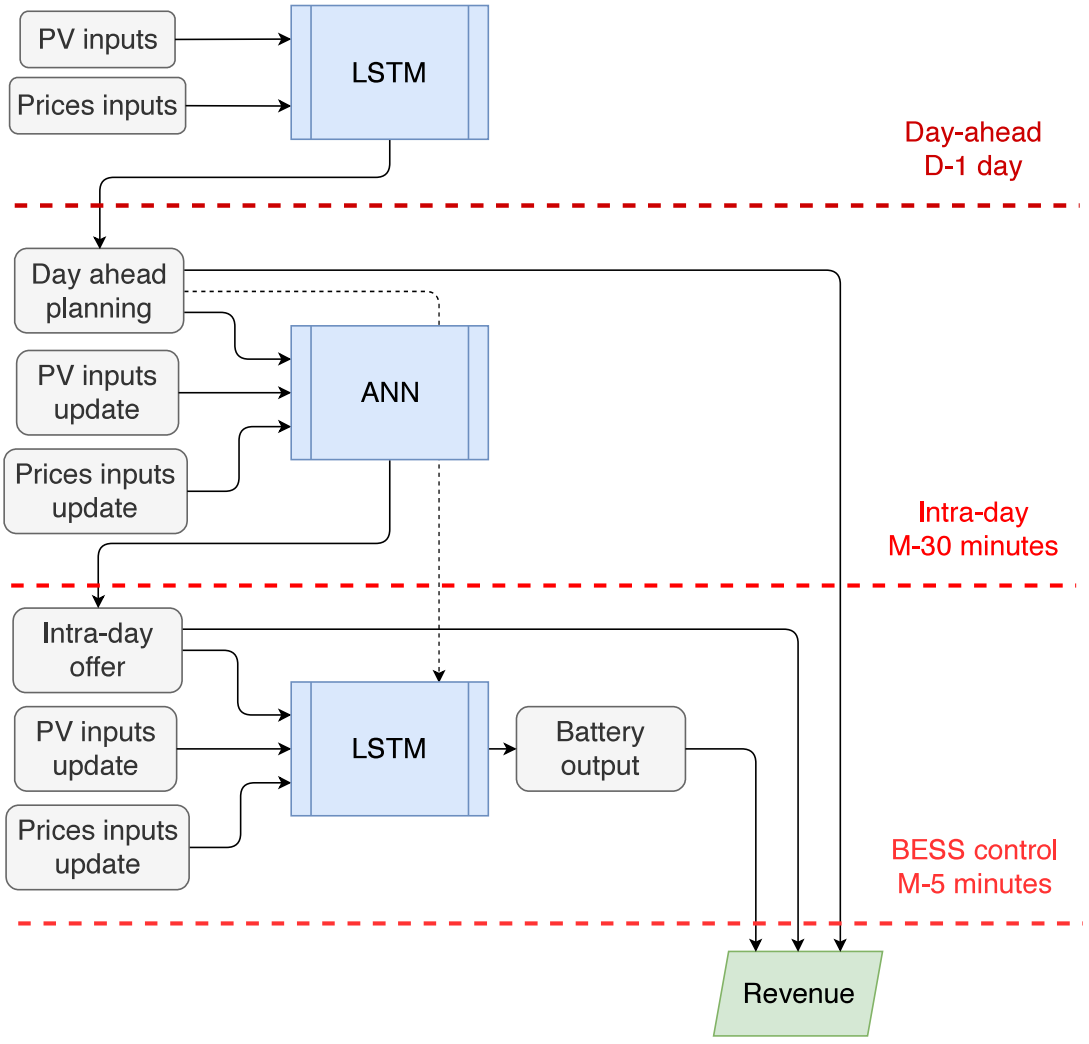

Figure 5.10: Flowchart of Approach 2

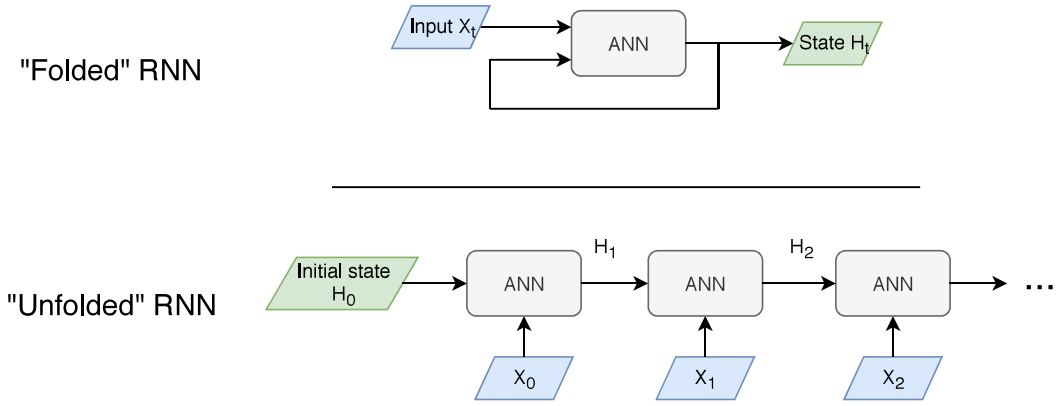

Figure 5.11: Schematic representations of a RNN

unconstrained output to enforce the constraints before computing the loss function. As long as the transformations have a gradient, the backpropagation can still be used to update the model parameters, and the transformations used to enforce the constraints can be seen as the output layer of the model.

Still, the model must have the time series of bids for the whole next day, from the time series of inputs. Although it would be possible to use a standard ANN that takes all features for each time step of the following day and that generates the bids, it is preferable to use a model architecture specifically designed for sequence-to-sequence forecasts. This naturally suggests RNNs, that have been developed for sequence predictions.

RNNs are a class of neural networks that are able to sequentially process a sequence of inputs. Basically, the input is combined with a hidden state. The resulting vector is fed to a neural network that generates the next hidden state. This new state can be combined with the next input to get the next state, until the whole input sequence is processed. RNNs can be schematically represented as folded or unfolded, as in figure 5.11.

The rationale behind this architecture is that the output of the neural network is conditional to the state, and thus to the previous inputs. This creates a form or memory, which allows the network to remember previous information when processing the next state. In the case of regression, the output of the RNN can simply be the hidden state of the RNN. Sometimes, a companion ANN is used to decode the hidden state into a value as the output. In our case, this representation seems useful, as the output is conditional to the state of charge of the BESS, which could be contained in the hidden state, and to the prices and weather data which could be contained in the inputs.

If standard RNNs are theoretically able to remember any event, they empirically have a

memory up to a few time steps ago and thus have trouble learning "long-term" dependencies [162]. To overcome this, another variant of RNNs called Long Short Term Memory networks (LSTM) was initially proposed in [163]. In such networks, the ANN that is used in standard RNNs is replaced by a memory cell that facilitates the propagation of information along time. Since they outperformed standard RNNs on a number of tasks (see [164], ,[165] or [166]), we chose to implement a LSTM.

To facilitate the implementation of the constraints, we also propose to separate the contracted energy as before with $E_c = E_{c,PV} + E_{c,BESS}$. Therefore, we train the LSTM network to provide an output of size $n_{mtu} \times 2$ where n_{mtu} is the number of MTUs for the following day. The two columns of the output are $E_{c,PV}$ and $E_{c,BESS}$.

In a similar manner to the ANN we trained on chapter 3, the features used by the LSTM are the union of all the features used in the first approach. They include:

- Weather-related features: NWP forecasts of wind speed, temperature, solar irradiance, cloud cover and precipitation at the surface, clear-sky profile
- Market-related features: TSO forecast of national demand, spot prices observed the day before the current trading day, day of the week and hour of the day.

Then the constraints are manually enforced on the LSTM output. The absolute maximum energy that can be moved from the battery is defined by the third constraint on the charging/discharging rate. Thus, this constrained is enforced first. To do so, a check is passed on the second column of the output, $E_{c,BESS}$. If any two consecutive time steps $i, i+1$ violate the third constraint, the amount of energy $E_{c,BESS,i+1}$ moved from the BESS at time $i+1$ is capped so that the maximum charging or discharging rate of the BESS is respected, while keeping the direction i.e. charging or discharging, of the BESS.

Then the second constraint is checked. A second check is passed on $E_{c,BESS}$. If the second constraint is violated for any time step, the energy moved from the BESS is again capped so that the BESS is not charged from the grid. Finally, the last constraint is checked in the same manner: if for any two consecutive time steps, the constraint is violated, the energy moved from the BESS is capped so that the state of charge of the BESS remains between 0 and 1.

Note that for each of these transformations, the direction of the BESS energy movement is preserved, and the absolute value of $E_{c,BESS}$ can only be lowered. Therefore, enforcing a constraint can not cancel the realization of a previously enforced constraint.

Finally, the total revenue generated from the transformed output is computed from equation (5.1), and the parameters of the LSTM are updated using backpropagation.

5.3.2 Intra-day bidding

For the intra-day bidding, there are no constraints on the possible offers, and the realization of a transaction does not influence the possible offers for the following time steps, as opposed to the control of the BESS. Thus, each MTU can be considered independently and consecutively when participating in the intra-day market. There is no incentive to use a sequence forecast as for the day-ahead planning, so we use a standard ANN to produce the intra-day offers.

We use the same intra-day market model as in 5.2.2. However, since the ANN model learns from the reward it gets with the intra-day market, there is no need to force the intra-day offer price to π_s to simplify the derivation of the offer as in 5.2.2. We can simply use the output π_{ID}, E_{ID} of the ANN, and then use it to evaluate the additional revenue. Since the evaluation is made *a posteriori*, we can use the real additional revenue by replacing the forecast PDF of the PV power by the actual energy generated E_{PV}. Finally, the loss we use to train the ANN is adapted from equation (5.13), which is the expected revenue with respect to the probability of acceptance of the offer, knowing the actual energy generation E_{PV}:

$$L_{ID}(\pi_{ID}, E_{ID}) = p_{ID}\left((\pi_{B,ID} - \pi_{ID})E_{ID} + (E_{PV} - E_c)(\pi_{B,ID} - \pi_B)\right) \tag{5.46}$$

Compared to the intra-day control method from approach 1, this bidding agent is able to offer both a volume and an offer price to maximize its additional revenue.

The features used to provide the intra-day offers are the same as the ones used for the day-ahead bidding. However, at this stage we are closer to real-time and so the features used are updated. They include:

- Updates of the NWP forecasts based on the last available NWP run.
- Update of the TSO national demand forecast.
- Actual spot price, which is known at the time of participation on the intra-day market.
- Clear-sky profile.
- Last observed injection from the PV plant. Since the intra-day market closes 30 minutes before delivery, we use the 30-minute lagged production as feature.

We also use the result of the previous decision-making process, that is the bids on the day-ahead market, as features.

5.3.3 Real-time control

The real-time control of the BESS is very similar to the day-ahead bidding agent. The control of the BESS must be done over several time steps, since the action for the next time step can prevent the realization of the day-ahead planning. This motivates again the use of a LSTM. The output is only the energy to charge or discharge from the BESS, and thus the output is a $\mathbb{R}^m$ sequence, where m is the length of the LSTM sequence.

To train the model, we use the reward obtained from the action of the BESS. We can use the actual energy generation E_{PV} to compute this reward. Thus, the loss used to train this second LSTM model is:

$$L_{LSTM}(E_{RT}) = \sum_{m} \pi_{B,BESS} E_{BESS} + (E_{PV} - E_c)(\pi_{B,BESS} - \pi_B) \tag{5.47}$$

Where $\pi_{B,BESS}$ denotes the imbalance price considering the action of the BESS:

$$\pi_{B,BESS} = \begin{cases} \pi_+ \text{ if } E_{realized} + E_{BESS} > E_c \\ \pi_- \text{ if } E_{realized} + E_{BESS} < E_c \end{cases} \tag{5.48}$$

Once again, the features used are the updates of the features used at the previous stage. They include updates of the NWP weather forecasts and TSO demand forecasts, clear-sky profile, last power measurement from the PV plant. The control of the BESS is made as close to the real-time as possible. In our case, we have the data with a 5-minute resolution and thus we use the 5-minute lagged production time series as a feature. We also use the decisions that resulted from the previous decision-making processes, that are the bids on the day-ahead market and the accepted offers on the intra-day markets.

5.3.4 Results

We performed the same simulation as with Approach 1. The control of the PV/BESS is simulated on a period of four months from 01/01/2018 to 01/05/2018 for the aggregated plant of 91 897 kWp. The size of the BESS used for the simulation is 91 897 kWh as for approach 1.

5.3.4.1 Day-ahead trading

The first decision to make is the day-ahead trading. Example results of the trading realized with Approach 2 are shown on figure 5.12.

With this approach, the shape of the bids is quite similar from one day to another. Since there are no dedicated PV power forecasting model in the decision chain, the model can not

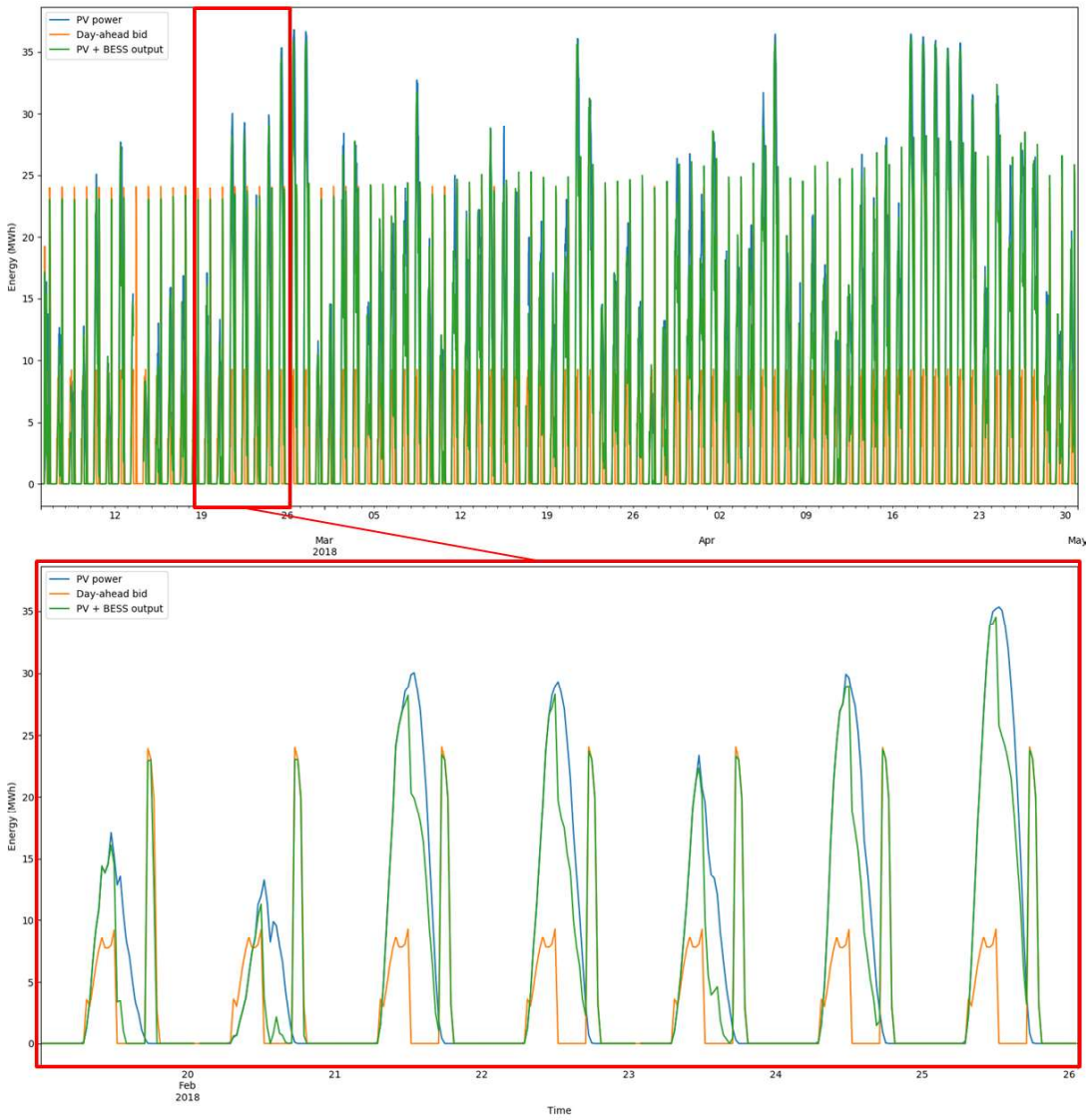

Figure 5.12: Example trading days with Approach 2 in the day-ahead market

Table 5.4: Results for the day-ahead bidding with Approach 2 and comparison with the best results obtained from Approach 1

	Approach 1 - strategy R3	Approach 2
Total imbalance (MWh)	4 239	14 563
Total revenue (€)	1 085 190	1 126 615

offer bids as precise as with the first approach. Thus, its strategy to maximize revenue is to offer bids at times when spot prices are high. The times of the day when prices are high are almost always the same for this market, that is in the morning and the evening at peak demand for France, and so the bids are almost the same every day.

Results regarding revenue and imbalance when using only this LSTM without participation in the intra-day market and real-time control are shown in table 5.4. The actual realization of the BESS used to derive this revenue is the output given by the enforcement of the constraints described in 5.3.1 applied on the BESS planning given by the LSTM at the day-ahead trading stage. These results set the benchmark for the following decision-making processes. Using approach 2, the revenue generated at the day-ahead bidding phase is higher than with approach 1, and so its usage of market information seems more efficient than approach 1.

5.3.4.2 Intra-day trading

The following decision is the intra-day bidding. We trained two models: one designed for minimizing the imbalance and another one designed to maximize the revenue.

The description of the model maximizing the revenue is presented in 5.2.2.1. The one minimizing the imbalance is similar. However, we made several changes:

- The price of the offer is not an output of the model, as this would encourage the model to make extremely poor bids regarding the revenue. For example, if a positive imbalance is expected, the model could sell excess energy for a negative price on the intra-day market, which would reduce the imbalance but be extremely harmful for the actual revenue. As we want the solution to be useful in an operation setting even if it does not focus on revenue, we removed this degree of freedom from the model and always set the intra-day offer price to π_s.

- The loss function is not the actual revenue but the imbalance reduction ΔImb. Since the probability of acceptance of the offer is a function of the offer price only, we did

Table 5.5: Results for the participation in the intra-day market with approach 2

	ANN reducing imbalance	ANN maximizing revenue
Total imbalance (MWh)	13 188	14 563
Imbalance variation	-10.0%	0%
Total revenue (€)	1 095 025	1 126 615
Revenue variation	-2.8%	0%

Table 5.6: Results for the participation in the intra-day market and real-time control with approach 2

	Imbalance Reduction	Revenue Maximization
Total imbalance (MWh)	15 023	25 517
Variation compared to benchmark	3.3%	75%
Variation compared to benchmark and intra-day	14.3%	75%
Total revenue (€)	968 677	1 013 699
Variation compared to benchmark	-14%	-10%

not take it into account in the loss function:

$$\Delta Imb = E_{realized} + E_{ID} - E_c \tag{5.49}$$

Complete results for these two models are reported in table 5.5. Although Approach 2 allows for a significant imbalance reduction, it does not necessarily increases the revenue. This comes from the high frequency of cases when $\pi_+ > \pi_s$ or $\pi_- < \pi_s$, in which case any imbalance is actually rewarded.

When trying to anticipate this effect and using market-related inputs to participate in the intra-day market to maximize revenue, the model learns to not participate in the intra-day market, as it found no way to reliably increase the revenue. This seems to suggest that the inherent uncertainty of imbalance prices is too important to have reliable methods to increase the revenue for this market.

5.3.4.3 Real-time control

Final results for the control of the BESS using the three consecutive decisions are reported on table 5.6.

As for the intra-day participation, we can see that the second approach is able to reduce the imbalance but not improve the revenue. This is a major distinction with the first approach which could improve both criteria. Besides, the imbalance reduction was higher with approach 1 than with this approach. However, the initial revenue generated with the benchmark was higher with the second approach, which shows that it still has value.

5.4 Conclusions

In this chapter we applied the methodology we proposed for PV power trading to the whole value chain, including and intra-day market and a storage system. To do so, we introduced new trading methods for intra-day markets, and we also performed some sensitivity analysis on the storage size and the market prices. We did not compare the two training methods M1 and M2 introduced in chapter 2, since the study from 4 suggested that training method M2 was more efficient regarding revenue. Therefore, we only studied the difference between the approaches based on individual forecasting models (approach 1) and ANNs (approach 2).

As in the first test case from chapter 4, the second approach used the market information more efficiently and so generated more revenue than the first approach in the day-ahead bidding phase, while creating more imbalances. However, for the intra-day participation and BESS control, there is almost no new market information that could help this model, and the improvement must be based solely on the update of the PV power forecasts, which improves a lot close to real-time. Thus, the first approach that uses a PV power forecasting model significantly improved the revenue in the operation phase with intra-day market and storage control, while the second approach that relies primarily on market trends and systematic tendencies could not improve the revenue during that phase. This also explains why the first approach, which uses much more accurate PV power forecasts, performed better in both imbalance and revenue on the intra-day market and real-time control.

However, the second approach performed much better than the first one in the bidding phase, and thus generated more revenue than the first approach even considering the additional revenue obtained by the first approach during the operation phase.

Chapter summary in French

Description du cas d'étude

Dans ce chapitre, nous étudions la chaîne de valorisation complète de l'énergie PV. Si nous nous plaçons toujours dans le cadre d'un marché day-ahead avec des prix de règlement des écarts en "dual-pricing", nous considérons également la possibilité de participer à un marché intra-day, ainsi le couplage de la centrale PV avec une batterie.

Le marché intra-day permet d'acheter ou de vendre de l'énergie jusqu'à 30 minutes avant la livraison. Ceci permet de réduire le volume d'écart et donc les pénalités. L'augmentation du revenu est alors égale à la réduction du volume d'écart multipliée par la différence entre le prix spot et le prix de la transaction intra-day. Cependant, les offres ne sont pas systématiquement acceptées sur le marché intra-day, puisqu'elles doivent trouver une contre-partie compatible en terme de prix.

La batterie permet deux façons d'améliorer le revenu. La première est de déplacer la production des instants où le prix spot est faible aux instants où le prix spot est élevé, ce qui permet d'améliorer le revenu du volume d'énergie déplacée multipliée par la différence de prix spot entre ces deux instants. Ceci s'effectue au moment de soumettre les offres de vente a marché de day-ahead. La seconde est d'utiliser la batterie en temps réel pour réduire le volume d'écart. L'augmentation du revenu est alors égale à la réduction de l'écart multipliée par la différence entre le prix spot et le prix de réglement des écarts.

De façon génerale, en notant E_{PV} la production PV, E_{BESS} l'énergie chargée ou déchargée de la batterie, E_{ID} l'énergie vendue ou achetée sur le marché intra-day, E_c, le revenu s'écrit :

$$\begin{aligned} R = \pi_s(E_{PV} + E_{BESS}) - (E_{PV} + E_{BESS} + E_{ID} - E_c)(\pi_s - \pi_B) \\ - C(E_{BESS}) \end{aligned} \tag{5.50}$$

Où $C(E_{BESS})$ est un terme qui traduit le coût lié à la perte de durée de vie de la batterie causée par son utilisation.

Il y a donc trois processus de prise de décision successifs :

- En J-1, déterminer la quantité d'énergie E_c à vendre sur le marché day-ahead en prenant en compte la capacité de la batterie à déplacer la production.
- A T-30 minutes, déterminer la quantité d'énergie E_{ID} à acheter ou vendre sur le marché intra-day en prenant en compte E_c.

- Au plus près possible du temps réel i.e. T-5 minutes avec nos données, déterminer la quantité d'énergie E_{BESS} à charger ou décharger de la batterie connaissant E_c et E_{ID}.

Nous reprenons les solutions proposées dans la thèse avec les approches A1 et A2 qui utilisent respectivement la chaîne classique de modèles de prévision individuels, ou un réseau de neurones artificiel. Cependant, nous ne conservons que la méthode d'entraînement M2, car elle a montré avoir de meilleurs performances en terme de revenu dans le chapitre 4. Ce chapitre permet donc de comparer les approches A1 et A2, ainsi que d'illustrer la valeur du modèle AnEn développé dans la thèse, puisque c'est cet unique modèle qui permet d'obtenir les prévisions PV à la fois pour les marchés day-ahead, intra-day et le contrôle de la batterie, sans nécessité d'entraînement.

Approche 1

Pour chaque prise de décision, il est nécessaire d'avoir une prévision des prix et de la production PV. Les mêmes modèles que ceux du premier cas d'étude sont utilisés ici. Notons cependant que pour la participation au marché intra-day et l'utilisation de la batterie, les prix spot sont déjà connus puisqu'ils sont communiqués quelques heures seulement après la cloture du marché en J-1.

Pour chacune des options de valorisation (day-ahead, intra-day et contrôle de la batterie), des algorithmes de contrôle spécifiques doivent être développés.

Pour la participation au marché day-ahead, nous comparons deux méthodes. La première, notée DA0 est une méthode benchmark dans laquelle la batterie n'est pas utilisée, et les offres sont calculées de la même façon que dans le premier cas d'étude. La deuxième consiste à réaliser une optimisation stochastique du revenu en générant des scénarios de production tenant en compte de l'auto-corrélation de la production PV à partir des prévisions probabilistes. Cette optimisation est également soumise aux contraintes opérationelles de la batterie : sa charge ne peut pas dépasser son état de charge maximal où être inférieure à zéro, et elle ne peut pas être chargée d'un volume d'énergie inférieur à la production PV. Nous rajoutons également une contrainte sur la puissance maximale de charge ou décharge de la batterie pour qu'elle soit plus représentative des solutions existantes dans le commerce.

Pour la stratégie de participation au marché d'intra-day, il faut déterminer l'offre optimale à soumettre. Une offre consiste en un couple (E_{ID}, π_{ID}) comprenant le volume et le prix de l'offre. Nous introduisons une modélisation probabiliste de l'acceptation ou non de l'offre sur le marché intra-day. Nous proposons de la modéliser comme une épreuve de Bernoulli dont la probabilité de succès dépend du prix d'offre. Plus le prix d'une offre de

vente (resp. d'achat) est bas (resp. élevé), plus l'offre a de chances d'être acceptée. A partir de ce modèle, nous avons pu établir que tout point critique (E^*_{ID}, π^*_{ID}) devait vérifier :

$$E^*_{ID} = E_c - F^{-1}_{PV}\left(\frac{\pi_s - \pi_+}{\pi_- - \pi_+}\right) \tag{5.51}$$

Cependant ce n'est pas nécessairement un maximum local. En posant $\pi_{ID} = \pi_s$, toute transaction acceptée est bénefique pour le revenu, et on peut alors montrer que le point critique est un maximum local. La stratégie de participation au marché intra-day est donc de soumettre ce point comme offre, et donc :

$$(E^*_{ID}, \pi^*_{ID}) = \left(E_c - F^{-1}_{PV}\left(\frac{\pi_s - \pi_+}{\pi_- - \pi_+}\right), , \pi_s\right) \tag{5.52}$$

Finalement, pour la méthode de contrôle en temps réel, nous proposons deux méthodes. La première, la méthode RT1, est obtenue de façon similaire à la stratégie de participation au marché intra-day. En négligeant le coût d'usage de la batterie, et en n'optimisant que pour le prochain pas de temps, nous pouvons montrer que le volume d'énergie à charger ou décharger de la batterie qui minimise les pénalités est :

$$E^*_{BESS} = E_c - F^{-1}_{PV}\left(\frac{1}{1 + \dfrac{\pi_- - \pi}{\pi_s - \pi_+}}\right) \tag{5.53}$$

La seconde méthode, la méthode RT2, est similaire à la méthode de participation au marché day-ahead. A chaque pas de temps, la fonction de revenu est optimisée de façon stochastique à partir de scénarios de production PV et de prévisions déterministes des prix de réglement des écarts, sous les contraintes opérationelles de la batterie. A la différence de la première méthode, le revenu est optimisé sur le futur proche i.e. jusqu'à la fin de la journée en cours, et pas uniquement pour le prochain pas de temps. Ceci est très utile pour le cas fréquent où la batterie doit se décharger en fin de journée, quand le prix est elevé. Sans prendre en compte le futur proche, le volume optimal calculé par la première méthode pourrait vider la batterie de façon prématurée pour compenser des erreurs de prévision, ce qui causerait de grandes pénalités en fin de journée. Cette méthodologie est appelée Model Predictive Control (MPC) dans la littérature.

Resultats de l'approche 1

La simulation de la participation à cette structure de marché est réalisée pour une centrale PV virtuelle constituée de l'aggrégation des 12 centrales du premier cas d'étude, sur une période couvrant Janvier à Mai 2018 sur le marché EPEX SPOT en France. Une différence

importante par rapport au premier cas d'étude est que les données étant plus récentes, les règles de calcul du prix des écarts ont changé et sont plus récentes. En particulier, les pénalités ne sont plus nécessairement négatives, ce qui signifie que le producteur peut être rémunéré dans certains cas pour son écart, s'il contribue à la réduction de l'écart au niveau national. La conséquence principale est que l'amélioration de revenu par la réduction des écarts devient difficile, car dans de nombreux cas, réduire un écart revient effectivement à diminuer son revenu. Ces nouvelles règles sont cohérentes avec les directives européennes qui préconisent une uniformisation des règles de calcul des prix des écarts vers une règle "single pricing" qui permettent ces pénalités positives [167].

Cinq stratégies sont comparées : la stratégie de benchmark R0 qui correspond à l'absence de batterie, puis les quatre stratégies R1 à R4 qui correspondent aux cas avec ou sans marché intra-day, et avec la méthode de contrôle RT1 ou RT2. Nous les comparons également aux stratégies I0 à I4 qui utilisent exactement les mêmes méthodes mais avec pour objectif de minimiser l'écart au lieu de maximiser le revenu.

Avec les stratégies I0 à I4, la réduction de l'écart est significative, jusqu'à 72% dans le meilleur des cas. Cependant, cela ne se traduit que par une faible augmentation du revenu, puisque certains écarts étaient rémunérés. A l'inverse, les méthodes R0 à R4 génèrent un écart plus élevé, mais également une augmentation de revenu significative. La plupart du revenu semble être généré par la participation de la batterie en day-ahead, et non pas par la compensation des écarts, ce qui favorise les méthodes R4 et R4. La méthode R4 est celle qui génère le plus de revenu, cependant il nous semble que la méthode R4 est plus fiable puisqu'elle préserve la durée de vie de la batterie, bien que le coût de vieillissement de la batterie soit malgré tout assez faible pour toutes les stratégies. En outre, la méthode R4 utilise un algorithme glouton ("greedy algorithm") qui l'expose à des risques plus importants.

Finalement, il faut remarquer que si les augmentations de revenu sont significatives, elles ne se comparent pas au coût d'investissement de la batterie. Les conditions sont défavorables au couplage PV/batterie sur le marché day-ahead, avec un temps de retour extrêmement long. Les marchés de services systèmes pourraient cependant offrir des opportunités de revenu bien plus intéressantes.

Approche 2

Avec l'approche 2, nous entraînons un modèle ANN pour chaque prise de décision. Cependant, deux problèmes rendent complexes l'utilisation de réseaux standards ("feedforward neural networks").

Le premier problème est que la solution doit répondre aux contraintes opérationnelles

de la batterie. En tout état de cause, la sortie d'un modèle ANN n'est pas contrainte. Nous proposons donc d'intégrer dans la fonction d'évaluation de la sortie du réseau une première étape préliminaire qui modifie cette sortie de façon à ce que les contraintes opérationelles soient respectées.

Le second problème est que la décision à prendre dépend grandement de la décision qui a été prise plus tôt, puisqu'il est nécessaire d'avoir une idée de l'état de charge de la batterie pour savoir combien d'énergie il est possible de charger ou décharger. Nous proposons donc d'utiliser un réseau de type Recurrent Neural Network (RNN) qui est spécifiquement fait pour la prévision de séquence, en utilisant une forme de mémoire qui permet au réseau de conditionner sa sortie par l'historique de ce qu'il s'est passé avant. Plus précisément, nous utilisons un modèle de type Long Short Term Memory (LSTM) qui a prouvé dans la littérature son efficacité.

Ainsi nous utilisons un réseau LSTM pour l'offre sur le marché day-ahead. Pour la participationi au marché intra-day, il n'y a pas de contraintes et donc nous utilisons un ANN standard. Par rapport à la première méthode, nous pouvons laisser le réseau libre de choisir le prix d'offre π_{ID} puisqu'il est censé apprendre par la fonction d'évaluation le fonctionnement du marché, à savoir que les offres à prix non-compétitifs sont refusées et donc de génèrent pas d'amélioration du revenu. Finalement, nous utilisons à nouveau un réseau LSTM pour le contrôle en temps réel, puisque le problème est très similaire à la participation au marché intra-day.

Résultats de l'approche 2

Les résultats sont très différents de ceux obtenus avec l'approche 1. Comme dans le cas d'étude précédent, le modèle exploite bien plus les tendances du marché que les données météorologiques, si bien que la sortie du réseau ne semble que très peu conditionnée par les prévisions météorologiques. Au contraire, le réseau s'appuie énormément sur le comportement systématique du marché, avec des offres très conservatrices le matin pour se protéger du prix de réglement des écarts négatifs plus élevé que le positif, puis un stockage de l'énergie toute l'après-midi dans la batterie avant de décharger le soir lorsque le prix est élevé.

Cette stratégie fonctionne puisque le revenu géneré de cette façon est supérieur à celui obtenu par l'approche 1, bien qu'il reste trop faible pour envisager l'installation d'un couplage PV/stockage. Il s'agit en fait d'un cas où l'incertitude sur les prix, notamment sur le fait que les écarts contributeurs à la réduction de l'écart national soient rémunerés ou non, est telle qu'il n'est pas judicieux d'essayer à tout prix de réduire son volume d'écarts. Au contraire, il vaut mieux exploiter les tendances moins incertaines du marché, c'est-à-dire

le fait que les prix soient plus élevés à la pointe de la demande autour de 19h.

Malgré cela, les décisions suivantes sur le marché intra-day et le contrôle en temps réel ne parviennent ni à réduire l'écart, ni à augmenter encore le revenu. Il semble logique que le réseau ne parvienne pas à réduire les écarts puisqu'il ne possède pas de moyen de prévision de la production à proprement parler, mais il est surprenant qu'il ne parvienne pas non plus à augmenter le revenu. Notre hypothèse est que toutes les informations du marché à faible incertitude sont déjà exploitées au moment de soumettre les offres en day-ahead, et que les informations apportées en se rapprochant du temps réel de réduisent pas suffisamment l'incertitude sur le prix de réglement des écarts pour permettre au réseau d'augmenter encore le revenu.

Chapter 6

Conclusions

Contents

6.1 Summary and main findings

In chapter 1, we introduced the context and the objectives of this study. The worldwide energy production, and especially electricity, is a large contributor to many global pollution issues such as global warming, air and water pollution or loss of the local biodiversity. Although they suffer from other problems, such as aesthetic impact or land occupation, renewable energies are usually considered more environmentally friendly than other electricity sources. Especially, they produce much less CO_2 emissions than burning fossil fuels, and generate almost no waste compared to thermal and nuclear power plants. As such, their development is much promoted since the 2000s.

However, the integration of renewable energies in the power grid causes many issues, as their production is weather dependent and thus both uncertain and not controllable. Traditionally, the cost caused by these integration issues was supported by a surcharge on electricity consumers such as the CSPE in France [168] or the EEG surcharge in Germany [169]. In the recent years, the installation costs of wind and especially photovoltaic power decreased greatly, and now new support mechanisms involve transferring a part of the renewable integration costs on renewable power plant operators, by making them financially responsible for their production forecast errors.

Since it very difficult to know what kind of support mechanisms will be available in the coming years, if any, the objective of this thesis is to maximize the revenue generated from

PV power plants in the absence of any supporting mechanism. To do so, we focused on addressing the systematic issues we found in the PV power trading value chain, instead of incrementally improving individual parts of the value chain. We identified the four following issues:

- The need for a seamless PV power forecasting model.
- The need for a PV power forecasting model that combines heterogenous sources of data.
- The complexity and the number of forecasting models involved in the value chain.
- The absence of link between the individual forecast performance of the models and the value they generate.

In chapter 2, we introduced the different options available for PV producers to valorize their production. Currently, the most simple way to generate revenue from PV power production is to participate in electricity markets. However, some new ways to valorize the power may appear e.g. ancillary services market, flexibility remuneration or tenders with specific remuneration rules. Thus, we proposed generic notations that allows for modeling any valorization process assuming that their remuneration rules are clearly defined. In that way, it is easy to participate in any subset of the existing valorization options, or to add new options to the existing ones. Using this generic notation, we described the solutions that we propose to improve PV power trading:

- First we proposed to train individual models together using the value of the decision they contribute to as the objective function. This allows linking the training of the model to the PV power value, and so addresses the fourth issue identified. The standard training method where each model is trained to maximize its own performance is called Method 1, while the simultaneous training of the models for value is Method 2.
- Then we proposed to implement an alternative approach to obtain the decisions for each market. The standard approach called Approach 1 is to use a chain of individual forecasting models. We propose to use a single ANN to obtain the decisons for each decision-making process, which is Approach 2. In that case, the decision-making is based only on existing data. ANNs are convenient because they can learn to minimize any objective function, and so we can directly use the revenue generated from a given valorization option as an objective to train the ANN. To our knowledge, this approach has never been proposed before. This addresses the third identified issue by greatly

simplifying the model chain. Generally, this alternative approach had similar or better results that the standard one, but showed a very different behavior.

In chapter 3, we presented the forecasting model that we developed to address the first and second issues identified above. To do so, we improved an AnEn model by reinforcing it with satellite data and in situ measurements, and also by implementing an automatic feature-weighting procedure to make the model seamless. The model showed good performances compared to other state-of-the-art models, especially for short-term forecasts i.e. forecasts with an horizon lower than five minutes. This work was published in article [C] in section 1.7.

In chapter 4, we used these two approaches and training methods to simulate the participation of twelve PV power plants in the French electricity market EPEX SPOT. To perform Approach 1, we used the AnEn model introduced in 3. We also performed approach 2 using a simple ANN as the trading agent, without any PV power forecasting model. We found that this approach focused a lot more on market and price signals, resulting in systematically conservative bids, because overproducing is penalized less heavily than underproducing. Results regarding revenue and penalties were in the same range as with approach 1, although they were obtained in a very different manner: the total imbalance was much higher with approach 2 than with approach 1, but the average financial penalty per MWh of imbalance was lower. This ultimately resulted in roughly similar penalties and revenue. The two training methods generated a similar effect, but in a less significant manner. This comparison of the two Approaches and training methods was published in article [A] in section 1.7.

In chapter 5, we enhanced the previous case study by adding a BESS coupled with the PV plant to increase revenue, along with an intra-day market. The BESS and intra-day market have similar roles, as they both allow modifying the production after the bids have been submitted. But they have structural differences:

- Intra-day markets close 30 minutes before delivery, while BESS usage goes up to real-time.

- Intra-day offers are subject to acceptation depending on the price of the offer while BESS usage is not. We modeled the probability of acceptation of the intra-day offers depending on their price and the imbalance prices to derive bidding rules on the intra-day market.

- BESS usage is limited by the operational constraints of the BESS.

Again, we used the notations from chapter 2 to perform Approaches 1 and 2. With Approach 1 we proposed increasingly complex control strategies for the BESS, taking into account BESS ageing and the near future. Sensitivity analyses revealed that more complex strategies had low added value compared to simpler ones, unless the BESS size was very small compared to the PV plant size. In such case, taking the near future into account would greatly reduce the occurence of saturation effects with the BESS. With both control strategies, participating in the intra-day market greatly reduced the BESS usage, allowing to have similar performances with lower BESS sizes compared to the case wihout intra-day. However, the increase in revenue was too low to make the BESS a viable financial investment, because both the intra-day variations of the spot price and the penalizations for forecast errors were too small. The control of the PV/BESS system with the quantification of the revenue improvement was published in article [B] in section 1.7 while the sensitivity of the results to the BESS size was presented at the EU PVSEC 2019 conference.

Approach 2 performed in a similar manner as in chapter 2. It used a lot of market information, resulting in bids that exploited systematic trends of the electricity market rather than weather data, which in the end resulted in bids that are very similar from one day to another. Still, using the day-ahead BESS command as the real-time control of the BESS without update resulted in an improved revenue compared to Approach 1, despite having a greater imbalance. Benefits from shifting productions to times when spot prices are higher are more reliable than reducing imbalance, because imbalance prices are very uncertain, and sometimes imbalances are remunerated if they help the system. On the other hand, the spot price is almost always higher in the evening and so shifting the production to the evening with the BESS almost always increases revenue. This is why focusing on market tendencies is more reliable than focusing on PV production.

However, Approach 2 was much less efficient for the intra-day market participation and BESS real-time control. For the intra-day market, it could reduce imbalance but not improve revenue, and for the real-time control it could not reduce imbalance nor improve revenue compared to participating only in the day-ahead market, using the day-ahead BESS command as the real-time control. When going closer to real-time, a lot of new information regarding PV power production appears, while market information does not change much. Thus, Approach 2, that mostly uses market information, had trouble improving the performance when going closer to real-time.

6.2 Conclusion and perspectives

In the introduction, we stated that the objective of the thesis was to maximize the value obtained from PV power generation in electricity markets under price and production uncertainty. We proposed to tackle the systematic issues of the PV power value chain instead of improving individual parts of the chain. Generic notations were introduced to model any trading option along with two concurrent approaches for taking decisions in the value chain: Approach 1 that takes decisions based on expert forecasting models adapted to the objective, and Approach 2 based on ANNs learning to maximize the objective from historical data. Two training methods were also introduced. Method 1 trains the individual models of the value chain to maximize their forecasting performance, while Method 2 trains them to maximize the revenue obtained from the related trading option.

We found that the most efficient option to valorize the PV production is to participate in a day-ahead and an intra-day market without a storage system. The increased revenue generated over the lifetime of the BESS would not compensate the initial investment required for installing it.

A general finding is that Approach 2 made more use of market information, while Approach 1 made more use of weather information. When a BESS was available, Approach 2 performed better because it was better at shifting the production when the spot price was high. Without this option, both approaches had similar results. Another advantage of Approach 2 is that it is simpler to maintain, as there is only one model involved for each decision. However, there are other elements to consider when choosing which approach to prefer.

For example, using Approach 2 generates more overall imbalance. As a result, from the TSO point of view, it is less righteous than Approach 1. It is an open question whether it is allowed to deliberately generate more imbalance by being more conservative in order to hedge against imbalance prices or not. Besides, in some tenders, participants have to give to the TSO a forecast of their production. In that case, a PV power forecasting model is required no matter what, which cancels the argument that Approach 2 is simpler to maintain thanks to having less models.

However, there is a last argument in favor of Approach 2. When participating in electricity markets, one cause of having large imbalance prices is that a lot of participants base their bids on the same weather forecasts, and so when the forecast is wrong, all the participants are either short or long at the same time, which causes very high costs for balancing the grid. Having a unique forecasting method or using different sources of information can hedge this risk, effectively giving a competitive advantage even if the overall forecast

precision is lower [170]. With Approach 2, decisions are taken mostly based on market information, and so using Approach 2 could hedge the risk of very high imbalances.

This thesis opens up several research directions. We identified some that look promising.

The first natural research direction that we could think of is to further improve the range of forecast horizons of the AnEn model by using more data. As stated in the thesis, the version we developed did not use data from all-sky imagers, or spatial data from neighboring PV power plants. Such data could improve again the performance of short-term forecasts in their respective forecast horizons. To improve the performance in the morning, infrared satellite images could be used to use information on the cloud cover that standard visible satellite images could not see. Also, the AnEn model could be used not only to combine features but directly forecasts from other models, either developed or bought from an external entity.

Another possibility would be to use more adapted ANN structures in order to improve the Policy Function Approximation performed in Approach 2. One good candidate is the RL paradigm that was already used in recent work to maximize the cumulated profit obtained from storage systems performing energy arbitrage, and so would shift the subject of this thesis towards prescriptive analytics. Also, recent advances in deep learning highlighted Generative Adversarial Networks (GANs) [171], which could be used to implement more sophisticated ANN models able to process the market and weather information in a more efficient manner. Although the ANN models used in this thesis performed well in terms of revenue, they focused much more on market information than on weather information. Using more sophisticated ANN structures could then improve the results in that regard. More generally, considering more advanced decision-making methods could significantly improve the results obtained in this thesis. For example, using RO techniques to control the BESS could help achieving optimal solutions instead of approximately solving the problem with an MPC approach. At the day-ahead bidding phase, we only considered stochastic programming, although there are a wealth of stochastic optimization methods that could perform the same task [43].

Extending the considered test cases is also a very direct research direction. For now, we restricted ourselves to spot and intra-day electricity markets. However, the participation of variable energies in ancillary services markets is now a significant field of research, especially in combination with storage systems. Thus, future works should consider the joint participation in both electricity and ancillary services markets. Another interest of this is that in our case studies, all the markets considered were sequential. With ancillary services markets, the decision should be taken at the same time for both markets, and so the

problem would be more complex. Power derivatives are also a useful tool to hedge against the weather or the electricity price risk that could be included in our approach.

Another limitation of the work is that we focused on existing solutions to sell the PV power production. However, it would be possible to model possible new options in prospective works, such as peer-to-peer energy trading with the blockchain technology [172], or alternative remuneration rules in electricity and ancillary services markets. This could serve as a source of information for PV plants operators willing to estimate their revenue depending on market conditions. Alternatively, by simulating the simultaneous participation of different actors, this could help identify possibly efficient market structures and imbalance settlement rules.

Résumé et observations principales

Dans le chapitre 1, nous avons présenté le contexte et l'objectif de cette étude. La production mondiale d'énergie, et en particulier d'électricité, contribue largement à de nombreux problèmes environnementaux à échemlle mondiale tels que le réchauffement climatique, la pollution de l'air et de l'eau ou la perte de la biodiversité locale. Bien qu'elles souffrent d'autres problèmes, tels que l'impact esthétique ou l'occupation des sols, les énergies renouvelables sont généralement considérées comme plus respectueuses de l'environnement que les autres sources d'électricité. En particulier, elles émettent beaucoup moins de CO2 que les combustibles fossiles et ne génèrent presque pas de déchets par rapport aux centrales thermiques et à l'énergie nucléaire. Ainsi, leur développement est très favorisé depuis les années 2000.

Cependant, l'intégration des énergies renouvelables dans le réseau électrique pose de nombreux problèmes, car leur production dépend des conditions météorologiques et est donc à la fois accompagnée d'incertitude et non-contrôlable. Historiquement, le coût causé par ces problèmes d'intégration était supporté par des taxes supplémentaires qui étaient redistribuées aux TSOs. Ces dernières années, les coûts d'installation des filières éoliennes et photovoltaïques ont fortement diminué, de sorte que les nouveaux mécanismes de soutien impliquent le report d'une partie des coûts d'intégration des énergies renouvelables aux exploitants de centrales électriques renouvelables, en les rendant financièrement responsables du coût causé par leurs erreurs de prévision de production.

Comme il est très difficile de savoir quels types de mécanismes de soutien seront disponibles dans les années à venir, l'objectif de cette thèse est de maximiser les revenus générés par les centrales électriques sur le marché de l'électricité en l'absence de tout mécanisme de soutien, sous incertitude des prix et de la production. Pour ce faire, nous nous sommes concentrés sur les problèmes structurels que nous avons trouvés dans la chaîne de valorisation de l'énergie PV, au lieu d'améliorer individuellement les différents maillons de la chaîne de valorisation. Nous avons identifié les quatre problèmes suivants :

- Le besoin d'un modèle de prévision de puissance adapté aux besoins des marchés de l'électricité.
- Le besoin d'un modèle de prévision de puissance PV à court terme qui combine des sources de données hétérogènes.
- L'absence de lien entre la performance de prévision des modèles individuels et la valeur qu'ils génèrent sur les marchés.

- La complexité et le nombre de modèles de prévision impliqués dans la chaîne de valeur.

Dans le chapitre 2, nous avons présenté les différentes options disponibles pour les producteurs de PV pour valoriser leur production. Actuellement, le moyen le plus simple de générer des revenus à partir de la production d'électricité à court terme est de participer aux marchés de l'électricité. Cependant, de nouvelles façons de valoriser la production peuvent apparaître, par exemple le marché des services systèmes ou des appels d'offres avec des règles de rémunération spécifiques. Ainsi, nous avons proposé des notations génériques qui permettent de modéliser tout processus de valorisation en supposant que leurs règles de rémunération soient clairement définies. De cette façon, il est facile de participer à n'importe quel sous-ensemble des options de valorisation existantes ou d'ajouter de nouvelles options à celles qui existent déjà. En utilisant cette notation générique, nous avons décrit les solutions que nous proposons pour améliorer la chaîne de valorisation de l'énergie PV :

- Entraîner les modèles individuels simultanément en utilisant la valeur de la décision à laquelle ils contribuent comme fonction objectif. Cela permet de relier l'entraînement des modèle au revenu , et donc d'aborder le troisième problème identifié. La méthode d'entraînement standard où chaque modèle est formé pour maximiser sa propre performance est appelée Méthode 1, tandis que l'entraînement simultané des modèles est la Méthode 2.

- Une approche alternative pour obtenir les décisions pour chaque marché. L'approche standard appelée Approche 1 consiste à utiliser une chaîne de modèles de prévision individuels. Nous proposons l'Approche 2 qui consiste à utiliser un seul ANN pour obtenir les vecteurs de décisions de chaque option de valorisation. Dans ce cas, la prise de décision s'appuie uniquement sur les données existantes. Les ANNs peuvent apprendre à minimiser n'importe quelle fonction objectif, et ainsi nous pouvons utiliser directement les revenus générés par une option de valorisation donnée comme objectif. A notre connaissance, cette approche n'a jamais été proposée auparavant, et répond au quatrième problème identifié en simplifiant considérablement la chaîne de valorisation.

Dans le chapitre 3, nous avons présenté le modèle de prévision que nous avons élaboré pour traiter les premiers et deuxièmes problèmes identifiés ci-dessus. Pour ce faire, nous avons amélioré un modèle AnEn en le renforçant avec des données satellite et des mesures locales, ainsi qu'en mettant en œuvre une procédure de pondération automatique des variable d'entrée pour rendre le modèle capable de fournir des prévisions pour n'importe quel horizon. Le modèle a montré de bonnes performances par rapport à l'état de l'art, en

particulier pour les prévisions à court terme, c'est-à-dire les prévisions dont l'horizon est inférieur à cinq minutes. Ce travail a été publié dans un article de journal [27].

Dans le chapitre 4, nous avons utilisé les approches et les méthodes 1 et 2 pour simuler la participation de douze centrales électriques PV au marché français de l'électricité EPEX SPOT. Pour réaliser l'approche 1, nous avons utilisé le modèle de prévision AnEn développé dans le chapitre 3. Nous avons également réalisé l'approche 2 en utilisant un ANN pour obtenir les offres de vente, sans modèle de prévision de puissance PV intermédiaire. Nous avons constaté que cette approche exploitait plus les informations liées au marché, ce qui se traduit par des offres généralement conservatrices, car la surproduction est moins pénalisée que la sous-production. Les résultats sont similaires qu'avec l'approche 1, mais ils sont obtenus d'une manière très différente : le montant total des écarts est bien plus élevé avec l'approche 2, mais la pénalité financière moyenne par volume d'écarts est moindre. Il en résulte des pénalités et un revenu total à peu près semblable. Les méthodes d'entraînement 1 et 2 ont eu un effet similaire, mais de manière moins importante. Cette comparaison des deux approches et méthodes de formation a été publiée dans [28].

Dans le chapitre 5, nous avons étendu le cas d'étude précédent en ajoutant un BESS couplé à la centrale PV pour augmenter les revenus, ainsi qu'un marché intra-day. Le BESS et le marché intra-day ont des rôles similaires, car ils permettent tous deux de modifier la production après que les offres ont été soumises, mais ils ont des différences structurelles :

- Les marchés intra-day ferment 30 minutes avant la livraison, tandis que l'utilisation d'un BESS va jusqu'au temps réel.
- Les offres intra-journalières sont sujettes à acceptation en fonction du prix de l'offre. Nous avons modélisé la probabilité d'acceptation des offres intrajournalières en fonction de leur prix et des prix de règlement des écarts pour traiter cet aspect.
- L'utilisation des BESS est limité par des contraintes opérationnelles.

Nous avons utilisé les notations présentées dans le chapitre 2 pour réaliser les approches 1 et 2. Avec l'approche 1, nous avons proposé différents stratégies de contrôle graduellement plus complexes pour le BESS, en tenant compte du vieillissement du BESS et du futur proche. Des analyses de sensibilité ont révélé que les stratégies plus complexes avaient une faible valeur ajoutée par rapport aux stratégies plus simples, à moins que la taille des BESS soit très petite par rapport à celle de l'installation PV. Dans un tel cas, la prise en compte du futur proche dans le contrôle du BESS réduit considérablement l'apparition d'effets de saturation. Pour toutes les stratégies de contrôle, la participation au marché intra-day

réduit considérablement l'utilisation du BESS, ce qui permet d'obtenir des performances similaires à celles des cas sans marché intrajournalier avec des tailles de BESS plus faibles. Toutefois, l'augmentation du revenu reste trop faible pour faire du BESS un investissement financièrement viable, car les variations intrajournalières du prix de l'électricité et les pénalités pour les erreurs de prévision sont trop faibles. Le contrôle du système PV/BESS a été publié dans [173] tandis que la sensibilité des résultats à la taille du BESS a été présentée à la conférence EU PVSEC 2019.

L'approche 2 s'est comportée de la même manière qu'au chapitre 2. Elle a plus utilisé les informations sur le marché de l'électricité, ce qui a donné lieu à des offres qui exploitent les tendances systématiques du marché de l'électricité plutôt que les données météorologiques. Cela aboutit à des offres très similaires d'un jour à l'autre (voir figure 5.12). Néanmoins, en utilisant la commande day-ahead du BESS comme contrôle en temps réel du BESS sans mise à jour, le revenu obtenu est supérieur à celui de l'approche 1, malgré un plus grand écart. Le profit obtenu en déplacant la productions vers des instants où le prix de l'électricité est plus élevé est plus fiable que celui obtenu en réduisant l'écart, car les prix de règlement des écarts sont très variables et imprévisibles, et parfois les écarts sont mêmes rémunérés s'ils aident à réduire le désequilibre au niveau national. D'autre part, le prix de l'électricité est presque toujours plus élevé le soir et donc le fait de déplacer la production vers le soir avec le BESS augmente presque toujours le revenu.

Toutefois, l'approche 2 a été beaucoup moins efficace pour la participation au marché intrajournalier et le contrôle en temps réel du BESS. Pour le marché intrajournalier, l'approche 2 a su réduire l'écart mais pas améliorer le revenu, et pour le contrôle en temps réel, il n'a su améliorer aucun de ces critères comparé à la participation au marché day-ahead uniquement. En se rapprochant du temps réel, beaucoup de nouvelles informations liées à la production d'énergie apparaissent, alors que les informations liées au marché changent peu. Ainsi, l'approche 2, qui utilise principalement l'information liée au marché, à une faible valeur ajoutée à l'approche du temps réel.

Conclusion et perspectives

Dans l'introduction, nous avons indiqué que l'objectif de la thèse était de maximiser la valeur obtenue à partir de la production d'électricité sur les marchés de l'électricité dans des conditions de prix et de production incertains. Nous avons proposé d'aborder les problèmes structurels de la chaîne de valorisation de l'énergie au lieu d'améliorer les différents maillons de la chaîne. Des notations génériques ont été introduites pour modéliser les différents options de marché. Deux approches sont ont été proposées pour prendre des décisions dans la

chaîne de valorisation : l'approche 1 qui prend des décisions en s'appuyant sur des modèles de prévision individuels adaptés à l'objectif, et l'approche 2 qui s'appuie sur des modèles ANNs pour maximiser l'objectif à partir de données historiques. Deux méthodes d'entraînement ont également été introduites. La méthode 1 entraîne les différents modèles de la chaîne de valorisation à maximiser leur performance de prévision, tandis que la méthode 2 les entraîne à maximiser le revenu obtenus pour l'option de valorisation à laquelle ils contribuent.

Nous avons constaté que l'option la plus efficace pour valoriser la production PV est de participer à un marché day-ahead et à un marché intrajournalier sans BESS. L'augmentation des revenus générés pendant la durée de vie du BESS ne compenserait pas l'investissement initial nécessaire à son installation.

Une conclusion générale est que l'approche 2 a fait un plus grand usage de l'information sur le marché, tandis que l'approche 1 a fait un plus grand usage de l'information météorologique. Lorsqu'un BESS était disponible, l'approche 2 a donné de meilleurs résultats parce qu'elle permettait de déplacer la production lorsque le prix de l'électricité était élevé. Sans cette option, les deux approches ont donné des résultats similaires. Un autre avantage de l'approche 2 est qu'elle est requiert moins de maintenance, car il n'y a qu'un seul modèle impliqué dans chaque décision. Toutefois, il y a d'autres éléments à prendre en considération au moment de choisir l'approche à privilégier.

Par exemple, l'utilisation de l'approche 2 génère un plus grand écart global. Par conséquent, du point de vue du TSO, cette approche est moins vertueuse. Reste à savoir s'il est permis de générer délibérément plus d'écarts en étant plus conservateur afin de se prémunir contre les prix de règlement des écarts élevés ou non. En outre, dans certains appels d'offres, les participants doivent donner au TSO une prévision de leur production. Dans ce cas, un modèle de prévision de puissance de PV est nécessaire quoi qu'il arrive.

Il reste un dernier argument en faveur de l'approche 2. L'une des raisons pour lesquelles les prix d'équilibrage sont élevés est qu'un grand nombre de participants renouvelables fondent leurs offres sur les mêmes prévisions météorologiques, de sorte que lorsque les prévisions sont fausses, tous les participants ont une erreur de prévision dans le même sens, ce qui entraîne des coûts très élevés pour équilibrer le réseau, et donc des pénalités élevés pour les producteurs qui se sont trompés dans ce sens. Utiliser une méthode de prévision originale ou qui exploite différentes sources d'information peut diminuer ce risque en étant moins susceptible de faire une erreur dans le même sens que les autres participants, ce qui donne effectivement un avantage concurrentiel même si la précision globale des prévisions est inférieure [170]. Avec l'approche 2, les décisions sont prises principalement sur la base des informations du marché, et l'utilisation de l'approche 2 pourrait donc couvrir le risque

d'écarts très importants.

Cette thèse ouvre plusieurs pistes de recherche. Nous en avons identifié quelques-unes qui semblent prometteuses.

La première direction de recherche est d'améliorer la gamme des horizons de prévision du modèle AnEn en utilisant plus de données. Comme indiqué dans la thèse, la version que nous avons développée n'a pas utilisé de données provenant de caméras hémishpériques, ni de données spatiales provenant de centrales PV voisines. De telles données pourraient améliorer encore la performance des prévisions à court terme.

Une autre possibilité serait d'utiliser les récents progrès en deep learning tels que les Generative Adversarial Networks (GAN) [171] pour mettre en œuvre des modèles ANN plus sophistiqués capables de traiter les informations sur le marché et la météo de manière plus efficace. Bien que les modèles ANN utilisés dans cette thèse aient donné de bons résultats en termes de revenus, ils se sont concentrés beaucoup plus sur les informations de marché que sur les informations météorologiques. L'utilisation de structures ANN plus sophistiquées pourrait alors améliorer les résultats à cet égard.

Une autre limitation de cette thèse est que nous nous sommes concentrés sur les solutions existantes pour vendre la production d'énergie PV. Il serait toutefois possible de modéliser de nouvelles options, telles que la vente d'énergie en pair à pair avec la technologie blockvhain [172], ou d'autres règles de rémunération sur les marchés de l'électricité et des services système. Cela pourrait servir de source d'information pour les exploitants de centrales PV souhaitant estimer leurs recettes en fonction des conditions du marché. Par ailleurs, en simulant la participation simultanée de différents acteurs, cela pourrait aider à identifier des structures de marché et des règles de pénalisation des écarts potentiellement plus efficaces.

Bibliography

[1] S. Arrhenius. 'On the Influence of Carbonic Acid in the Air upon the Temperature of the Earth'. In: *Publications of the Astronomical Society of the Pacific* 9 (Feb. 1897), p. 14. DOI: 10.1086/121158.

[2] D.H. Meadows et al. *The limits to growth. A report for the Club of Rome's project on the predicament of mankind.* New York, USA: Universe Books, 1972.

[3] Wissenschaftlicher Beirat der Bundesregierung Globale Umweltveränderungen (Germany). *Climate change as a security risk*. Routledge, 2009.

[4] T.F. Stocker et al. 'Climate Change 2013: The Physical Science Basis. Contribution of Working Group I to the Fifth Assessment Report of the Intergovernmental Panel on Climate Change'. In: Cambridge, United Kingdom and New York, NY, USA: Cambridge University Press, 2013. Chap. Technical Summary, pp. 33–115. ISBN: ISBN 978-1-107-66182-0. DOI: 10.1017/CBO9781107415324.005.

[5] J. Hansen et al. 'Global surface temperature change'. In: *Reviews of Geophysics* 48 (2010), RG4004. DOI: 10.1029/2010RG000345.

[6] Monique Grooten and REA Almond. 'Living Planet Report-2018: Aiming Higher'. In: *WWF, Gland, Switzerland* (2018).

[7] Rashid Hassan, Robert Scholes and Neville Ash. *Ecosystems and Human Well-Being: Current State and Trends: Findings of the Condition and Trends Working Group (Millennium Ecosystem Assessment Series)*. Washington, DC (USA) Island Press, Jan. 2005.

[8] Robert Costanza et al. 'Changes in the global value of ecosystem services'. In: *Global environmental change* 26 (2014), pp. 152–158.

[9] Jos Lelieveld et al. 'The contribution of outdoor air pollution sources to premature mortality on a global scale'. In: *Nature* 525.7569 (2015), p. 367.

[10] International Energy Agency. *World Energy Balances 2018*. 2018, p. 762. DOI: https://doi.org/10.1787/world_energy_bal-2018-en.

[11] Roberto Turconi, Alessio Boldrin and Thomas Astrup. 'Life cycle assessment (LCA) of electricity generation technologies: Overview, comparability and limitations'. In: *Renewable and sustainable energy reviews* 28 (2013), pp. 555–565.

[12] International Renewable Energy Agency. *Renewable Power Generation Costs in 2018*. Tech. rep. IRENA, May 2019.

[13] P Bailly Du Bois et al. 'Estimation of marine source-term following Fukushima Dai-ichi accident'. In: *Journal of Environmental Radioactivity* 114 (2012), pp. 2–9.

[14] Atsuki Hiyama et al. 'The biological impacts of the Fukushima nuclear accident on the pale grass blue butterfly'. In: *Scientific reports* 2 (2012), p. 570.

[15] Timothy A Mousseau and Anders P Møller. 'Genetic and ecological studies of animals in Chernobyl and Fukushima'. In: *Journal of Heredity* 105.5 (2014), pp. 704–709.

[16] Jeffrey A Frankel. *The Natural Resource Curse: A Survey*. Working Paper 15836. National Bureau of Economic Research, Mar. 2010. DOI: 10.3386/w15836.

[17] Daniele La Porta Arrobas et al. 'The growing role of minerals and metals for a low carbon future'. In: *The World Bank: Washington, DC, USA* (2017).

[18] Indra Overland. 'The geopolitics of renewable energy: Debunking four emerging myths'. In: *Energy Research & Social Science* 49 (2019), pp. 36–40.

[19] Simon Philipps and Werner Warmuth. 'Photovoltaics report'. In: *Fraunhofer Institute for Solar Energy Systems, ISE* (2017).

[20] Miguel de Simón-Martín, Montserrat Díez-Mediavilla and Cristina Alonso-Tristán. 'Shadow-band radiometer measurement of diffuse solar irradiance: Calculation of geometrical and total correction factors'. In: *Solar Energy* 139 (2016), pp. 85–99.

[21] Ph Blanc and Lucien Wald. 'The SG2 algorithm for a fast and accurate computation of the position of the Sun for multi-decadal time period'. In: *Solar Energy* 86.10 (2012), pp. 3072–3083.

[22] M. Lefèvre et al. 'McClear: A new model estimating downwelling solar radiation at ground level in clear-sky conditions'. In: *Atmospheric Measurement Techniques* 6.9 (2013), pp. 2403–2418. ISSN: 1867-8548. DOI: 10.5194/amt-6-2403-2013.

[23] KH Solangi et al. 'A review on global solar energy policy'. In: *Renewable and sustainable energy reviews* 15.4 (2011), pp. 2149–2163.

[24] *Cahier des charges de l'appel d'offres portant sur la réalisation et l'exploitation d'Installations de production d'électricité à partir de l'énergie solaire « Centrales au sol ».* Commision de Régulation de l'Energie. 2019.

[25] *Programmation Pluriannuelle de l'Energie - Synthèse.* Ministère de la Transition écologique et Solidaire. 2019.

[26] Hannah E Murdock et al. *Renewables 2019 Global Status Report.* Tech. rep. Ren21, 2019.

[27] Thomas Carriere et al. 'A Novel Approach for Seamless Probabilistic Photovoltaic Power Forecasting Covering Multiple Time Frames'. In: *IEEE Transactions on Smart Grid* (2019).

[28] Thomas Carriere and George Kariniotakis. 'An Integrated Approach for Value-oriented Energy Forecasting and Data-driven Decision-making. Application to Renewable Energy Trading'. In: *IEEE Transactions on Smart Grid* (2019).

[29] S.J. Deng and S.S. Oren. 'Electricity derivatives and risk management'. In: *Energy* 31.6 (2006). Electricity Market Reform and Deregulation, pp. 940–953. ISSN: 0360-5442. DOI: https://doi.org/10.1016/j.energy.2005.02.015.

[30] Sergei Kulakov and Florian Ziel. 'The impact of renewable energy forecasts on intraday electricity prices'. In: *arXiv preprint arXiv:1903.09641* (2019).

[31] CE Delft and Microeconomix. *Refining Short-Term Electricity Markets to Enhance Flexibility.* Tech. rep. Study on behal of Agora Energiewende, 2016.

[32] Anuj Banshwar et al. 'Renewable energy sources as a new participant in ancillary service markets'. In: *Energy strategy reviews* 18 (2017), pp. 106–120.

[33] AS Chuang and Christine Schwaegerl. 'Ancillary services for renewable integration'. In: *2009 CIGRE/IEEE PES Joint Symposium Integration of Wide-Scale Renewable Resources Into the Power Delivery System.* IEEE. 2009, pp. 1–1.

[34] Anuj Banshwar et al. 'Market based procurement of energy and ancillary services from Renewable Energy Sources in deregulated environment'. In: *Renewable Energy* 101 (2017), pp. 1390–1400.

[35] Tiago Soares et al. 'Optimal offering strategies for wind power in energy and primary reserve markets'. In: *IEEE Transactions on Sustainable Energy* 7.3 (2016), pp. 1036–1045.

[36] Simon Camal, A. Michiorri and G. Kariniotakis. 'Optimal Offer of Automatic Frequency Restoration Reserve from a Combined PV/Wind Virtual Power Plant'. In: *IEEE Transactions on Power Systems* 99.c (2018), p. 1. ISSN: 08858950. DOI: 10.1109/TPWRS.2018.2847239.

[37] Xin Ai et al. 'Robust operation strategy enabling a combined wind/battery power plant for providing energy and frequency ancillary services'. In: *International Journal of Electrical Power & Energy Systems* 118 (2020), p. 105736.

[38] Jose L Crespo-Vazquez et al. 'Evaluation of a data driven stochastic approach to optimize the participation of a wind and storage power plant in day-ahead and reserve markets'. In: *Energy* 156 (2018), pp. 278–291.

[39] Erik Ela et al. 'Effective ancillary services market designs on high wind power penetration systems'. In: *2012 IEEE Power and Energy Society General Meeting*. IEEE. 2012, pp. 1–8.

[40] Tiago Soares, Pierre Pinson and Hugo Morais. 'Wind offering in energy and reserve markets'. In: *Journal of Physics: Conference Series (Online)*. IOP Publishing. 2016.

[41] Pierre Pinson, Christophe Chevallier and George N. Kariniotakis. 'Trading wind generation from short-term probabilistic forecasts of wind power'. In: *IEEE Transactions on Power Systems* 22.3 (2007), pp. 1148–1156. ISSN: 0885-8950. DOI: 10.1109/TPWRS.2007.901117.

[42] Franck Bourry. 'Management of uncertainties related to renewable generation participating in electricity markets'. PhD thesis. 2010, pp. 1–254.

[43] Warren B Powell. 'A unified framework for stochastic optimization'. In: *European Journal of Operational Research* 275.3 (2019), pp. 795–821.

[44] Yujian Ye et al. 'Deep Reinforcement Learning for Strategic Bidding in Electricity Markets'. In: *IEEE Transactions on Smart Grid* (2019).

[45] Gilles Bertrand and Anthony Papavasiliou. 'Reinforcement-Learning Based Threshold Policies for Continuous Intraday Electricity Market Trading'. In: *IEEE PES General Meeting, Atlanta*. 2019.

[46] Daniel R Jiang and Warren B Powell. 'Risk-averse approximate dynamic programming with quantile-based risk measures'. In: *Mathematics of Operations Research* 43.2 (2018), pp. 554–579.

[47] Carlos Adrian Correa-Florez, Andrea Michiorri and Georges Kariniotakis. 'Robust optimization for day-ahead market participation of smart-home aggregators'. In: *Applied energy* 229 (2018), pp. 433–445.

[48] Warren B Powell and Stephan Meisel. 'Tutorial on stochastic optimization in energy—Part I: Modeling and policies'. In: *IEEE Transactions on Power Systems* 31.2 (2015), pp. 1459–1467.

[49] Javier Sanz Rodrigo et al. 'The role of predictability in the investment phase of wind farms'. In: *Renewable Energy Forecasting*. Elsevier, 2017, pp. 341–357.

[50] Antonio Bracale et al. 'New advanced method and cost-based indices applied to probabilistic forecasting of photovoltaic generation'. In: *Journal of Renewable and Sustainable Energy* 8.2 (2016). ISSN: 19417012. DOI: 10.1063/1.4946798.

[51] Markus Peters et al. 'Autonomous data-driven decision-making in smart electricity markets'. In: *Joint European Conference on Machine Learning and Knowledge Discovery in Databases*. Springer. 2012, pp. 132–147.

[52] Javier Saez-Gallego et al. 'A data-driven bidding model for a cluster of price-responsive consumers of electricity'. In: *IEEE Transactions on Power Systems* 31.6 (2016), pp. 5001–5011.

[53] Jim Sanchez, Javier Pantoja and Juan C Vera. 'Data Driven Robust Static Hedging of Weather and Price Risks in the Electricity Market'. In: (2019).

[54] Georges Kariniotakis. *Renewable Energy Forecasting: From Models to Applications*. Woodhead Publishing, 2017.

[55] Pierre Pinson, Christophe Chevallier and Georges Kariniotakis. 'Optimizing benefits from wind power participation in electricity market using advanced tools for wind power forecasting and uncertainty Assessment'. In: *EWEC*. London, United Kingdom, Nov. 2004.

[56] Franck Bourry, M Costa and George Kariniotakis. 'Advanced Strategies for Wind Power Trading in Short-term Electricity Markets'. In: *European Wind Energy Conference*. April. Brussels, 2008.

[57] Ricardo Bessa et al. 'Towards Improved Understanding of the Applicability of Uncertainty Forecasts in the Electric Power Industry'. In: *Energies* 10.9 (2017), p. 1402. ISSN: 1996-1073. DOI: 10.3390/en10091402.

[58] George N Kariniotakis and Pierre Pinson. 'Uncertainty of short-term wind power forecasts a methodology for on-line assessment'. In: *2004 International Conference on Probabilistic Methods Applied to Power Systems*. IEEE. 2004, pp. 729–736.

[59] Tilmann Gneiting, Fadoua Balabdaoui and Adrian E Raftery. 'Probabilistic forecasts, calibration and sharpness'. In: *Journal of the Royal Statistical Society: Series B (Statistical Methodology)* 69.2 (2007), pp. 243–268.

[60] Jochen Bröcker and Leonard A Smith. 'Scoring probabilistic forecasts: The importance of being proper'. In: *Weather and Forecasting* 22.2 (2007), pp. 382–388.

[61] Pierre Pinson et al. 'Non-parametric probabilistic forecasts of wind power: required properties and evaluation'. In: *Wind Energy: An International Journal for Progress and Applications in Wind Power Conversion Technology* 10.6 (2007), pp. 497–516.

[62] Caleb M DeChant and Hamid Moradkhani. 'On the assessment of reliability in probabilistic hydrometeorological event forecasting'. In: *Water Resources Research* 51.6 (2015), pp. 3867–3883.

[63] Alexandre Costa et al. 'A review on the young history of the wind power short-term prediction'. In: *Renewable and Sustainable Energy Reviews* 12.6 (2008), pp. 1725–1744.

[64] GN Kariniotakis, GS Stavrakakis and EF Nogaret. 'Wind power forecasting using advanced neural networks models'. In: *IEEE transactions on Energy conversion* 11.4 (1996), pp. 762–767.

[65] Lars Landberg. 'Short-term prediction of the power production from wind farms'. In: *Journal of Wind Engineering and Industrial Aerodynamics* 80.1-2 (1999), pp. 207–220.

[66] George Sideratos and Nikos D Hatziargyriou. 'An advanced statistical method for wind power forecasting'. In: *IEEE Transactions on power systems* 22.1 (2007), pp. 258–265.

[67] Sobrina Sobri, Sam Koohi-Kamali and Nasrudin Abd Rahim. 'Solar photovoltaic generation forecasting methods: A review'. In: *Energy Conversion and Management* 156.May 2017 (2018), pp. 459–497. ISSN: 01968904. DOI: 10.1016/j.enconman.2017.11.019.

[68] Philippe Lauret, Mathieu David and Hugo Pedro. 'Probabilistic Solar Forecasting Using Quantile Regression Models'. In: *Energies* 10.10 (2017), p. 1591. ISSN: 1996-1073. DOI: 10.3390/en10101591.

[69] L. Mazorra Aguiar et al. 'Combining solar irradiance measurements, satellite-derived data and a numerical weather prediction model to improve intra-day solar forecasting'. In: *Renewable Energy* 97 (2016), pp. 599–610. ISSN: 18790682. DOI: 10.1016/j.renene.2016.06.018.

[70] A. Ayet and P. Tandeo. 'Nowcasting solar irradiance using an analog method and geostationary satellite images'. In: *Solar Energy* 164 (2018), pp. 301–315. ISSN: 0038092X. DOI: 10.1016/j.solener.2018.02.068.

[71] Xwegnon Ghislain Agoua, Robin Girard and George Kariniotakis. 'Short-Term Spatio-Temporal Forecasting of Photovoltaic Power Production'. In: *IEEE Transactions on Sustainable Energy* 9.2 (2018), pp. 538–546. ISSN: 19493029. DOI: 10.1109/TSTE.2017.2747765.

[72] X. G. Agoua, R. Girard and G. Kariniotakis. 'Probabilistic Models for Spatio-Temporal Photovoltaic Power Forecasting'. In: *IEEE Transactions on Sustainable Energy* 10.2 (Apr. 2019), pp. 780–789. ISSN: 1949-3029. DOI: 10.1109/TSTE.2018.2847558.

[73] Hugo T C Pedro et al. 'Assessment of machine learning techniques for deterministic and probabilistic intra-hour solar forecasts'. In: *Renewable Energy* 123 (2018), pp. 191–203. ISSN: 18790682. DOI: 10.1016/j.renene.2018.02.006.

[74] P Mathiesen et al. 'Improved Solar Power Forecasting Using Cloud Assimilation into WRF'. In: *LII Annual Conference Australian Solar Energy Society*. 2014, pp. 703–708.

[75] Henrik Aalborg Nielsen et al. 'From wind ensembles to probabilistic information about future wind power production–results from an actual application'. In: *2006 International Conference on Probabilistic Methods Applied to Power Systems*. IEEE. 2006, pp. 1–8.

[76] Simone Sperati, Stefano Alessandrini and Luca Delle Monache. 'An application of the ECMWF Ensemble Prediction System for short-term solar power forecasting'. In: *Solar Energy* 133 (2016), pp. 437–450.

[77] Javier Antonanzas et al. 'Review of photovoltaic power forecasting'. In: *Solar Energy* 136 (2016), pp. 78–111.

[78] Hugo T C Pedro and Carlos F M Coimbra. 'Assessment of forecasting techniques for solar power production with no exogenous inputs'. In: *Solar Energy* 86.7 (2017), pp. 2017–2028. ISSN: 0038-092X. DOI: 10.1016/j.solener.2012.04.004.

[79] Joao Gari da Silva Fonseca et al. 'On the use of maximum likelihood and input data similarity to obtain prediction intervals for forecasts of photovoltaic power generation'. In: *Journal of Electrical Engineering and Technology* 10 (2015), pp. 1342–1348. ISSN: 19750102. DOI: 10.5370/JEET.2015.10.3.1342.

[80] Jidong Wang et al. 'A short-term photovoltaic power prediction model based on the gradient boost decision tree'. In: *Applied Sciences* 8.5 (2018), p. 689.

[81] Can Wan et al. 'Probabilistic Forecasting of Photovoltaic Generation: An Efficient Statistical Approach'. In: *IEEE Transactions on Power Systems* 32.3 (2017), pp. 2471–2472. ISSN: 0885-8950. DOI: 10.1109/TPWRS.2016.2608740.

[82] Bo Jing et al. 'Ultra short-term PV power forecasting based on ELM segmentation model'. In: *The Journal of Engineering* 2017.13 (2017), pp. 2564–2568. ISSN: 2051-3305. DOI: 10.1049/joe.2017.0790.

[83] Faranak Golestaneh, Pierre Pinson and H B Gooi. 'Very Short-Term Nonparametric Probabilistic Forecasting of Renewable Energy Generation— With Application to Solar Energy'. In: *IEEE Transactions on Power Systems* 31.5 (2016). DOI: 10.1109/TPWRS.2015.2502423.

[84] Hanmin Sheng et al. 'Short-Term Solar Power Forecasting Based on Weighted Gaussian Process Regression'. In: *IEEE Transactions on Industrial Electronics* 65.1 (2017), pp. 1–1. ISSN: 0278-0046. DOI: 10.1109/TIE.2017.2714127.

[85] Mohammad Javad Sanjari and H. B. Gooi. 'Probabilistic Forecast of PV Power Generation Based on Higher Order Markov Chain'. In: *IEEE Transactions on Power Systems* 32.4 (2017), pp. 2942–2952. ISSN: 08858950. DOI: 10.1109/TPWRS.2016.2616902.

[86] Ye Ren, PN Suganthan and N Srikanth. 'Ensemble methods for wind and solar power forecasting—A state-of-the-art review'. In: *Renewable and Sustainable Energy Reviews* 50 (2015), pp. 82–91.

[87] Tao Hong et al. 'Probabilistic energy forecasting: Global Energy Forecasting Competition 2014 and beyond'. In: *International Journal of Forecasting* 32 (2016), pp. 896–913. DOI: 10.1016/j.ijforecast.2016.02.001.

[88] Gábor I. Nagy et al. 'GEFCom2014: Probabilistic solar and wind power forecasting using a generalized additive tree ensemble approach'. In: *International Journal of Forecasting* 32.3 (2016), pp. 1087–1093. ISSN: 01692070. DOI: 10.1016/j.ijforecast.2015.11.013.

[89] Jing Huang and Matthew Perry. 'A semi-empirical approach using gradient boosting and k-nearest neighbors regression for GEFCom2014 probabilistic solar power forecasting'. In: *International Journal of Forecasting* 32 (2016), pp. 1081–1086. ISSN: 01692070. DOI: 10.1016/j.ijforecast.2015.11.002.

[90] Bella Espinar et al. 'Photovoltaic Forecasting: A state of the art'. In: *5th European PV-Hybrid and Mini-Grid Conference*. Tarragona, Spain, Apr. 2010.

[91] Lorenzo Gigoni et al. In: *IEEE Transactions on Sustainable Energy* 9.2 (2018), pp. 831–842. ISSN: 19493029. DOI: 10.1109/TSTE.2017.2762435.

[92] Xinmin Zhang et al. 'A solar time based analog ensemble method for regional solar power forecasting'. In: *IEEE Transactions on Sustainable Energy* 10.1 (2018), pp. 268–279.

[93] Deockho Kim and Jin Hur. 'Short-term probabilistic forecasting of wind energy resources using the enhanced ensemble method'. In: *Energy* 157 (2018), pp. 211–226.

[94] Jooyoung Jeon, Anastasios Panagiotelis and Fotios Petropoulos. 'Probabilistic forecast reconciliation with applications to wind power and electric load'. In: *European Journal of Operational Research* (2019).

[95] Li Bai and Pierre Pinson. 'Distributed Reconciliation in Day-Ahead Wind Power Forecasting'. In: *Energies* 12.6 (2019), p. 1112.

[96] Emil B Iversen et al. 'Probabilistic forecasts of solar irradiance using stochastic differential equations'. In: *Environmetrics* 25.3 (2014), pp. 152–164.

[97] Emil B Iversen et al. 'Short-term probabilistic forecasting of wind speed using stochastic differential equations'. In: *International Journal of Forecasting* 32.3 (2016), pp. 981–990.

[98] Emil B Iversen et al. 'Leveraging stochastic differential equations for probabilistic forecasting of wind power using a dynamic power curve'. In: *Wind Energy* 20.1 (2017), pp. 33–44.

[99] Luca Delle Monache et al. 'Probabilistic Weather Prediction with an Analog Ensemble'. In: *Monthly Weather Review* 141.10 (2013), pp. 3498–3516. ISSN: 0027-0644. DOI: 10.1175/MWR-D-12-00281.1.

[100] Claudio Monteiro et al. 'Short-term power forecasting model for photovoltaic plants based on historical similarity'. In: *Energies* 6 (2013), pp. 2624–2643. ISSN: 1996-1073. DOI: 10.3390/en6052624.

[101] S. Alessandrini et al. 'An analog ensemble for short-term probabilistic solar power forecast'. In: *Applied Energy* 157 (2015), pp. 95–110. ISSN: 03062619. DOI: 10.1016/j.apenergy.2015.08.011.

[102] Bengu Ozge Akyurek et al. 'TESLA: Taylor expanded solar analog forecasting'. In: *2014 IEEE International Conference on Smart Grid Communications, SmartGridComm 2014*. Venice, Italy, 2015, pp. 127–132. ISBN: 9781479949342. DOI: 10.1109/SmartGridComm.2014.7007634.

[103] Constantin Junk et al. 'Predictor-weighting strategies for probabilistic wind power forecasting with an analog ensemble'. In: *Meteorologische Zeitschrift* 24.4 (2015), pp. 361–379. ISSN: 0941-2948. DOI: 10.1127/metz/2015/0659.

[104] André Gensler, Bernhard Sick and Vitali Pankraz. 'An analog ensemble-based similarity search technique for solar power forecasting'. In: *Proceedings of the IEEE International Conference on Systems, Man, and Cybernetics (SMC16)*. Budapest, Hungary, 2016, pp. 2850–2857. ISBN: 978-1-5090-1897-0. DOI: 10.1109/SMC.2016.7844672.

[105] Guido Cervone et al. 'Short-term photovoltaic power forecasting using Artificial Neural Networks and an Analog Ensemble'. In: *Renewable Energy* 108 (2017), pp. 274–286. ISSN: 18790682. DOI: 10.1016/j.renene.2017.02.052.

[106] Bw. Silverman. 'Density estimation for statistics and data analysis'. In: *Chapman and Hall* 37.1 (1986), pp. 1–22. ISSN: 00359254. DOI: 10.2307/2347507.

[107] S. Alessandrini et al. 'A novel application of an analog ensemble for short-term wind power forecasting'. In: *Renewable Energy* 76 (2015), pp. 768–781. ISSN: 18790682. DOI: 10.1016/j.renene.2014.11.061.

[108] Claude E Shannon and Warren Weaver. *The mathematical theory of communication*. University of Illinois press, 1998.

[109] Hanchuan Peng, Fuhui Long and Chris Ding. 'Feature selection based on mutual information: criteria of max-dependency, max-relevance, and min-redundancy'. In: *IEEE Transactions on Pattern Analysis & Machine Intelligence* 8 (2005), pp. 1226–1238.

[110] James Dougherty, Ron Kohavi and Mehran Sahami. 'Supervised and Unsupervised Discretization of Continuous Features'. In: *Machine Learning: Proceedings of the Twelfth International Conference*. San Francisco, USA, 1995.

[111] Luis F. Zarzalejo et al. 'A new statistical approach for deriving global solar radiation from satellite images'. In: *Solar Energy* 83.4 (2009), pp. 480–484. ISSN: 0038-092X. DOI: 10.1016/j.solener.2008.09.006.

[112] Philippe Blanc et al. 'The HelioClim project: Surface solar irradiance data for climate applications'. In: *Remote Sensing* 3.2 (2011), pp. 343–361. ISSN: 20724292. DOI: 10.3390/rs3020343.

[113] J. L. Bosch and J. Kleissl. 'Cloud motion vectors from a network of ground sensors in a solar power plant'. In: *Solar Energy* 95 (2013), pp. 13–20. ISSN: 0038092X. DOI: 10.1016/j.solener.2013.05.027.

[114] Robert Tibshiranit. *Regression Shrinkage and Selection via the Lasso*. 1. 1996, pp. 267–288.

[115] Hirotogu Akaike. 'Information theory and an extension of the maximum likelihood principle'. In: *Selected papers of hirotugu akaike*. Springer, 1998, pp. 199–213.

[116] Leo Breiman. 'Random forests'. In: *Machine Learning* 45.1 (2001), pp. 5–32. ISSN: 0885-6125. DOI: 10.1023/A:1010933404324. eprint: /dx.doi.org/10.1023{\%}2FA{\%}3A1010933404324 (http:).

[117] Nicolai Meinshausen. 'Quantile Regression Forests'. In: *Journal of Machine Learning Research* 7 (2006), pp. 983–999. ISSN: 1532-4435. DOI: 10.1111/j.1541-0420.2010.01521.x.

[118] Michael E Tipping. 'Sparse Bayesian Learning and the Relevance Vector Machine'. In: *Journal of Machine Learning Research* 1 (2001), pp. 211–245.

[119] H Madsen et al. 'A protocol for standardising the performance evaluation of short-term wind power prediction models'. In: *Proceedings of the Global WindPower 2004 Conference*. 2004.

[120] Jochen Bröcker and Leonard A. Smith. 'Increasing the Reliability of Reliability Diagrams'. In: *Weather and Forecasting* 22.3 (2007), pp. 651–661. DOI: 10.1175/WAF993.1.

[121] Pierre Pinson, Patrick McSharry and Henrik Madsen. 'Reliability diagrams for non-parametric density forecasts of continuous variables: Accounting for serial correlation'. In: *Quarterly Journal of the Royal Meteorological Society* 136.646 (2010), pp. 77–90. ISSN: 00359009. DOI: 10.1002/qj.559.

[122] F.X. Diebold and R.S. Mariano. 'Comparing Predictive Accuracy'. In: *Journal of Business and Economic Statistics* 13 (1995), pp. 253–263.

[123] Martín Gastón-Romeo et al. 'A Morphological Clustering Method for daily solar radiation curves'. In: *Solar Energy* 85.9 (2011), pp. 1824–1836. ISSN: 0038092X. DOI: 10.1016/j.solener.2011.04.023.

[124] Graeme N Bathurst, Jennie Weatherill and Goran Strbac. 'Trading wind generation in short term energy markets'. In: *IEEE Transactions on Power Systems* 17.3 (2002), pp. 782–789.

[125] Julija Matevosyan and Lennart Soder. 'Minimization of imbalance cost trading wind power on the short-term power market'. In: *IEEE Transactions on Power Systems* 21.3 (2006), pp. 1396–1404.

[126] E Bitar, R Rajagopal and P Khargonekar. 'Bringing Wind Energy to Market'. In: *IEEE Transactions on Power Systems* (2011).

[127] Marco Zugno, Tryggvi Jónsson and Pierre Pinson. 'Trading wind energy on the basis of probabilistic forecasts both of wind generation and of market quantities'. In: *Wind Energy* 16.6 (2013), pp. 909–926.

[128] Ting Dai and Wei Qiao. 'Trading wind power in a competitive electricity market using stochastic programing and game theory'. In: *IEEE Transactions on Sustainable Energy* 4.3 (2013), pp. 805–815.

[129] Ershun Du et al. 'Managing wind power uncertainty through strategic reserve purchasing'. In: *IEEE Transactions on Power Systems* 32.4 (2016), pp. 2547–2559.

[130] Rafał Weron. 'Electricity price forecasting: A review of the state-of-the-art with a look into the future'. In: *International Journal of Forecasting* 30.4 (2014), pp. 1030–1081. DOI: 10.1016/j.ijforecast.2014.08.008.

[131] Adam Paszke et al. *Automatic differentiation in PyTorch*. 2017.

[132] Diederik P Kingma and Jimmy Ba. 'Adam: A method for stochastic optimization'. In: *arXiv preprint arXiv:1412.6980* (2014).

[133] R. Girard, K. Laquaine and G. Kariniotakis. 'Assessment of wind power predictability as a decision factor in the investment phase of wind farms'. In: *Applied Energy* 101 (2013), pp. 609–617. ISSN: 03062619. DOI: 10.1016/j.apenergy.2012.06.064.

[134] Council of European Union. *Council regulation (EU) no 2019/944*. 2019.

[135] Igor Rychlik. 'A new definition of the rainflow cycle counting method'. In: *International journal of fatigue* 9.2 (1987), pp. 119–121.

[136] Mahera Musallam and C. Mark Johnson. 'An efficient implementation of the rainflow counting algorithm for life consumption estimation'. In: *IEEE Transactions on Reliability* 61.4 (2012), pp. 978–986. ISSN: 0018-9529. DOI: 10.1109/TR.2012.2221040.

[137] Chanaka Keerthisinghe, Gregor Verbič and Archie C Chapman. 'Evaluation of a Multi-stage Stochastic Optimisation Framework for Energy Management of Residential PV-storage Systems'. In: *Australasian Universities Power Engineering Conference (AUPEC)*. Perth, Australia, 2014, pp. 1–6.

[138] Huajie Ding et al. 'Integrated bidding and operating strategies for wind-storage systems'. In: *IEEE Transactions on Sustainable Energy* 7.1 (2015), pp. 163–172.

[139] Francesco Conte, Stefano Massucco and Federico Silvestro. 'Day-ahead Planning and Real-time Control of Integrated PV-storage Systems by Stochastic Optimization'. In: *IFAC-PapersOnLine* 50.1 (2017), pp. 7717–7723.

[140] Francesco Conte et al. 'A Stochastic Optimization Method for Planning and Real-Time Control of Integrated PV-Storage Systems : Design and Experimental Validation'. In: *IEEE Transactions on Sustainable Energy* 9.3 (2018), pp. 1188–1197. DOI: 10.1109/TSTE.2017.2775339.

[141] Tiago Rodrigues, Pedro J Ramírez and Goran Strbac. 'Risk-averse bidding of energy and spinning reserve by wind farms with on-site energy storage'. In: *IET Renewable Power Generation* 12.2 (2017), pp. 165–173.

[142] Ahmad Attarha et al. 'Adaptive robust self-scheduling for a wind producer with compressed air energy storage'. In: *IEEE Transactions on Sustainable Energy* 9.4 (2018), pp. 1659–1671.

[143] Yuwei Wang, Huiru Zhao and Peng Li. 'Optimal Offering and Operating Strategies for Wind-Storage System Participating in Spot Electricity Markets with Progressive Stochastic-Robust Hybrid Optimization Model Series'. In: *Mathematical Problems in Engineering* 2019 (2019).

[144] A. Saez-de-Ibarra et al. 'Management Strategy for Market Participation of Photovoltaic Power Plants Including Storage Systems'. In: *IEEE Transactions on Industry Applications* 52.5 (2016), pp. 4292–4303. ISSN: 0093-9994. DOI: 10.1109/TIA.2016.2585090.

[145] Amparo Núñez-Reyes et al. 'Optimal scheduling of grid-connected PV plants with energy storage for integration in the electricity market'. In: *Solar Energy* 144 (2017), pp. 502–516. ISSN: 0038092X. DOI: 10.1016/j.solener.2016.12.034.

[146] Anders Skajaa, Kristian Edlund and Juan M Morales. 'Intraday trading of wind energy'. In: *IEEE Transactions on Power Systems* 30.6 (2015), pp. 3181–3189.

[147] E Perez et al. 'Predictive Power Control for PV Plants With Energy Storage'. In: *IEEE Transactions on Sustainable Energy* 4.2 (2013), pp. 482–490.

[148] Hussein Hassan Abdeltawab and Yasser Abdel-Rady I Mohamed. 'Market-Oriented Energy Management of a Hybrid Wind-Battery Energy Storage System Via Model Predictive Control With Constraint Optimizer'. In: *IEEE Transactions on Industrial Electronics* 62.11 (2015), pp. 6658–6670. ISSN: 0278-0046. DOI: 10.1109/TIE.2015.2435694.

[149] A Damiano et al. 'Real-Time Control Strategy of Energy Storage Systems for Renewable Energy Sources Exploitation'. In: *IEEE Transactions on Sustainable Energy* 5.2 (2014), pp. 567–576. ISSN: 1949-3029. DOI: 10.1109/TSTE.2013.2273400.

[150] H Ding et al. 'Optimal Offering and Operating Strategies for Wind-Storage Systems with Linear Decision Rules'. In: *IEEE Transactions on Power Systems* 31.6 (2017), pp. 4755–4764. DOI: 10.1109/TPWRS.2016.2521177.

[151] Hao Wang and Baosen Zhang. 'Energy storage arbitrage in real-time markets via reinforcement learning'. In: *2018 IEEE Power & Energy Society General Meeting (PESGM)*. IEEE. 2018, pp. 1–5.

[152] Hanchen Xu et al. 'Arbitrage of energy storage in electricity markets with deep reinforcement learning'. In: *arXiv preprint arXiv:1904.12232* (2019).

[153] Jun Cao et al. 'Deep Reinforcement Learning Based Energy Storage Arbitrage With Accurate Lithium-ion Battery Degradation Model'. In: *IEEE Transactions on Smart Grid* (2020).

[154] Andrea Michiorri et al. 'Storage sizing for grid connected hybrid wind and storage power plants taking into account forecast errors autocorrelation'. In: *Renewable energy* 117 (2018), pp. 380–392.

[155] Faranak Golestaneh, Hoay Gooi and Pierre Pinson. 'Generation and evaluation of space – time trajectories of photovoltaic power'. In: *Applied Energy* 176 (2016), pp. 80–91. ISSN: 0306-2619. DOI: 10.1016/j.apenergy.2016.05.025.

[156] Michael JD Powell. 'A Direct Search Optimization Method that Models the Objective and Constraint Functions by Linear Interpolation'. In: *Advances in Optimization and Numerical Analysis*. Springer, 1994, pp. 51–67.

[157] I Duggal and B Venkatesh. 'Short-term scheduling of thermal generators and battery storage with depth of discharge-based cost model'. In: *2016 IEEE Power and Energy Society General Meeting (PESGM)* 30.4 (2016), p. 1. DOI: 10.1109/PESGM.2016.7741255.

[158] Georg Fuchs et al. *Technology Overview on Electricity Storage - Overview on the potential and on the deployment perpectives of electric storage technologies*. Tech. rep. June. 2012, p. 66. DOI: 10.13140/RG.2.1.5191.5925.

[159] David Meyer et al. *e1071: Misc Functions of the Department of Statistics, Probability Theory Group (Formerly: E1071)*. R Package Version 1.6-8. TU Wien, 2017.

[160] Steven G. Johnson. *The NLopt Nonlinear-optimization Package*. MIT, 2018.

[161] Carl Johan Rydh and Björn A. Sandén. 'Energy analysis of batteries in photovoltaic systems. Part I: Performance and energy requirements'. In: *Energy Conversion and Management* 46.11-12 (2005), pp. 1957–1979. ISSN: 0196-8904. DOI: 10.1016/j.enconman.2004.10.003.

[162] Yoshua Bengio, Patrice Simard, Paolo Frasconi et al. 'Learning long-term dependencies with gradient descent is difficult'. In: *IEEE transactions on neural networks* 5.2 (1994), pp. 157–166.

[163] Sepp Hochreiter and Jürgen Schmidhuber. 'Long short-term memory'. In: *Neural computation* 9.8 (1997), pp. 1735–1780.

[164] Alex Graves et al. 'A novel connectionist system for unconstrained handwriting recognition'. In: *IEEE transactions on pattern analysis and machine intelligence* 31.5 (2008), pp. 855–868.

[165] Felix A Gers, Jürgen Schmidhuber and Fred Cummins. *Learning to forget: Continual prediction with LSTM*. Tech. rep. IET, 1999.

[166] Klaus Greff et al. 'LSTM: A search space odyssey'. In: *IEEE transactions on neural networks and learning systems* 28.10 (2016), pp. 2222–2232.

[167] *Feuille de route de l'équilibrage du système électrique français*. 2016.

[168] 'LOI n° 2003-8 du 3 janvier 2003 relative aux marchés du gaz et de l'électricité et au service public de l'énergie (1)'. In: *Journal Officiel de la République Française* (Jan. 2004).

[169] Naturschutz und Reaktorsicherheit Bundesministerium für Umwelt. *Informationen zur Kalkulation der EEG-Umlage für das Jahr 2012*. 2012.

[170] Carolina Möhrlen, John Zack and Gregor Giebel. *Recommended Practice on Renewable Energy Forecast Solution Selection*. Tech. rep. International Energy Agency, 2019.

[171] Ian Goodfellow et al. 'Generative adversarial nets'. In: *Advances in neural information processing systems*. 2014, pp. 2672–2680.

[172] Merlinda Andoni et al. 'Blockchain technology in the energy sector: A systematic review of challenges and opportunities'. In: *Renewable and Sustainable Energy Reviews* 100 (2019), pp. 143–174.

[173] Thomas Carriere et al. 'Strategies for combined operation of PV/storage systems integrated into electricity markets'. In: *IET Renewable Power Generation* (2019).

RÉSUMÉ

La décarbonation de la production d'électricité à échelle mondiale est un élément de réponse clé face aux pressions exercées par les différents enjeux environnementaux. Par ailleurs, la baisse des coûts de la filière photovoltaïque (PV) ouvre la voie à une augmentation significative de la production PV dans le monde. Cependant, la forte variabilité de la production PV ainsi que des prix du marché de l'énergie impose aux producteurs d'energie PV de prendre de nombreuses décisions sous incertitude pour valoriser leur production. Dans cette thèse, nous proposons une formulation génerique de ces problèmes de prise de décision afin de formuler différentes façons de les résoudre. L'approche classique consistant à prévoir la production ainsi que les prix avant de résoudre un problème d'optimisation stochastique est comparée à une approche de Policy Function Approximation (PFA) où des réseaux de neurones artificels apprennent directement à formuler la prise de décision à partir des données. Cette seconde approche permet en particulier de résoudre certaines problématiques auxquels font face les producteurs d'énergie PV tels que la disparité entre les produits de prévisions commerciaux disponibles et la finalité de leur utilisation, ainsi que la multiplication des modèles requis pour valoriser la production.

MOTS CLÉS

Energies renouvelables, Stockage, Optimisation, Prévision, Policy Function Approximation, Photovoltaïque, Marchés de l'électricité, Smart grids

ABSTRACT

The decarbonation of electricity generation on a global scale is a key response to the pressures of various environmental issues. In addition, the falling costs of the photovoltaic (PV) industry are paving the way for a significant increase in PV production worldwide. However, the high variability of PV production and energy market prices means that PV power producers have to make many decisions under uncertainty in order to increase the value of their production. In this thesis, we propose a generic formulation of these decision-making problems in order to formulate different ways to solve them. The classical approach of predicting the PV power output as well as prices before solving a stochastic optimization problem is compared to a Policy Function Approximation (PFA) approach where artificial neural networks learn directly to formulate the decision making from the data. This second approach allows in particular to solve some of the problems faced by PV power producers such as the disparity between the available market forecast products and the finality of their use, as well as the multiplication of models required to value the PV production.

KEYWORDS

Renewable energies, Storage, Optimization, Forecasting, Policy Function Approximation, Photovoltaics, Electricity markets, Smart grids